A STUDY OF THE IGNEOUS INTRUSIVE ROCKS OF
THE DUNNAGE MELANGE, NEWFOUNDLAND

BRENNA ELLEN LORENZ

CANADIAN THESES ON MICROFICHE

I.S.B.N.

THESES CANADIENNES SUR MICROFICHE

National Library of Canada
Collections Development Branch

Canadian Theses on
Microfiche Service

Ottawa, Canada
K1A 0N4

Bibliothèque nationale du Canada
Direction du développement des collections

Service des thèses canadiennes
sur microfiche

NOTICE

The quality of this microfiche is heavily dependent
upon the quality of the original thesis submitted for
microfilming. Every effort has been made to ensure
the highest quality of reproduction possible.

If pages are missing, contact the university which
granted the degree.

Some pages may have indistinct print especially
if the original pages were typed with a poor typewriter
ribbon or if the university sent us a poor photocopy.

Previously copyrighted materials (journal articles,
published tests, etc.) are not filmed.

Reproduction in full or in part of this film is gov-
erned by the Canadian Copyright Act, R.S.C. 1970,
c. C-30. Please read the authorization forms which
accompany this thesis.

AVIS

La qualité de cette microfiche dépend grandement de
la qualité de la thèse soumise au microfilmage. Nous
avons tout fait pour assurer une qualité supérieure
de reproduction.

S'il manque des pages, veuillez communiquer
avec l'université qui a conféré le grade.

La qualité d'impression de certaines pages peut
laisser à désirer, surtout si les pages originales ont été
dactylographiées à l'aide d'un ruban usé ou si l'univer-
sité nous a fait parvenir une photocopie de mauvaise
qualité.

Les documents qui font déjà l'objet d'un droit
d'auteur (articles de revue, examens publiés, etc.) ne
sont pas microfilmés.

La reproduction, même partielle, de ce microfilm
est soumise à la Loi canadienne sur le droit d'auteur,
SRC 1970, c. C-30. Veuillez prendre connaissance des
formules d'autorisation qui accompagnent cette thèse.

THIS DISSERTATION
HAS BEEN MICROFILMED
EXACTLY AS RECEIVED

LA THÈSE A ÉTÉ
MICROFILMÉE TELLE QUE
NOUS L'AVONS REÇUE

Canada

A STUDY OF THE IGNEOUS INTRUSIVE ROCKS OF

THE DUNNAGE MELANGE, NEWFOUNDLAND

BY

Brenna Ellen Lorenz, B.S., M.A.

A thesis submitted to the School of Graduate

Studies in partial fulfillment of the

requirements for the degree of

Doctor of Philosophy

Department of Earth Sciences

Memorial University of Newfoundland

January 1984

St. John's   Newfoundland

Abstract

The Dunnage Melange, located in the central mobile belt of the Appalachian Orogen, in north-central Newfoundland, is host to several suites of igneous intrusions. These include mafic through felsic dikes, stocks, and batholiths ranging in age from Early Ordovician through Jurassic.

The tectonic environment and mode of origin of the Dunnage Melange, as well as the origin and significance of its intrusions, have long been a subject of controversy. The purpose of this study was to examine the field relationships between the intrusions and the host melange, and the geochemistry and petrography of the intrusions, in the context of this controversy.

It was concluded that the melange and its intrusions were part of a complex and dynamic igneous, sedimentary and tectonic system, the local history of which was characterized by penecontemporaneous sedimentation, block faulting, olistostrome deposition, intrusion, and sediment slumping and sliding in Ordovician time. The earliest intrusions are mafic tholeiites with a chemistry indicative of a tensional environment, interpreted to be related to back-arc basinal rifting. The Dunnage Formation was then intruded, penecontemporaneously with sedimentation and melange formation, by a suite of silicic rocks (the Coaker Porphyry) that have a sedimentary source. These intrusions were followed closely in time by a calc-alkaline suite that was derived from an igneous or mantle source.

On a regional scale, melange formation and intrusion of the Coaker Porphyry are interpreted to have taken place in a back-arc setting during the Early Ordovician subduction of the leading edge of the continental margin of North America, with partial melting of sediments from the continental margin giving rise to large quantities of silicic magma that permeated the overlying mantle wedge. Later calc-alkaline magmas were derived from the partial melting of this contaminated mantle.

Acknowledgements

I gratefully acknowledge my advisor, Bob Stevens, and my
committee, Hank Williams and Lars Fahraeus, for their guidance
and financial and moral support during three trying years. I also
thank Dave Strong for his financial assistance, and Steve Papezik
for his advice and support. Thanks also to Gert Andrews, Trish
Davis, and Dave Press for their assistance in the laboratory,
and to Foster Thornhill and Lloyd Warford for the many thin sections.
Wilf Marsh taught me everything I know about photography. A
special thanks to Wilf, Wins Howell, and Pat Browne for their
friendship and special sense of humour.

Finally, I most gratefully thank Stella and Elmo Small for
being my hosts, my teachers, and my family.

CONTENTS

v

CHAPTER 6

CHAPTER 9

viii

List of Tables

List of Figures

x

Chapter 1

Introduction

The Dunnage Melange is a prominent and controversial component of the central mobile belt of the Appalachian Orogen, located in the northeasternmost extension of the orogen, on the Island of Newfoundland.

The Dunnage Melange is host to a suite of felsic igneous intrusions. The Coaker Porphyry is unique to the northeast portion of the melange terrane, where it comprises approximately one third of the outcrop area. Minor mafic intrusions, the Puncheon Diorite and the Grapnel Gabbro, also occur in this area. The southwest portion of the Dunnage Melange was intruded by gabbro sills which, together with blocks of gabbro in the melange, are correlative with the New Bay Gabbros in the adjacent Exploits Group. The age, abundance, physical characteristics, and distribution of these intrusions suggest that they were penecontemporaneous with, and possibly related to, melange formation (Williams and Hibbard 1976).

The Dildo Porphyry is a suite of Late Ordovician dikes and stocks that intrudes surrounding formations, but is absent, oddly, from the Dunnage Melange itself.

A suite of Acadian batholiths (the Loon Bay granodiorites) and associated dikes and stocks intrude the southern and northwestern part of the melange. Diabase dikes of probable Devonian age intrude the melange in a swarm parallel to Dildo and Reach Runs. The youngest intrusions in the area are Jurassic lamprophyres that permeate the Notre Dame Bay area.

1.1 Statement of problem

The purpose of this study is twofold. Firstly, it is a petrological study of several suites of igneous rocks, to determine their sources, evolution, modes of emplacement, and interrelationships. The Coaker Porphyry in particular is an interesting rock, with its abundant ultramafic xenoliths, muscovite and garnet phenocrysts, and spectacular interactions with the host mudstones of the Dunnage Melange matrix.

The second purpose of this study is the determination of the physical and temporal relationships between the intrusions and the formation of the Dunnage Melange. It is also hoped that the petrogenetic part of the study would help to elucidate the tectonic environment of formation of the melange. The tectonic significance of the Dunnage Melange has long been a subject of dispute, with the theories of its origin ranging from that of an olistostromal deposit in a fore- or back-arc basin to tectonic deformation in the trench of a subduction zone. The conclusions reached have had a profound influence on the models by which the geologic history of central Newfoundland has been interpreted.

1.2 Methods

Two summers of field work were undertaken, during which the relationships between the intrusions and their host rocks were studied, distribution of igneous rock types were mapped, contacts between the northeast part of the Dunnage Melange and surrounding units were examined, and samples were collected in the Dunnage Melange and surrounding units.

Following recognition of the importance of mud-magma interactions in the Dunnage Melange, similar and well-documented occurrences in Wales and Ireland were examined during the Geological Society of London's conference, "Volcanic Processes in Marginal Basins".

Thin sections of the samples were examined for the petrographic part of the study; microscopic observations were supplemented by electron microprobe data, obtained using a fully automated JEOL JXA-50A electron probe microanalyser.

Trace elements, including rare earth elements, were analyzed by x-ray fluoresence, using a Phillips 1450 automatic X-ray flourescence spectrometer. Major elements were analyzed by atomic absorption (Perkin Elmer 360). A whole-rock Rb/Sr isochron was obtained for the Coaker Porphyry by mass spectrometry.

1.3 Format of dissertation

The first part of this report, Chapters 2 through 5, is concerned with the presentation and interpretation of field relationships and previous work. Chapter 2 sets the stage with a description of the geologic setting of the Dunnage Melange and the igneous rocks under study. Chapter 3 is an outline of previous and current work in the area. The behaviour of the igneous rocks during emplacement is discussed in Chapter 4. Chapter 5 presents conclusions based on the material in Chapters 2 through 4, and discusses the local geologic history of the Dunnage Melange as interpreted according to these conclusions.

The second part of the dissertation deals with the petrography, geochemistry, and petrogenesis of the igneous rocks under study: the Coaker Porphyry (Chapter 6), the Dildo Porphyry and Loon Bay suites (Chapter 7), and the mafic rocks (Chapter 8).

Chapter 9 summarizes the main points of the study and draws together the field and petrogenetic interpretations into a unified story.

Geologic Setting of the Dunnage Melange and its Intrusions

        The igneous rocks that intruded the Dunnage Melange are the

principle subjects of this dissertation, as well as intrusions

occurring in neighboring units and the rocks that serve as hosts to

these intrusions. This chapter is a brief overview of the geology and

geologic setting of the Dunnage Melange, and the igneous environment

of which the intrusions are a part. For further information on this

material, the reader is referred to previous work; only new

information and observations are presented in detail in this section.

2.1 Regional setting

        The Dunnage Melange is located in the north-central part of the

Appalachian orogen in Newfoundland. The orogen in Newfoundland has

been divided into four major tectonostratigraphic zones (Williams

1979) (fig. 2.1a). The Dunnage Zone, named after and including the

Dunnage Melange, consists of early Palaeozoic mafic volcanics,

ophiolites, and marine sediments, and comprises the remnants of the

ancient Iapetus Ocean. The Humber Zone to the west is the ancient

continental margin of North America, the easternmost part of which was

deformed and metamorphosed during the emplacement of the Taconic

allochthons onto the continental margin during early to middle

Ordovician time. The Gander and Avalon Zones to the east are

enigmatic suspect terranes (Williams and Hatcher 1982) whose

Figure 2.1 The Appalachian Orogen in Newfoundland

A. The Appalachian Orogen in Newfoundland has been divided into four major tectonostratigraphic zones (Williams 1979):

1) The Humber Zone = ancient continental margin of North America

2) Dunnage Zone = remnants of Iapetus Ocean

3) Gander and Avalon Zones = possible continental fragments annexed onto North America following the closing of the Iapetus Ocean.

B. A schematic cross-section (Early-Middle Ordovician) depicting a generalized model for the formation of the Appalachian Orogen, showing proposed location of the Dunnage Melange.

Baie Verte Lineament
Island arc Volcanics
Dunnage Melange

Humber Zone

Allochthons

Dunnage Zone

Gander Zone

Avalon Zone

N

A

Dunnage Zone
??
Gander Zone

Humber Zone

back arc basin
assemblages
including Dunnage
Melange
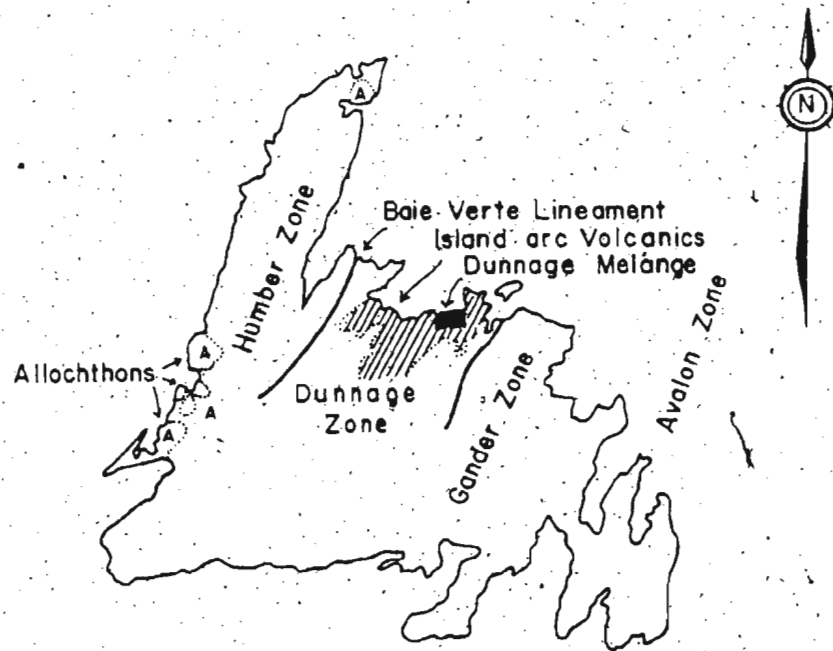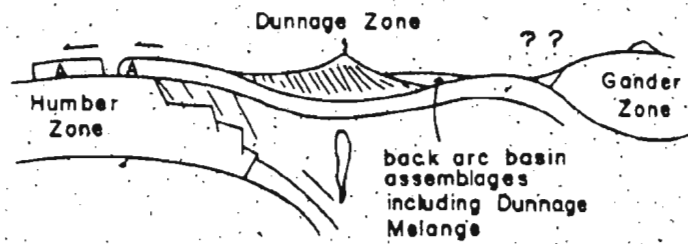
B

relationships to the Appalachian orogen are poorly understood. They are interpreted as continental masses from the eastern side of the Iapetus Ocean (see Coleman-Sadd 1980, 1982).

The Dunnage Zone is underlain by an ophiolitic basement that is exposed along the western edge of the zone, and in a horst in the central part of the zone (Haworth et al. 1978, Strong 1977, Dean 1978, Lorenz and Fountain 1982). Thick piles of Lower Ordovician volcanic and volcaniclastic rocks in the western and central parts of the Dunnage Zone have been universally accepted as having formed in an island arc environment (see Hibbard and Williams 1979 for complete references).

The Dunnage Melange is part of an assemblage of arc-derived basinal sediments that lies to the east of the island arc volcanics. Previous workers have disagreed as to whether this basinal assemblage was located in a fore-arc or a back-arc position. The advocates of a fore-arc environment based their conclusions on the presence of the Dunnage Melange itself, which they interpreted to be analogous to the Franciscan melanges, formed in the trench of a west-dipping subduction zone (Dewey 1969, Kay 1976, McKerrow and Cocks 1978). Hibbard and Williams (1979) advocated that the Dunnage Melange is an arc-flanking olistostrome rather than a trench-fill melange, but were unable to distinguish between the fore- and back-arc environments on the basis of local relationships.

The bulk of regional evidence favors the now widely-accepted model for Newfoundland in which closure of the Iapetus Ocean was effected by an eastward-dipping subduction zone located along the Baie Verte Lineament (fig. 2.1a) (see Coleman-Sadd 1983 for discussion). This model places the Dunnage Melange in a back-arc setting (fig. 2.1b).

2.2 Geology and local setting of the Dunnage Melange

The Dunnage Melange occupies an area approximately 40 km long and up to 13 km wide in the Bay of Exploits area of eastern Notre Dame Bay (fig. 2.2). It is part of a stratigraphically and structurally complex assemblage of island-arc volcanic and arc-derived sedimentary rocks that range in age from Middle Cambrian through Silurian. The lithologies comprising the Dunnage Melange are pre-Caradocian, and the melange is one of several distinct pre-Caradocian assemblages in the eastern Notre Dame Bay area. The geology of these assemblages and their possible relationships to the Dunnage Melange (stratographic or facies equivalence, source of melange lithologies) are summarized in Table 2.1, and discussed in section 2.2.3 below. The pre-Caradocian assemblages are overlain by Caradocian black shales, distal turbidites and minor chert, followed by flysch sequences that pass upwards (not without complications!) into Silurian terrestrial red-beds.

Figure 2.2   The Bay of Exploits region. Modified from Dean 1978.

Key

Loon Bay Granite	⬛
Undifferentiated Silurian groups	USi
Sansom Greywacke	OSs
Point Leamington Greywacke	OSp
Dark Hole Formation	mOD
Chapel Formation	⬛
Lawrence Harbour Shale	mOL
Summerford Group	Os
Lawrence Head Volcanics	OEi
New Bay Gabbro	⬛
New Bay Formation	OEn
Dunnage Melange	⬛
Twillingate Trondjhemite	⬛
Moreton's Harbour Group	EOM
Sleepy Cove Group	EOMs
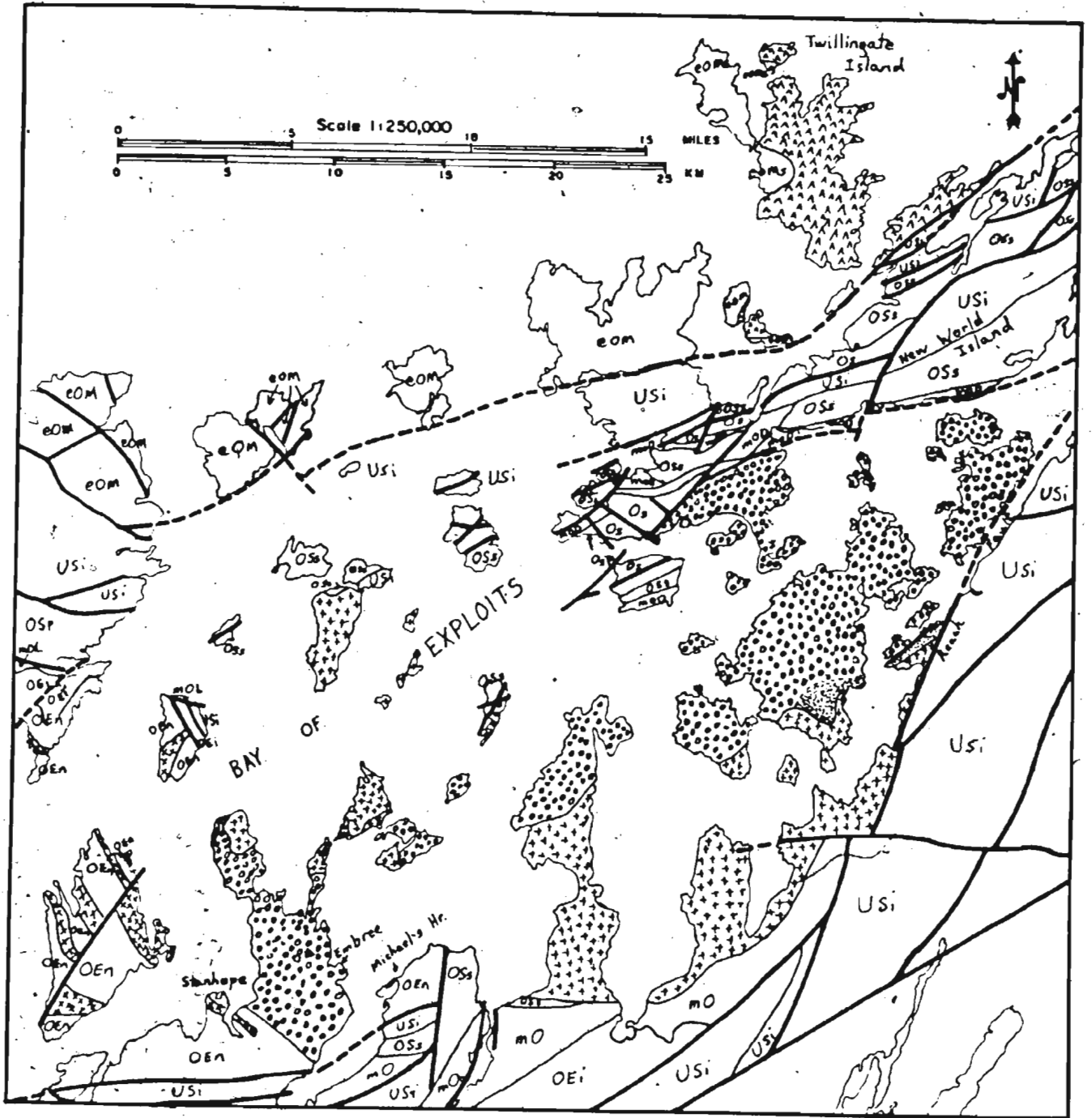
TABLE 2.1

Possible Sources and Stratigraphic Correlatives
of the Dunnage Melange

AGE AND UNIT	LITHOLOGIES	RELATIONSHIP TO DUNNAGE MELANGE
Exploits Group ? to Caradocian	Mafic Tea Arm Volcanics, New Bay Formation: tuff turbidites, conglomerates, greywackes	Interdigitates with SW portion of the Dunnage Melange, which is possibly a distal equivalent; New Bay Formation + Dunnage Melange matrix, but is coarser; Lawrence Head = volcanic blocks (Hibbard and Williams 1979)
Summerford Group Tremadocian(?) to Caradocian	Volcanics, Caradocian argillites, slumped argillites, limy tuff, arkose	Fault contact against Dunnage Melange on New World Island. Possibly share common source of lithologies, or represent the same formation but with different structural history.
Dunnage Melange Mid-Cambrian (blocks) Tremadocian (matrix) Arenig (blocks) to Caradocian	See tables 2.2 and 2.3	
Loon Harbour ? to Caradocian (Dean 1978, p 107)	Mafic volcanics, chert, Caradocian argillites	Possibly same sources as Dunnage Melange; could be stratigraphic equivalent of Exploits Group, emplaced as a block (Dean 1978, p 108)
Twillingate Moreton's Harbour Cambrian to ?	Mafic Sleepy Cove Formation, trondhjemite, volcanics, tuff turbidites, dike swarms	Separated from Dunnage Melange and other rocks by the Chanceport Fault. May be source or similar to source of Cambrian pillow basalts, tuff turbidites, trondhjemite in the Dunnage Melange

2.2.1 Geology of the Dunnage Melange

The Dunnage Melange is a chaotically disrupted unit consisting of an inhomogeneous sedimentary matrix, lacking consistent or continuous bedding, that supports a large number of clasts and blocks that are inhomogeneous in lithology and distribution. Clasts and blocks range in size from granular to dimensions of up to a kilometer across, and comprise less than 30% of the melange. Table 2.2 details the matrix types, and Table 2.3 the types of blocks and clasts, that were observed by the author. Localities are shown on the map, figure 2.3. The matrix is most commonly a dark, massive, non-fissile mudstone with coarse, anastamosing cleavage (type 1), or cobbly mudstone (type 4). The predominant block types are mafic volcanics (mostly tuffs, agglomerates, pillow breccia, and pillow basalts - types 1a, 1b, and 1d), greywackes (type 2a), and carbonates (type 3). Notably absent from the Dunnage Melange are ophiolitic lithologies: serpentinites or other ultramafics, layered gabbros, and sheeted dikes. Gabbros in the southwest portion of the melange are related to the New Bay Gabbro sills rather than to ophiolite (Hibbard 1976, p. 37). Chromite has not been observed in the melange matrix. Pillow lavas and minor chert occur in the Dunnage Melange, but these litholgies alone are not sufficient evidence for an ophiolitic source for the melange.

For further description of the Dunnage Melange see Hibbard and Williams (1979).

TABLE 2.2

Dunnage Melange Matrix Types

Type	Field locality (See map fig. 2.3)

1) Dark massive mudstone, non-fissile, with coarse, irregular, anastamosing cleavage, few or no clasts.
    a) with abundant pyrite nodules
    b) manganiferous
    c) with siderite porphyroblasts
    d) with graptolites
    e) with sparse large blocks but few or no small clasts
    f) micaceous
    g) silty
	a) 77,83,229,522,544,a67
	b) 154,173,a79
	c) 96
	d) 879.
	e) One of most abundant matrix types, particularly on New World I,
	f) 63
	g) 63,212,238,271,279

2) Streaky, variagated mudstone, usually a combination of any of black, grey, green, red.
    a) discontinuous, contorted bedding
    b) isoclinally folded and kink-banded
	Extremely common matrix type: 30,64,81,83,84, 85,86,98,250,278,323, 334,503,561,645,654, 692,730

3) Mudstone – greywacke combinations
    a) well-preserved sand - shale interbeds persisting for short distances (up to 10 m)
    b) discontinuous lenses, broken and boudinaged beds, of siltstone and sandstone in mudstone
	a) 209,284,344,374,415
	
	b) 80,179,234,235,403, 432,736,766,767,868

4) Cobbly mudstone
    a) swarms of rounded and angular cobbles in mudstone
    b) volcanic breccia with mudstone matrix, commonly gradational into volcanic blocks
    c) plutonic pebble conglomerate
    d) stretched pebble conglomerates or extreme boudinage of beds
	a) one of most abundant matrix types
	b) one of most abundant matrix types
	c) a47,a51,a53
	d) Peculiar to SW portion of the melange: Michael's Harbour, Embree.

5) Intermingled mudstone and non-brecciated mafic volcanic extrusives
    a) pillowed flows
    b) ropy lava
    c) tuffs and ash flows
	a) 450
	b) 65
	c) 310,311,312,314,316, 340,341,399,401,405, 449,450,451,455,500, 615,674,668,669,672, 673

TABLE 2.3

Dunnage Melange Block Types

Type	Field Localities (See map fig. 2.3)
1) Mafic volcanics	
a) pillow breccia	a) 16,78,89,90,330,361, 468,530,539,572,588, 713,721,786,830,852, 874,923,a34,a48,a62
b) tuffs and agglomerates	b) 205,242,276,302,618, 633,651,771,833,848, a31
i) coarse, unsorted, agglomerate, some with argillaceous matrix (See matrix type 4b)	b-i) 332,452,586,709,a86
ii) coarse, poorly-sorted volcanic breccia with glassy or fragmental volcanic matrix	b-ii) 149,263,485,770
iii) tuff with graded bedding, some intruded by parallel dikes, similar to Moreton's Harbour Group	b-iii) 112,290,291,621, 834,836
c) scoria	c) 216,696,846
d) well-developed pillow basalts	d) 28,53,167,169,272,277, 328,362,383,421,456, 465,481,516,520,610, 612,643,651,683,711, 872,875,a34,a49,a71
i) with carbonate mesostasis	d-i) 59,89,90,469,548, 659,685,737,786,a75
ii) variolitic	d-ii) 201,289,467,532,578, 642,675,685,851,896
e) massive basalts, commonly mineralized with pyrite, chalcopyrite	e) 34,62,82,99,a84
f) amygdaloidal volcanic glass blebs in calcite matrix	f) a119
g) mixture of massive and pillowed volcanics containing pods of hornblende diorite and trondhjemite, volcanic breccia, and carbonate breccia	g) See 5d

TABLE 2.3 (continued)

Type	Field Locality
2) Clastic sediments	
a) greywacke	a) 68,74,117,231,271,285, 410,557,847,a95
i) massive	a-1) See 2a
ii) bedded	a-ii) 238,924
iii) with shale fragments	a-iii) 281,772
iv) interbedded with shale	a-iv) 286
b) massive or bedded mudstone	b) 72,154
c) clast-supported platy pebble conglomerate	c) 351
3) Carbonates	206,207,213,239,265,293, 341,407,413,432,466,499, 572,629,672,693,695,a59, a67,a69,a87
a) highly recrystallized dolomitic carbonate breccia	a) 60,63,143,146,592,604
b) carbonate breccia with argillite matrix	b) 71
c) cone-in-cone structure	c) 237
d) bedded carbonate sandstone	d) a46
4) Chert - Blood-red jasper breccia in a matrix of magnetite and manganese oxides, with minor malachite. Adjacent to mineralized diabase dike (chalcopyrite, pyrrhotite, pentlandite). Both chert block and dike were mined approximately 50 years ago (E. C. Small, pers. com. 1982)	645
5) Siliceous and/or plutonic igneous rocks	
a) gabbro, diorite	a) SW Dunnage Melange
b) Coaker Porphyry	
i) small cobbles in conglomerate	b-1) 403,619
ii) breccia in argillite matrix	b-ii) 399,a93
c) trondhjemite	c) a47,a51,a53
d) hornblende diorite and trondhjemite associated with block type (1-g) above	d) 48,52,56,812,917

2.2.2 Contacts

The Dunnage Melange is bounded to the east by the Reach Fault, to the south by the Loon Bay batholith, and to the west by the Long Island batholith. To the west, the melange interdigitates with the sediments and volcanics of the Exploits Group, where a ghost stratigraphy within the melange reflects Exploits Group stratigraphy (Hibbard and Williams 1979). The base of the Dunnage Melange is not exposed. To the south on Chapel Island, the melange passes upwards into the Chapel Island Formation (described below, section 2.2.2.2). To the north, it is in contact with the Caradocian Dark Hole Formation.

The following is a description of the contacts between the Dunnage Melange and the Dark Hole Formation, the Holmes Point and Reach Faults, and a newly discovered unit on Chapel Island, based on observations by the author.

2.2.2.1 Dunnage Melange - Dark Hole Shale

The Dark Hole Formation was named and its contacts with the Dunnage Melange described by Horne (1969). The contacts have been variously interpreted as conformable (Horne 1969, McKerrow and Cocks 1978, Karlstrom et al. 1983), unconformable and faulted (Kay 1976), and locally conformable (Hibbard and Williams 1979). The contacts are exposed, from west to east, on southern Farmer's Island, Dark Hole, and intermittently along the southern coast of eastern New World Island and the northern coast of Coaker Island. Contact relationships

are best exposed on a shoreline traverse from Dark Hole southward.

The Dark Hole shale is a vertically-dipping, N-facing distal turbidite that is characterized by isoclinal folds, tightly crenulated cleavage, phyllitic fabric, and a silvery sheen indicative of the development of secondary muscovite. These features are consistent from localities as widely separated as Farmer's Island and Coaker Island. On Farmer's Island, Dark Hole shale locally contains abundant limonite cubes pseudomorphic after pyrite. On New World Island, carbonate concretions are common.

The matrix of the Dunnage Melange near its contacts with the Dark Hole Shale is typically of type 1e (see Table 2.2), contains anastomosing veinlets of siliceous material, and is black.

The contact between the Dunnage Melange and the Dark Hole shale is laterally and stratigraphically gradational. Passing from Dark Hole shale through the transition to Dunnage Melange, the following changes occur:

1) bedding becomes progressively less distinct,

2) veining becomes more abundant,

3) the colour darkens — the silvery sheen of the Dark Hole shale fades out and

4) blocks occur locally.

Deformation (shearing, folding, crenulation) does not increase noticeably from the Dark Hole shale to the melange, possibly because little structure is discernable in the relatively massive, non-fissile mudstone characteristic of the melange matrix at the contacts.

One particularly puzzling characteristic of the contact is the difference between igneous rocks on either side of it. The Dark Hole shale is intruded by tiny stocks (usually about 3 to 8 m across) of intermediate to rhyolitic composition (the Dildo Porphyry - see section 2.4). These cut across bedding and are found right up to the contact. South of Dark Hole, they occur in tiny patches of Dark Hole shale that are surrounded on three sides by Dunnage Melange, and perhaps totally engulfed by the melange. However, intrusions of Dildo Porphyry are not found in the Dunnage Melange.

The Dunnage Melange contains abundant intrusions of Coaker Porphyry, some stocks of which occur near (but not on) the contact on Coaker Island. Coaker Porphyry is not found outside the Dunnage Melange.

The Dildo and Coaker Porphyries (see Table 2.4) are distinguished in part by different degrees of alteration. The Dildo Porphyry suffered a more pervasive alteration than did the Coaker Porphyry, and its broken and strained quartz phenocrysts contrast with the unstrained phenocrysts of the Coaker Porphyry. These differences, coupled with the extensive development of secondary muscovite and a phyllitic fabric in the Dark Hole shale, indicate that the Dunnage Melange and the Dark Hole shale were exposed to contrasting

environments of deformation and hydrothermal activity. Because the Dark Hole shale and the Dunnage Melange are lithologically similar, as are the Dildo and Coaker Porphyries, differences in the responses of contrasting lithologic types to similar environmental conditions is not a likely explanation of the observed differences between these units.

Although there is no obvious fault separating the Dunnage Melange and the Dark Hole shale, and lithologies are similar (see discussions by Hibbard and Williams 1979, Karlstrom et al. 1983), the factors discussed above indicate that displacement between them has taken place. Particularly critical is the lack of younger Dildo Porphyry in the older Dunnage Melange, and the occurrence of the Dildo Porphyry right up to, but not across, contacts.

Discussion concerning this possible displacement and interpretations regarding its significance are reserved for Chapter 5.

2.2.2.2 Dunnage Melange — Chapel Formation (new informal name — definition in preparation)

Located between the Dunnage Melange and the Loon Bay Batholith on Holmes Point and on southern Chapel Island is a unit of bedded, vertically-dipping, south-facing siltstones, sandstones, and conglomerates, named here the Chapel Formation. It is best exposed in its widest portion in central Chapel Island, where access is by logging roads.

The Chapel Formation is folded into open, low-amplitude folds. It is characterized by graded bedding, small (up to 25 cm) soft-sediment faults that locally displace bedding, and small-scale slumps that are most prominent in conglomeratic horizons. It passes down-sequence into cobbly Dunnage Melange. It is thermally altered by the intrusion of the Loon Bay Batholith. The stratigraphic thickness of the Chapel Formation is impossible to assess because the unit is truncated by the batholith, although its maximum exposed thickness is approximately 2.5 km.

No fossils have been discovered in the Chapel Formation. It is possibly correlative with the Dark Hole Formation although it is coarser-grained and does not possess the phyllitic fabric characteristic of the Dark Hole shale. The contact between the melange and the Chapel Formation appears to be conformable.

The contacts between the Dunnage Melange and a south-facing younger unit to the south and a north-facing younger unit to the north indicate that the melange forms the core of an anticline.

2.2.2.3 The Reach and Holmes Point Faults

The Reach and Holmes Point Faults (Kay 1976) separate the Dunnage Melange from Silurian strata to the east, and from the "Boyd's Cove Complex" to the southeast. The Boyd's Cove Complex of Kay (1976, map notes) in part corresponds spatially to the Chapel Formation; however, Kay's description does not correspond well to the appearance of the Chapel Formation: "Boyd's Cove Complex: greywacke, quartzite,

and rhyolite intruded by basalt; 30 m band of plutonic pebble conglomerate...; complex mylonitized toward Reach Fault on southeast." The Boyd's Cove Complex is apparently a combination of Chapel Formation and cataclastized Dunnage Melange and Coaker Porphyry. Use of the term "Boyd's Cove Complex" should be discontinued.

The Reach Fault is a broad fault zone, the effects of which can be observed across a 2 km zone. The community of Boyd's Cove South sits on highly sheared Dunnage Melange and Coaker Porphyry which give way to the north to sheared pillow basalts and bedded sediments. The transition from Dunnage lithologies to the volcanics is taken to be the locus of the displacement.

The Holmes Point Fault appears to be a minor splay off the Reach Fault. It is manifest as a shear zone in Boyd's Harbour, but is not obvious at Holmes Point, unless it occupies the site of a cobble beach that separates the Dunnage Melange from the Chapel Formation. It was not observed on Chapel Island.

2.2.3 Possible sources and stratigraphic equivalents

The Dunnage Melange is one of several distinct pre-Caradocian assemblages in the eastern Notre Dame Bay area. These assemblages, described in Table 2.1, are the Sleepy Cove Formation/ Twillingate trondhjemite/ Moreton's Harbour sequence, the New Bay Formation and the Lawrence Head Volcanics of the Exploits Group, and the Loon Harbour Volcanics. An overview of the geology and stratigraphy of

these units can be found in Dean (1978).

Of these assemblages, only the Exploits Group is in unfaulted contact with the Dunnage Melange. Hibbard and Williams (1979) regard the melange as a distal, disrupted equivalent of the Exploits Group.

The Summerford Group (Horne 1970) is a structurally and lithologically complex unit exposed on southwest New World Island and on Farmer's Island. It is faulted against the Dunnage Melange on New World Island. The Summerford Group is characterized by localized debris flows, extensive slump folding, and large volcanic blocks (tens of meters across) in a volumetrically minor matrix. Horne (1970; personal communication 1982) has suggested that Summerford Group and Dunnage Melange lithologies may have a common source, and that fragmentation and mixing of the two units were a result of the same episode(s) of local instability. Volcanics of the Summerford Group and the Dunnage Melange are chemically identical (J. Wasowski, pers. com. 1983).

The Dunnage Melange is separated from the Loon Harbour Volcanics to the south by the Loon Bay Batholith. Kay (1975) had interpreted the Loon Harbour volcanics to be Cambro-Ordovician oceanic crust forming the base of the Dunnage Melange. However, this unit appears to be identical to the pre-Caradocian island arc volcanics to the west, and is overlain by Caradocian black shales (Dean 1978, p. 107).

The oldest rocks in the area are the Cambrian plutonic and volcanic rocks of the Twillingate trondhjemite and the Sleepy Cove Formation, which form the basement to the Ordovician Moreton's Harbour Group, an assemblage of volcanic and volcanogenic rocks. These rocks are separated from the younger sequences to the south by a major fault, the Chanceport Fault (see Dean 1978, p. 77). This assemblage or an equivalent one was a likely source of some of the Dunnage Melange clasts, including trondhjemite cobbles in the Boyd's Cove plutonic pebble conglomerate, mid-Cambrian pillow basalts (Kay and Eldredge 1968), and graded tuff-turbidites intruded by parallel dikes resembling the distinctive Moreton's Harbour Group.

2.2.4 Younger units

The Dunnage Melange and other pre-Caradocian assemblages of eastern Notre Dame Bay are overlain by a fairly uniform unit of Caradocian black shales, distal turbidites and minor chert, of which the Dark Hole Formation is an example. Locally intermixed with the lowermost horizon of the Dark Hole Formation is a conglomerate (the Cheneyville Conglomerate) that includes clasts of Coaker Porphyry (Kay 1976). The Dark Hole Formation passes up-sequence into the proximal turbidites of the Sansom Greywacke (Horne 1969), a post-Caradocian flysch sequence. Post-Caradocian through Silurian units on New World Island have been structurally repeated, and include horizons of Silurian melange. The stratigraphy and structure of New World Island are currently undergoing extensive study by several research teams and have suffered numerous reinterpretations and name-changes.

2.3 Igneous setting

The majority of intrusive rocks in central Newfoundland are Silurian or younger and are associated with the Acadian orogeny. Of the older (pre-Caradocian) intrusions, many are related to ophiolites or are parts of the basement to the island arc. These rocks are granodiorites, trondhjemites, tonalites, and quartz diorites and include the Twillingate trondhjemite, the South Lake Igneous Complex, and silicic rocks associated with the Annieopsquatch Ophiolite of Dunning (1980). The ophiolitic Lush's Bight Group is intruded by the Colchester and Wellman's Cove plutons. The latter contains ultramafic xenoliths (Dean 1978, p. 111) as does the Coaker Porphyry. The pre-Caradocian island arc-related sequences are intruded by small granitoid stocks, the largest of which is the Burlington Granodiorite, which appear to be sub-volcanic equivalents of associated felsic extrusions (Dean 1978, p. 109). The most abundant rock type intrusive into these assemblages, however, are mafic sills, such as the New Bay Gabbro. Of the rocks intruding the Dunnage Melange and vicinity, the New Bay Gabbro, the Puncheon Diorite, the Coaker Porphyry, and the Grapnel Gabbro belong to the group of pre-Caradocian intrusions of Notre Dame Bay. Slightly younger (Caradocian to Ashgillian (?)) are the stocks comprising the Dildo Porphyry. (See Chapter 5.)

The granitic rocks of central Newfoundland, most of which are Silurian and Devonian, have been divided into four groups (Strong 1981):

1) the calc-alkaline hornblende-bearing suites, characteristically intrusive into shallow crustal levels. Post-Ordovian granites of this type are abundant in the Dunnage Zone. Older suites occur in the Avalon Zone.

2) biotite-bearing granites and granodiorites, most commonly intrusive into amphibolite facies rocks of the Gander and eastern Humber Zones, less commonly into lower-grade rocks of the Dunnage and Avalon Zones. Ages range from 440 to 312 Ma.

3) muscovite +/- biotite granites are characteristic of the Gander Zone, are Silurian in age, and appear to be a result of in situ partial melting.

4) alkaline-peralkaline granites are Silurian to Devonian in age and intrude the margins of the orogen.

The distribution of these granite types reflects the tectonostratigraphic zonation of the orogen, and is interpreted to be a reflection of crustal differences among the zones (Strong and Dickson 1978, Strong 1981). The Dunnage Zone is characterized largely by the occurrence of the hornblende-bearing granites of which the Loon Bay and Long Island granodiorites are examples. Because the Loon Bay and Long Island Granodiorites are cogenetic (Strong and Dickson 1978), and because a granite in western Notre Dame Bay is also called the Long Island Granite, the names Long Island Batholith, Long Island Granite, and Long Island Granodiorite should be discontinued and both bodies of granodiorite should be refered to as belonging to the Loon Bay granodiorite suite. Related to the Loon Bay granodiorites is a

suite of small dikes and stocks that intrude the Dunnage Melange and surrounding units.

Diabase dikes occur in sub-parallel swarms throughout the Dunnage Zone, and have been observed in southern Newfoundland (L. Chorlton, pers. com. 1982), eastern White Bay (H. Williams, pers. com., 1983), in the Buchans area (P. Stewart, pers. com. 1983), within the South Lake Igneous Complex (Lorenz and Fountain 1982), and are abundant in the Dunnage Melange. These dikes are possibly part of a suite of alkalic diabase dikes that are abundant in the Gander Zone (Jayasinghe 1978), that have an $Ar(40)/Ar(39)$ age of 375 +/- 10 Ma (Reynolds and Murthy in press).

Mafic alkalic dikes and lamprophyric dikes of Jurassic age, related to the opening of the Atlantic Ocean, occur throughout Notre Dame Bay (Strong and Harris 1974). A small number of these dikes cut the Dunnage Melange, and a nephelinite sill (concordant with cleavage) in Stanhope is probably part of this suite.

2.4 Distribution of igneous rocks in the field area

Table 2.4 presents a summary of the igneous rocks under discussion in this dissertation.

Sills of New Bay Gabbro intrude the New Bay Formation and the southwestern portion of the Dunnage Melange (Hibbard 1976 p. 37.). The Puncheon Diorite occurs as small stocks on northwest Chapel Island (Puncheon Head) and Pomeroy's Island. The Grapnel Gabbro occurs as small stocks on Pyke Island and at two locations on central Chapel

TABLE 2.4

Igneous Intrusive Rocks in the Field Area

INTRUSION	ROCK TYPE AND MODE OF	LOCATION	APPROXIMATE AGE
New Bay Gabbro	gabbro sills	New Bay Formation, SW Dunnage Melange	Early Ordovician
Puncheon Diorite	diorite-gabbro stocks	Puncheon Head on Chapel Island, Pomeroy's Island	Early Ordovician
Grapnel Gabbro	phlogopite gabbro stocks	Pyke Island, Chapel Island	in range Arenig to Caradoc
Coaker Porphyry	dacite to rhyolite stocks, dikes	NE Dunnage Melange	LLandeilian
Dildo Porphyry	andesite to rhyolite stocks, dikes	Dark Hole Fm. Sansom Greywacke, Cobbs Arm Fault Zone, Summerford Gr., Campbellton shales	Caradocian to early Silurian
Loon Bay suite	granodiorite to tonalite batholiths, associated stocks, dikes	Bay of Exploits	early Silurian
Late dikes	diabase dikes	throughout Dunnage and Gander Zones	Devonian
Alkalic suite	lamprophyric and nephelinite dikes	Notre Dame Bay	Jurassic

Island.   These three rock types   are the only pre-Caradocian mafic rocks to intrude the Dunnage Melange, and comprise a volumetrically minor portion of the intrusive rocks in the melange.

Coaker Porphyry intrudes the northeast portion of the Dunnage Melange, where it comprises approximately a third of the total outcrop area.   Individual intrusions occur most commonly as irregular stocks that are weakly elongate in a northeast-southwest direction. Coaker Porphyry is not found outside this area.   It is distinguished from other silicic intrusions in the eastern Notre Dame Bay area by the large size and high concentration of its component intrusions, its intrusive characteristics (Chapter 4), the occurrence of ultramafic and mafic xenoliths, and its distinctive geochemistry (Chapter 6). With the exception of the Loon Bay granodiorites, the Coaker Porphyry is the volumetrically most significant intrusive rock type in the field area.

The Dildo Porphyry occurs as small stocks and dikes in the Dark Hole Formation, the lowermost horizons of the Sansom Greywacke, the Cobb's Arm Fault Zone in Fairbanks, the Summerford Group, and the Campbellton Shales south of the Dunnage Melange. It is not found in the Dunnage Melange.

The Loon Bay granodiorite suite is composed of two batholiths that intrude the Dunnage Melange and younger rocks of the post-Caradocian flysch. Geomagnetic data indicate the presence of a third batholith of this kind underneath Farmer's Island (Geological Survey of Canada 1964a,b). Rocks on Farmer's Island are baked to

greenschist grade, and Loon Bay dikes in the area are common. Dikes associated with the Loon Bay granodiorite intrude the Dunnage Melange, the Summerford Group, and the Sansom Greywacke.

Late dikes of the Devonian diabase suite are abundant in the Dunnage Melange, where they occur in swarms parallel to Dildo and Reach Runs.

2.5 Summary

The Dunnage Melange and its intrusions are interpreted as part of an arc-flanking basinal assemblage in a stratigraphically and structurally complex part of the Dunnage Zone. The Dunnage Melange probably correlates stratigraphically with some of the intact and disrupted pre-Caradocian assemblages in its immediate vicinity; others are possible sources of lithologies found within the melange. Complicated contact relationships exist between the Dunnage Melange and surrounding units. Intrusions within the Dunnage Melange and neighboring units belong primarily to the volumetrically minor group of pre-Caradocian intrusions intruding island arc and ophiolitic units in Notre Dame Bay. Younger igneous rocks in the area belong to the family of Acadian calc-alkaline granites of central Newfoundland, to a widespread suite of Devonian diabase dikes, and to the suite of Jurassic lamprophyres.

Previous and Current Work

The emphasis of this chapter will be on previous and current work pertaining to the igneous petrology of the Dunnage Melange. For a more general survey of work done in the Dunnage Melange, the reader is referred to Hibbard (1976) and Hibbard and Williams (1979).

The first detailed mapping in the area was done by Heyl (1936). He gave detailed descriptions of the Loon Bay and Long Island Batholiths, and of the numerous varieties of associated dikes, as well as a description of the gabbro (the New Bay Gabbro) that intrudes the southwest portion of the melange. He mentioned and briefly described the oligoclase porphyries (the Coaker Porphyry) that are older than and intruded by the batholiths. Although he did not recognize the chaotic nature of the melange terrane, he did remark that in places, the rock "breaks into irregular chunks".

Patrick (1956) mapped the distribution in the Comfort Cove area of intrusions which he interpreted to be Devonian. These included quartz diorite porphyry, quartz and/or feldspar porphyry, and a mottled variation of the quartz diorite porphyry (all of which are probably different forms of the Coaker Porphyry), in addition to the granodiorite of the Loon Bay Batholith. He interpreted the Loon Bay granodiorite to be a more felsic equivalent of the porphyries. (Actually, the Loon Bay granodiorites are less felsic than the Coaker

Porphyry.) Patrick also noted the deformed and heterogeneous nature of the melange mudstones, and referred to the melange as a "slump breccia".

Williams (1963) published a map of the Twillingate map area, on which he depicted the Coaker Porphyry as Devonian porphyritic granodiorites. In 1964, he reported K/Ar age dates of 440 m.y. and 450 m.y. for the Long Island and Loon Bay Batholiths, respectively, and noted that these Ordovician ages contradict the field observation that these batholiths intrude younger (as young as Silurian) rocks.

Helwig, in 1967, established the stratigraphy of the Exploits Group, and described the gabbros of the New Bay Formation, including gabbros in what is now considered to be part of the Dunnage Melange (Horne 1968, Hibbard 1976, p. 37).

Kay and Eldredge (1968) defined the Dunnage Formation as a sedimentary (mainly boulder-bearing mudstone) and volcanic unit. They noted the lack of regular bedding and the presence of "gravity slide structures". They reported the occurrence of Middle Cambrian trilobites (Kootenia and Bailiella) in carbonate associated with a volcanic block on Dunnage Island, the type locality of the Dunnage Formation.

Horne (1968) and later Horne and Helwig (1969) and Horne (1969) gave the first detailed descriptions of the Dunnage terrane, noted its chaotic character, and compared it with the argille scagliose of the Appenines. They suggested that no nappes are associated with the Dunnage Melange, although Karlstrom et al. (1983) are currently

advocating that the Dunnage Melange and other local and regional structures are the result of nappe emplacement. Horne viewed the Dunnage Formation as being essentially conformable with surrounding units, and interpreted the chaotic structure to be a result of slumping from steep depositional slopes, triggered by seismic or volcanic activity in a eugeosynclinal environment.

Dewey (1969) proposed that the Dunnage Melange is a fore-arc trench-fill deposit formed in a Paleozoic northwest-dipping subduction zone.

Horne (1970) discussed soft-sediment deformation (slump folds) in the Sansom Greywacke and proposed that the melange was produced by sliding and slumping of sediments as a result of dip-slip faulting caused by subduction.

Kay, in a series of publications (1970, 1972, 1973, 1975, 1976), portrayed the Dunnage Melange as a fault-bounded tectonic unit deformed in the trench of a subduction zone. He also named and described the igneous intrusions of the northeast Dunnage Melange: the Coaker Porphyry after the type locality on Coaker Island, the Causeway diorite or Causeway xenolith-bearing phase of the Coaker Porphyry after its type locality on the Curtis Causeway, and the Puncheon Diorite or Syenite after its type locality on Puncheon Head, Chapel Island. He published Rb/Sr ages (454 or 480 Ma depending upon the decay constant used - neither decay constants nor errors were reported) and K/Ar (428 +/- 13 and 435 +/- 13 Ma) ages for the Causeway xenolith phase, and K/Ar ages for the Loon Bay granodiorite

(372 +/- 10 and 365 +/- 10 Ma). He identified boulders within the Cheneyville Conglomerate as being Coaker Porphyry, and proposed an erosional unconformity between the melange and the Cheneyville.

Floran (1971), in an unpublished M.Sc. thesis, described the petrography and physical characteristics of the Loon Bay granodiorite.

Williams and Hibbard (1976), Hibbard (1976) and Hibbard and Williams (1979) reported their results of a detailed study of the Dunnage Melange. They found the melange to be essentially conformable with surrounding units and suggested a back-arc basinal olistostromal origin for the melange. Hibbard (1976, pp. 37-39) briefly discussed the New Bay Gabbros and mentioned a newly-discovered intrusion, the Grapnel Gabbro. He discussed the thermal effects of the intrusion of the Loon Bay granodiorites. Williams and Hibbard (1976) suggested that the Coaker Porphyry intruded unconsolidated sediments of the melange matrix, and that intrusion was penecontemporaneous with melange formation.

Jacobi and Schweikert (1976) described north-facing, vertical cumulate cross-bedding in the Puncheon Diorite. (The cross-bedding has proven to be schlieren structures.) They suggested that the presence of the Coaker Porphyry ruled out a subduction zone origin for the Dunnage Melange. They proposed a back-arc marginal basin setting for the melange and surrounding rocks, with the melange to the west of the island arc.

McKerrow and Cocks (1977, 1978) interpreted the Reach Fault as a major suture zone, with the Dunnage Melange as a trench-fill deposit. They revised the stratigraphic nomenclature of New World Island and depicted it as an uninterrupted stratigraphic sequence composed essentially of olistostromes and olistoliths.

Pajari et al. (1979) suggested that the Dunnage and Carmanville Melanges are correlative and related to post-obduction slumping associated with nappe transport.

Current work in the area is concerned mainly with structural and stratigraphic details of the units to the north of the Dunnage Melange. Karlstrom et al. (1983) have extended their theories concerning the structural geology of easternmost Notre Dame Bay to include the Dunnage Melange. They interpret the Dunnage Melange to be an Acadian tectonic melange continuous with the melanges of New World Island and Carmanville, and the Coaker Porphyry to be a Devonian intrusion identical to other silicic intrusions in the area (for example, on Change Islands).

Robert Jacobi and his students are currently studying various stratigraphic and tectonic problems in the Dunnage Melange. Wasowski and Jacobi (1983) reported that the geochemistry of the mafic volcanic blocks in the melange is indicative of an oceanic island origin for these basalts. Jacobi (pers. com. 1982, 1983) proposes that the Dunnage Melange is an ophiolitic melange despite the lack of ophiolite blocks and maintains that it originated as an olistostrome in the trench of a Silurian west-dipping subduction zone.

Greg Horne (pers. com. 1982, 1983) is currently studying the structural geology of the Summerford Group. He advocates that all rash speculation concerning tectonic models for the eastern Notre Dame Bay area, and for Newfoundland based on the geology of this area, should be suspended until we have more facts.

Relationships Between the Intrusions and Their Hosts

The relationships between the intrusions and their host rocks were examined to determine (1) condition of the host material at the time of intrusion (consolidated versus unconsolidated), (2) depths of emplacement, and (3) timing of intrusion. Factors such as condition of host material and depth of emplacement place important constraints on palinspastic restoration and structural modelling. Conclusions based on material presented in this chapter will be discussed in Chapter 5.

4.1 New Bay Gabbro

The relationship between the New Bay Gabbro and the New Bay Formation and the Dunnage Melange has been discussed in detail by Hibbard (1976, pp 37-45). The gabbro occurs as sills in both units, supporting Hibbard's conclusion that the Dunnage Melange and the New Bay Formation are correlative. In addition to the sills, blocks of New Bay Gabbro are found in the melange, indicating that melange formation and intrusion were penecontemporaneous. Sills and blocks of New Bay Gabbro are restricted to the southwest portion of the melange. The intrusions have distinct chilled margins and have aureoles of hornfels in the host argillites (Heyl 1936).

4.2 Puncheon Diorite

The Puncheon Diorite (Kay 1972) occurs as small stocks on northwest Chapel Island and Pomeroy's Island. The stocks display gradational textural and compositional variations, becoming progressively finer-grained and more mafic from the center to the peripheries. Near its peripheries, the Chapel Island stock displays well-developed schlieren structures that resemble sedimentary cross-bedding, and were interpreted as such by Kay (1976) and Jacobi and Schweikert (1976). Also in the peripheral areas are lenses and enclaves of more mafic cognate material. Schlieren have been interpreted by Didier (1973) to be cognate inclusions broken up and attenuated by magmatic processes. The Puncheon Diorite bakes the host mudstone to a purple, biotite-rich hornfels in an aureole approximately 5 meters wide.

The Puncheon Diorite is intruded by Coaker Porphyry on both Puncheon Head and Pomeroy's Island. On Puncheon Head, the Coaker Porphyry intrusion is a dike with straight contacts, cutting medium-grained Puncheon Diorite, indicating that the latter is older than the Coaker Porphyry.

4.3 Grapnel Gabbro

The Grapnel Gabbro (Hibbard 1976, p 39) occurs as small stocks on Pyke Island and at two locations on central Chapel Island. Margins are chilled and completely altered to an assemblage of chlorite, carbonate, biotite, and serpentine, whereas the interior portions are

coarser-grained and relatively fresh, indicating that the magma absorbed fluids from the host sediments. Grapnel Gabbro occurs together with Coaker Porphyry on Pyke Island. As noted by Hibbard and Williams(1979), the contact between them is irregular and complex, and neither rock type appears to be chilled against the other, suggesting that the two were intruded simultaneously. Examination of thin sections from the contact reveals that the Coaker Porphyry has been baked, resulting in the formation of secondary biotite and the elimination of volatiles from the rock, suggesting that the Grapnel Gabbro is younger than the Coaker Porphyry. However, the mafic magma was probably hotter than the silicic magma, and could have produced the observed thermal effects even under the condition of penecontemporaneous intrusion.

4.4 Coaker Porphyry

The Coaker Porphyry occurs in the following forms: (1) stocks, (2) dikes, (3) complexly interlayered with mudstone and folded, (4) lobes, in isolation or as part of above types, (5) breccia, and (6) cobbles in the Dunnage Melange and the Cheneyville Conglomerate.

4.4.1 Stocks

Stocks are the most abundant intrusive form and range in size from a few meters to about 3000 m across. They are irregular but rounded in shape and commonly have undulose, lobate, or pillowed contacts (fig. 4.1). Their surfaces are generally corrugated with the wavelengths of the corrugations greater than the amplitude (fig.

Figure 4.1 Lobate contact on a Coaker Porphyry stock.
Mudstone has eroded away from the contact,
exposing the lobate surface of the stock. Mudstone
is preserved in corrugations on the erosional
surface. Birchy Island.

Figure 4.2 Large-scale corrugations on the contact surface of
a Coaker Porphyry stock. More commonly, the
corrugations have an amplitude of less than 1 cm.
Chapel Island, west of Emily's Pond.
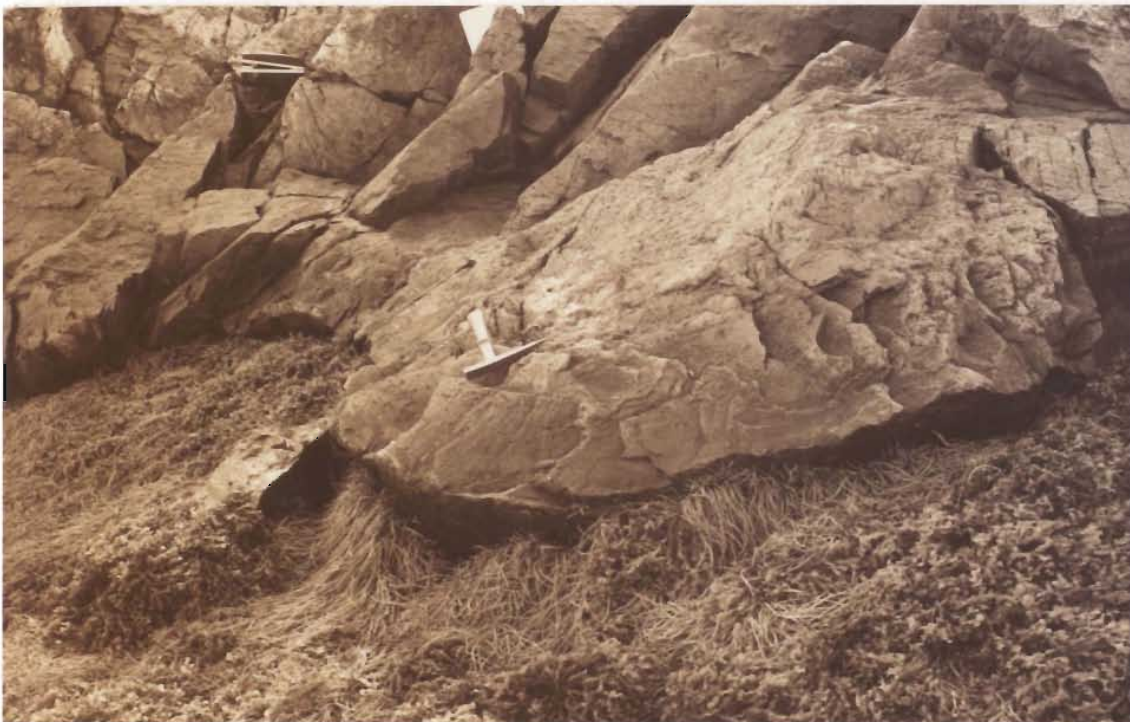
4.2). Wavelength is usually a centimeter or less but locally attains 6 or 7 centimeters. A few stocks display cracked surfaces (fig. 4.3). The stocks rarely have chilled margins and vescicles are uncommon. Around the margins of stocks, trachytic-textured rhyodacite shows pronounced flow-banding and alignment of mica flakes and plagioclase laths parallel to contacts.

Contact aureoles around stocks vary from non-existent to (most commonly) a few centimeters to a meter to the extensive purple hornfels associated with the Coaker Porphyry on Dog Island. On Dog Island, a xenolith-rich phase of Coaker Porphyry intrudes a body of xenolith-poor Coaker Porphyry. The hornfels on Dog Island preserved earlier structures (folded and contorted sediments). Commonly, baked contacts can be found only in mudstones surrounded on three sides by Coaker Porphyry. Lenses of hornfels are commonly found within the matrix of the melange near, but not in contact with, stocks of Coaker Porphyry, suggesting that relative movement of materials within the melange stripped the hornfels away from the contacts after intrusion of the stock.

4.4.2 Lobes

Bulbous or lobate protuberances of trachytic rhyodacite occur on the sides of stocks, the ends of dikes, and the hinges of folds of rhyodacite interlayered with mudstone (fig. 4.1, 4.4, 4.5). They range in size from about 3 cm to 4 m in diameter. Mostly they occur singly but in places as clusters with intervening mudstone. Commonly a flow lineation defined by plagioclase laths and colour banding

Figure 4.3 "Breadcrust" cracks on the contact surface of a
Coaker Porphyry stock. Birchy Island.

Figure 4.4 A lobate, pillow-like fold hinge consisting of Coaker Porphyry containing discontinuous stringers of mudstone (dark). Sample from South Dildo Island.

Figure 4.5 Rolled, lobate fold hinges consisting of Coaker Porphyry (light) in mudstone (dark). Note two detached lobes (under keys and immediately to the left) and glove-shaped structure (lower center of photograph). Inspector Island.

parallels the contacts.

4.4.3 Dikes

Dikes are irregular in thickness and shape; in shales, they split, then abruptly pinch out. Some terminate in pillow form. Dikes display straight, smooth, parallel contacts where they intrude brittle materials such as volcanic blocks and hornfels. They are composed of trachytic-textured dacite, and some are rich in xenoliths. In xenolith-rich dikes, the xenoliths are clumped in the center of the dike by flow-segregation. Unlike the stocks, Coaker dikes commonly have chilled margins.

4.4.4 Interlayered Coaker Porphyry and mudstone

Intimately interlayered and folded Coaker Porphyry and mudstone is the scarcest and most complex form in which the Coaker Porphyry occurs.

On Inspector Island, in an area approximately 500 m long and 150 m wide, an elongate, flow-banded stock of rhyolite is bordered by rhyolite dikelets that split into sheets interlayered with the host mudstone (fig. 4.6, 4.7). The interlayered rhyolite and mudstone are complexly folded together (fig. 4.8, 4.9). The limbs and hinges commonly consist of several layers of rhyolite and sediment that bear no systematic relationship to other fold structures occurring adjacently. Individual layers display complex folding within large folds, pinch and swell structures, boudinage, bifurcation, and

Figure 4.6 Coaker Porphyry dikelet (light) in mudstone (dark) bifurcates or splits (lower part of photograph) and breaks up into interlayered mudstone and porphyry. Note also that this dikelet is a three-limbed fold (upper part of photograph). Inspector Island.

Figure 4.7 Bifurcation of a Coaker Porphyry dikelet. Inspector Island.

Figure 4.8 Interlayered and folded Coaker Porphyry (light) and mudstone (dark). Core of upper fold is flow-banded Coaker Porphyry containing no mudstone. It is enclosed by a layer of mudstone and a thin, irregularly folded dikelet of Coaker Porphyry. The lower fold consists of a Coaker Porphyry dikelet with an angular hinge and a core of mudstone and discontinuous Coaker Porphyry layers. Inspector Island.

Figure 4.9 Interlayered and isoclinally folded Coaker Porphyry and mudstone. Inspector Island.

brecciation (fig. 4.10, 4.11, 4.12, 4.13). Rhyolite fold hinges commonly thicken into lobate structures that locally contain subparallel, discontinuous layers of mudstone (fig. 4.4). Other hinges give rise to third limbs that extend parallel to the axial surface or are folded around with the original limbs (fig. 4.14, 4.15a). The surfaces of the rhyolite dikelets are commonly convoluted into ropy structures resembling pahoehoe (fig. 4.16, 4.17). Other surface textures include knobbly extensions, and delicate wrinkles. The layers show a variation from being dominantly rhyolite, containing narrow (1 mm) stringers of sediment, to being dominantly sediment with narrow (2-3 cm) stringers of rhyolite.

On Birchy Island, similar complex relationships occur in an area about 200 m long and 15 to 20 m wide. Although the overall structure is of a recumbently folded isoclinal antiform (fig. 4.18), the internal layering is chaotic. The inner part of the antiform consists of interlayered mudstone and trachytic rhyodacite, and the outer part of massive trachytic rhyodacite (fig. 4.19). The interlayering occurs on a fine scale, with some layers only millimeters thick, giving the rock the appearance of a laminated shale (fig. 4.20). Rhyodacite layers range in thickness up to a meter across. Individual layers display the same kinds of disruption as do those of Inspector Island. However, the mixing of the two lithologies on Birchy Island appears to be more thorough locally, with stringers of Coaker Porphyry fading out into wisps and streaks within the mudstone. The resulting rock resembles paints of two different colours stirred together (fig. 4.21). Spherical globules of mudstone and small cobbles from the

Figure 4.10 Interlayered and folded Coaker Porphyry and mudstone. Complex internal structure within a large-scale isoclinal fold, Birchy Island. (See figures 4.18 and 4.20.)

Figure 4.11 Break-up of Coaker Porphyry layers in mudstone along the limb of a fold. Note also bifurcation of the thick dikelet, upper right. Inspector Island.

Figure 4.12 Tightly folded discontinuous layers of Coaker
Porphyry in dark mudstone. Birchy Island.

Figure 4.13 Brecciation of Coaker Porphyry layers.
Continuous Coaker Porphyry layers (left) break up
to form breccia with a mudstone matrix (right).
Birchy Island.

Figure 4.14 Three-limbed fold of Coaker Porphyry. (Above knife; see arrow). Inspector Island. Also see figure 4.6.

Figure 4.15 Structure and proposed origin of three-limbed folds.

A. A three-limbed fold of Coaker Porphyry (light) in mudstone (dark).

B. 1) Magma dikelet penetrates mud, moving in a downslope direction.

2) Mud and magma are rolled together during slumping.

3) Liquid magma breaks out of the hinge zone under the influence of gravity to produce a third limb.

4) The third limb is folded along with the first two as slumping continues.

0.5 m.
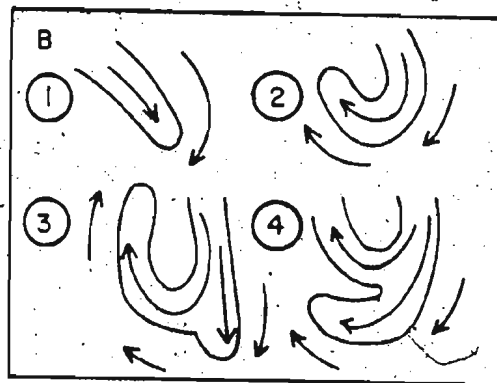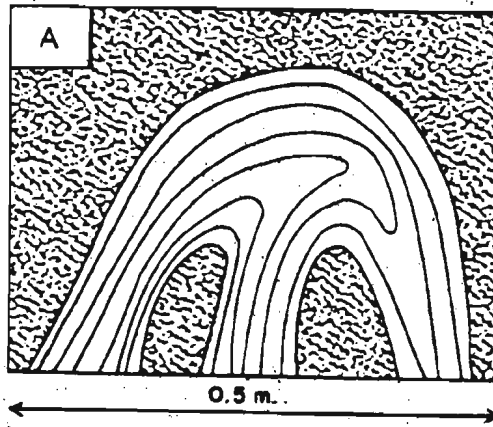
Figure 4.16 Deeply corrugated, ropy surface of a Coaker Porphyry dikelet. Inspector Island.

Figure 4.17 Twisted, ropy, pahoehoe-like surface of a Coaker Porphyry dikelet. Sample from Inspector Island.
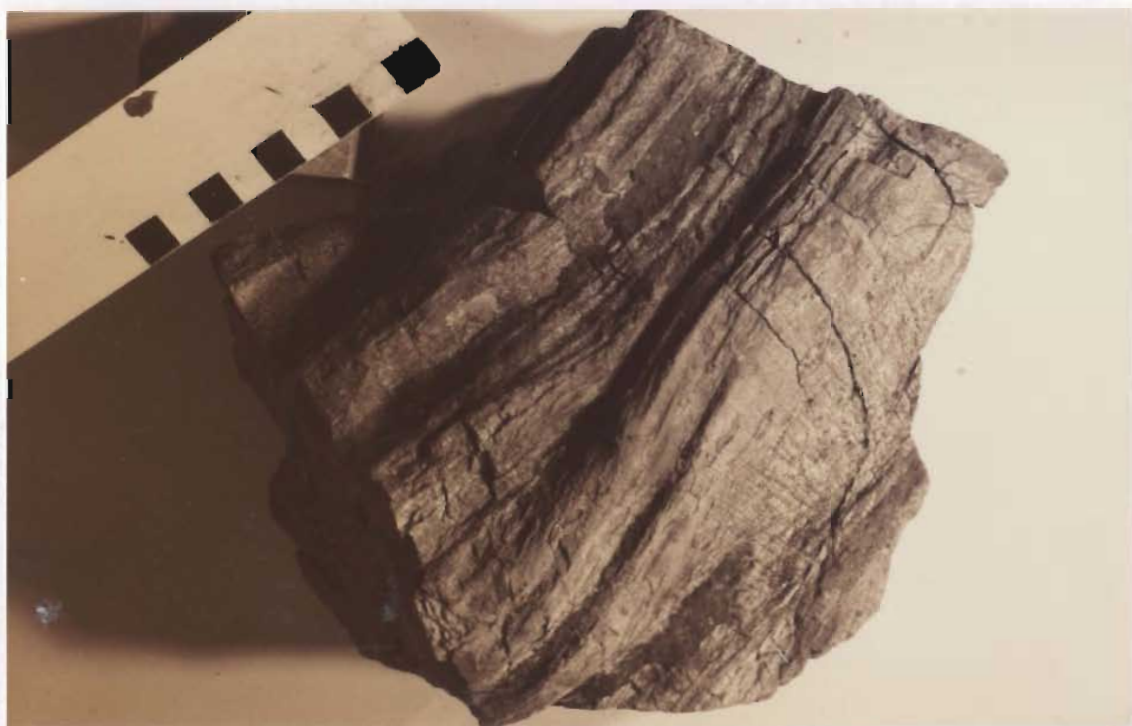
Figure 4.18 Structure and proposed origin of folded, interlayered Coaker Porphyry and mudstone on Birchy Island.

A. The structure consists of a recumbently-folded isoclinal antiform with a massive rhyodacite exterior and interlayered interior, and has an undulating axial surface. (See figure 4.20.)

B. 1) A sill-like body of Coaker Porphyry intrudes unconsolidated mud. 2) Stringers and blebs of magma sag into the underlying mud. 3) Slumping of molten magma and wet mud roll the sill and associated materials into an isoclinal antiform, with a massive exterior and an interlayered interior.

A.

Interlayered dacite and
mudstone interior

Massive dacite
exterior

Trace of axial surface

←—20 m—→

B.

(1)

(2)

(3)
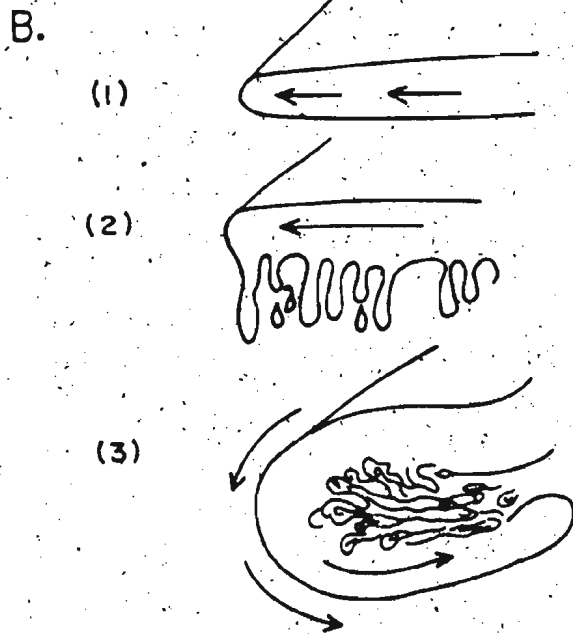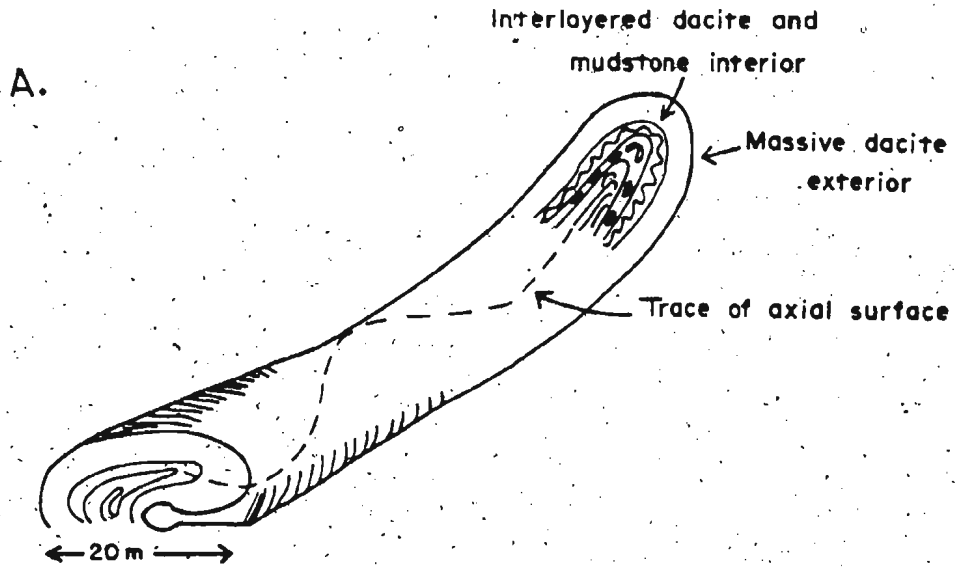
Figure 4.19 The Birchy Island structure. Massive exterior
portion (left) and interlayered interior (right).

Figure 4.20 The interlayered mudstone and Coaker Porphyry
interior of the Birchy Island structure.
Interlayers are thin, producing a laminated, shaly
appearance. Hinge of the fold is to the right of
the hammer.

Figure 4.21. Thorough mixing of Coaker Porphyry and mudstone, showing the resemblance to paint of two different colours stirred together. This photograph is a close-up of fig. 4.10 (bottom center). Birchy Island.

mudstone occur within the rhyodacite.

4.4.5 Breccia

Breccia is scarce, occurring locally in association with the stocks in two distinct forms. The first is as a mantle of breccia gradational into massive dacite. Dacite fragments in the breccia are set in a matrix composed primarily of coarse, elongate, anhedral quartz crystals with a weak subparallel alignment, with minor carbonate and wisps of mudstone. The quartz crystals do not appear to be phenocrysts released from the rhyodacite. Some of the fragments display a jigsaw-puzzle fit near the contact with the massive body of the stock. The breccias commonly contain small (< 1 cm) drusy cavities. Because of the gradational contacts between the breccia and the massive stocks and the silicification of the matrix, these breccias are interpreted to be peperites, i.e.: breccias formed as a result of explosive release of gasses. (See discussion by Kokelaar 1982).

Rhyodacite breccia with mudstone matrix also occurs in dikes that cut some Coaker stocks. Similar features, developed during cooling of viscous rhyolite, are described by Kokelaar (1982), who ascribes them to the opening of cooling joints with simultaneous injection of hot fluidized mud and peperite formation.

A third type of breccia occurs on Chapel Island near Birchy Island. It consists of fragments and clusters of fragments of Coaker Porphyry in a matrix consisting of mudstone and fine-grained slivers

of Coaker Porphyry. The breccia occurs in the form of lobate, flow-banded masses (fig. 4.22) that vary in size from 10 cm to 1.5 m across.

4.4.6 Interpretation

The Coaker Porphyry is interpreted, in agreement with Williams and Hibbard (1976), to have been intruded into the unconsolidated wet sediments that comprised the matrix of the Dunnage Melange. The evidence supporting this interpretation is as follows. (1) Corrugated contact surfaces are similar to features on the surface of a rhyolite sill intruding Ordovician unconsolidated, wet sediments, on Ramsey Island, Wales, described by Kokelaar (1982). Cooling cracks on Coaker stocks resemble the "breadcrust" structures from the Hammond Sill, interpreted by Hoyt (1961) as intrusive into wet sediment. Pahoehoe-like surfaces on some of the Coaker rhyolite layers suggest that both magma and host were fluid at the time of intrusion. (2) Lobate structures appear to be analogous to similar structures (pillows) produced by the extrusion of magma into water. (3) The occurrence of peperite, particularly peperite dikes in stocks, is indicative of intrusion into and fluidization of wet sediment.

The interlayering and folding of Coaker Porphyry and mudstone are also interpreted to have occurred during intrusion of the magma into wet sediment. The thickening and extension of hinges, the pinching out of mudstone layers within igneous material and of igneous layers within mudstone, suggest deformation of unconsolidated materials. The igneous (trachytic) textures of the rhyolites and rhyodacites, and the

Figure 4.22 Coaker Porphyry - mudstone breccia. This breccia
is interpreted to be completely disrupted layers of
Coaker Porphyry intermixed with mud.

lack of indications of strain in euhedral phenocrysts of quartz, muscovite, and feldspar, indicate that the structures displayed by the interlayered igneous and sedimentary rocks are primary igneous features rather than tectonic. In this case, the following require explanation: (1) the mechanism of interlayering of mud and magma, (2) the origin of folding, and (3) the persistence of very thin magma layers in sediment.

Kokelaar (1982) has ascribed the complex intermingling of magma and mud to be the result of fluidization of sediments by steam generated at contacts. Fluidized sediments offer little resistence to intrusion, and extremely complex contacts between magma and sediment can result, because magma can extend unrestricted in any direction. Fluidized sediments also serve to insulate the magma from immediate chilling, thus allowing the persistence of very thin layers of magma.

The style of folding indicates that the magma and mud were involved in slumping in an unconsolidated state. Slumping may have been triggered by the intrusion of the magma into muds at the edge of an escarpment or on a slope. A situation of magma intrusion contemporaneous with slumping is envisaged such that a dikelet of magma is folded into mud as the combined mass of mud and magma rolls down a slope. Because the rhyolite is still molten, the magma entering the hinge continues to flow downslope, producing the third limb, which may in turn be folded over during slumping (fig. 4.14b).

Two factors support the interpretation that the folding and interlayering are slope-controlled rather than a primary function of intrusion, for example, by squirting of the magma into mud. Firstly, the scarcity of the phenomenon, in contrast to the abundance of dikes and other simple forms, suggests that special conditions (ie.: the presence of a slope) are required for its occurrence. A second factor is an apparently gravity-controlled asymmetry inherent in these and similar forms elsewhere. Dikes intrusive into wet sediments occur on Ramsey Island, Wales, and near Waterford, Ireland, that are smooth on their upper contact surfaces, and have bulbous, udderlike protrusions extending from their lower surfaces. This asymmetry would appear to be the result of sagging of the denser magma into the less dense sediments under the influence of gravity. On Inspector Island, the dikelets emerge from an elongate stock, not simply sagging as they might in a pile of stagnant mud, but folding into complex forms. On Birchy Island, the recumbently folded isoclinal antiform probably originated as a simple sag dike, in which its massive outer layer was a dike from which the thin dikelets of its inner part emerged, the whole unit rolling into its present form due to slumping (fig. 4.17b).

Clearly, the Coaker Porphyry intruded unconsolidated sediments. Fluidization of sediments indicates depths of intrusion of less than 1.6 km (Kokelaar 1982), and the presence of dacite cobbles in conglomerates in the Dunnage Melange indicates penecontemporaneous erosion of extrusive or very shallow intrusive Coaker units. Shallow emplacement is thus implied.

4.5 Dildo Porphyry

The Dildo Porphyry is a suite of mafic to silicic stocks and dikes that intrudes the Dark Hole Shale, the lowermost horizons of the Sansom Greywacke, the Summerford Group, the Cobbs Arm Fault Zone at Fairbanks, and the Campbellton Shale. The stocks are small (3 to 8 m across), and dikes range from 30 cm to 2 m in thickness.

Stocks and dikes of Dildo Porphyry in the Dark Hole Shale and the Sansom Greywacke cut across bedding and have smooth contact surfaces. Their host sediments appear to have been consolidated at the time of intrusion. However, units of Dildo Porphyry intruding the Summerford Group commonly have irregular surfaces characterized by bulbous protrusions and pillow-like lobes, indicative of intrusion into unconsolidated materials. Such features can be observed on Farmer's Head. A dike of Dildo Porphyry that is characterized by complicated intermingling with host sediments and the occurrence of peperite intrudes Summerford Group shales containing Caradocian graptolites described by Horne (1970) at Fish Head on Farmer's Island. Intrusions of Dildo Porphyry do not have chilled or vesicular margins; nor did they cause noticeable hornfelsing of the host rocks.

4.6 Loon Bay Granodiorite

The intrusive characteristics of the Loon Bay granodiorite were studied by Floran (1971), who noted that cataclasis and straining of mineral grains occur at and near the contacts, and suggested that these structures related to the emplacement of the granodiorite by

forceful intrusion. Hibbard (1976, p 54) studied the thermal effects of the intrusion on the Dunnage Melange, documenting the mineralogy and grade of the contact aureole. The granodiorite produced a greenschist grade baked zone approximately 2 km wide. Shales within the aureole have a paragenesis of quartz, biotite, muscovite, cordierite, and garnet. Coaker Porphyry within the aureole displays a number of metamorphic changes, including recrystallization of the groundmass accompanied by the development of granophyric textures, the crystallization of pale brown secondary biotite in clumps replacing original mafic phases, the formation of tourmaline (rare), the elimination of apatite, and reversal of hydrothermal alteration and removal of volatile-containing phases such as carbonate.

The Loon Bay batholiths are accompanied by swarms of fine-grained dikes and small stocks that intrude the host in the immediate vicinity of the batholiths. Some of these, presumably late liquid fractions of the magma, intrude the batholiths themselves. These are physically and geochemically indistinguishable from Dildo Porphyry, and are distinguished only on the basis of their close proximity to the Loon Bay Batholiths.

4.7 Late Dikes

Late dikes intrude the Dunnage Melange in a swarm parallel to Dildo and Reach Runs. The dikes range in thickness from approximately 8 cm to 10 m across, but are most commonly about 1.5 m in width. They cut across all rock-types and small-scale structures within the Dunnage Melange, but are affected by some of the large-scale Acadian

structures (see Chapter 5). On Boyd's Island their pattern of intrusion was affected both by the presence of joints related to the Reach Fault and by the presence of Coaker Porphyry. The dikes have chilled margins, commonly amygdular, and produce a baked zone approximately 15 cm wide in the host rocks.

4.8 Summary

The New Bay Gabbro occurs both as sills and as blocks in the Dunnage Melange, indicating that emplacement bracketed the time of melange formation (Hibbard 1976, p 37). The Puncheon Diorite is older than the Coaker Porphyry. Coaker Porphyry intruded the Dunnage Melange at shallow depths while the matrix of the melange was wet and unconsolidated, giving rise to spectacular mud-magma interactions. Intrusion apparently occurred during melange formation. The Grapnel Gabbro was emplaced at the same time as the Coaker Porphyry. The Dildo Porphyry intruded unconsolidated sediments of the Summerford Group containing Caradocian graptolites, but the Caradocian Dark Hole Shale appears to have been consolidated at the time of intrusion of the Dildo Porphyry. The Loon Bay Granodiorite baked the host melange and the Coaker Porphyry to greenschist grade. The Late Dikes cross-cut all lithologies and most small-scale structures in the Dunnage Melange and occur in a swarm paralleling the Dildo and Reach Runs.

Timing of Events

This chapter is concerned with the local geologic history of the Dunnage Melange, based on observations presented in the previous chapters. The ages of Dunnage lithologies, the relationships between the melange and surrounding units, and the nature and timing of igneous activity are examined and interpreted to produce the conclusions presented below.

5.1 The age of Dunnage Melange lithologies

The oldest known rock in the Dunnage Melange is a volcanic block containing the Middle Cambrian trilobites Kootenia and Bailiella in associated carbonate (Kay and Eldredge 1968). Tremadocian graptolites (mainly Dictyonema of flabilliforme type) have been collected from the melange matrix in two localities (Williams 1972, Hibbard et al. 1977). Intermixture of extrusive volcanics with matrix muds indicates that volcanism was penecontemporaneous with sedimentation (Williams and Hibbard 1976). Arenigian conodonts have been found in a carbonate block in the southwest portion of the melange (Hibbard et al. 1977). If the Dark Hole Formation overlying the Dunnage Melange were conformable, as proposed by Hibbard and Williams (1979) and others, then the presence of Upper Caradocian graptolites in this formation (Kay 1976) would place an upper age limit on the deposition of Dunnage lithologies. Unfortunately, however, evidence exists that the contact

is not conformable (see section 2.2.2.1). However, the correlative relationship between the Dunnage Melange and the New Bay Formation and Lawrence Head Volcanics of the Exploits Group (Hibbard and Williams 1979), implies that the Dunnage lithologies should be approximately the same age as the Exploits Group correlatives - pre-Caradocian.

The history of clastic sedimentation from Tremadocian to Caradocian time is unknown due to the lack of fossils in the Dunnage Melange from this time interval.

5.2 Significance of the Coaker Porphyry

The Coaker Porphyry is restricted to the northeast portion of the Dunnage Melange. Taking into account the caprices of preservation, this limited distribution suggests a temporal and possibly a genetic relationship between the intrusion and the melange. Several lines of evidence indicate that intrusion occurred during melange formation, and that these were surficial events. Firstly, some undisrupted Coaker Porphyry dikes cut volcanic and carbonate blocks as well as the melange matrix, indicating that at least some of the blocks had already been intermixed with the matrix at the time of intrusion. Hornfels associated with Coaker Porphyry on Dog Island preserves earlier structures (folded and contorted sediments). Secondly, the melange matrix was unconsolidated at the time of intrusion of the Coaker Porphyry, strongly supporting penecontemporaneous intrusion and melange formation. Thirdly, fluidization of host sediments as a result of intrusion of Coaker Porphyry is inconsistent with the existence of a large tectonic overburden at the time of intrusion.

This evidence, combined with the localized occurrence of slumping during intrusion of the Coaker Porphyry, supports an olistostromal rather than a tectonic origin for the melange. Well-preserved contact relationships between the Coaker Porphyry and the host melange are inconsistent with an Acadian origin for the melange, as proposed by Karlstrom et al (1982). If melange formation had occurred after intrusion of the Coaker Porphyry, these units would then occur as blocks in the melange. However, local separation of Coaker Porphyry from its hornfels indicates that some structural activity continued after the intrusive event.

Intrusions of silicic magmas into unconsolidated sediments appear commonly to be associated with debris flow in areas undergoing block faulting (in southwest Wales - Kokelaar 1982, in southeast Ireland - M. Boland, pers. com. 1982, in California - Hanson and Schweikert 1982).

A whole-rock Rb/Sr age of 445 +/- 8 Ma was obtained for Coaker Porphyry (fig. 6.19). Keeping in mind the vagaries of the Ordovician time scale, and in light of field relationships, this date places the time of intrusion of the Coaker Porphyry at approximately the Llandeilian-Caradocian boundary.

5.3 The Dark Hole Shale and Dildo Porphyry

Hibbard and Williams (1979) present several lines of evidence in support of a conformable contact between the Dunnage Melange and the Dark Hole Shale, the most important of which is the relative ages of

the two units (see Chapter 2). Aside from the geometric difficulties of thrusting younger rocks on top of older ones, the relationship implied by a displacement at this contact is the opposite of those observed on New World Island, where all major faults emplaced older strata over and to the north of younger strata.

However, a displacement between the two units is strongly implicated by the absence of the younger Dildo Porphyry in the older Dunnage Melange, and its occurrence in the Dark Hole shale right up to, but not across, contacts with the Dunnage Melange. Such a relationship seems unlikely to have occurred in a conformable sequence; the two units could not have been in contact at the time of intrusion of the Dildo Porphyry.

The observed contact relationships could have occurred as a result of sliding of the Dark Hole Formation slice onto unconsolidated Dunnage muds, following the intrusion of Dildo Porphyry into the Dark Hole Formation. The gradational nature of the contact and the apparent break-up and dispersal of chunks of Dark Hole shale along the contact suggest that the Dark Hole Formation itself may have been poorly consolidated at the time of emplacement.

The age of the Dildo Porphyry places a limit on the timing of the displacement. Its age is not known, but can be estimated to be Late Ordovician due to its distribution in the Dark Hole Formation and the Sansom Greywacke (section 2.4) and its intrusion into unconsolidated Caradocian sediments of the Summerford Group (sec. 4.5). Thus an earliest late Ordovician age for the emplacement of the Dark Hole

Formation and Sansom Greywacke sequence onto the Dunnage Melange is implied. That this is an early structure rather than an Acadian structure can account for the difference in style between it and the major faults on New World Island.

5.4 An Ordovician Scenario

The proposed mechanism for the evolution of the Dunnage Melange and associated units is essentially that proposed by Horne (1970), in which the observed soft-sediment deformation in the Dunnage Melange, the Summerford Group, and parts of the Sansom Greywacke were the result of dip-slip faulting and crustal instability.

1) Dunnage Formation distal turbidites (?) and intermixed extrusive volcanics were deposited on a basement possibly consisting of a thick pile of pillow lavas with or without trondhjemite.
(Tremadocian - Caradocian: deposition.)

2) Block faulting and associated seismicity created unstable slopes, resulting in the local redeposition of the Dunnage Formation as a large olistostrome or series of olistostromes. Similar disturbances elsewhere created the disruption of the volcanic-rich Summerford Group. Other units in the area (the Exploits Group) were undisturbed. Block faulting exposed basement material in fault scarps, creating a source for old pillow basalts and trondhjemite in the Dunnage Melange. Fractures facilitated the ascent of silicic magmas (the Coaker Porphyry).
***(Arenigian (?) - Caradocian: block faulting, olistostromes,

intrusion)***

3) Substrate instability continued, perhaps diachronously in different areas. Local uplift of part of the Dunnage Melange resulted in the deposition of cobbles of Coaker Porphyry onto down-dropped portions of the melange. Slump folding and sediment slides occurred in Caradocian sediments of the Summerford Group and in the Sansom Greywacke (Horne 1970). The Dildo Porphyry intruded debris flows in Caradocian black shales of the Summerford Group and distal - turbidites of the Dark Hole Formation and lowermost horizons of the Sansom Greywacke. A slice of this material slid onto the Dunnage Melange. What happened to the sediments of equivalent age that already should have been on top of the Dunnage Melange? Perhaps they are preserved locally (the Chapel Island Formation, the Cheneyville Conglomerate). Perhaps they were displaced by the invading slice. Perhaps they were incorporated into the melange.

(Caradocian - Ashgillian: slump folding, intrusion, sediment sliding)

This scenario is summarized in fig. 5.1.

5.5 Later events

Later (Acadian) events are for the most part beyond the scope of this study, and are being examined in detail by several research teams working on New World Island. A brief summary of these events is given here, in which the timing of igneous intrusions is emphasized.

Figure 5.1 Ordovician – Silurian development of the Dunnage
Melange.

A. Pelagic sediments and intermixed volcanics
(Dunnage Formation) are deposited on a
Twillingate/Moreton's Harbour-type basement. Reef
development around volcanic cones (Arenig)
contributes carbonate breccia to the Dunnage
Formation.

B. Block-faulting causes redeposition of the
Dunnage Formation as olistostrome. Basement rock
exposed in fault scarps contributes pillow basalts,
tuffs, and trondhjemite to the Dunnage Melange.
Fractures facilitate the ascent of Coaker Porphyry
magmas into unconsolidated muds of the Dunnage
Melange.

C. Sedimentation continues. Calc-alkaline
batholiths are intruded at depth, preceeded,
accompanied, and succeeded by related dike swarms
and minor stocks (Loon Bay/Dildo Porphyry suite),
some of which intrude the sedimentary pile.

D. Continued block faulting causes a block of
turbiditic sediments containing stocks and dikes
(Dark Hole Formation) to slide onto the Dunnage
Melange.

A

reef development
(Arenig)

Dunnage
Formation

Cambrian→Arenig

B

Cooker
Porphyry

Llandeilian → Caradorian

C

Dunnage
Melange

Dark Hole Fm

Loon Bay
magmas

Caradorian→ Silurian

D

(X)

Dark Hole
Formation

Silurian
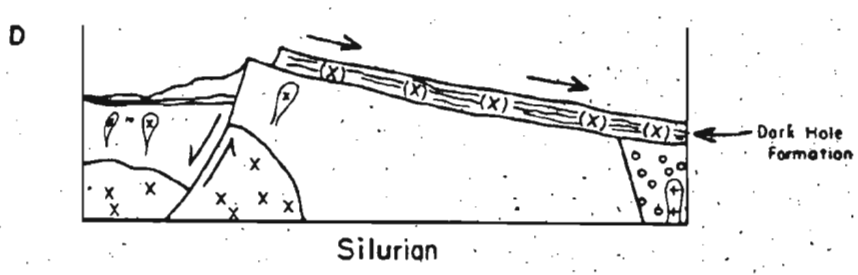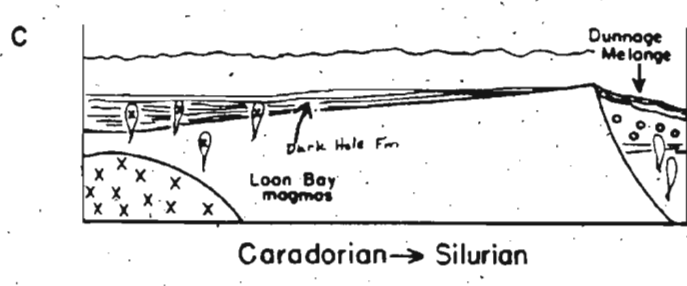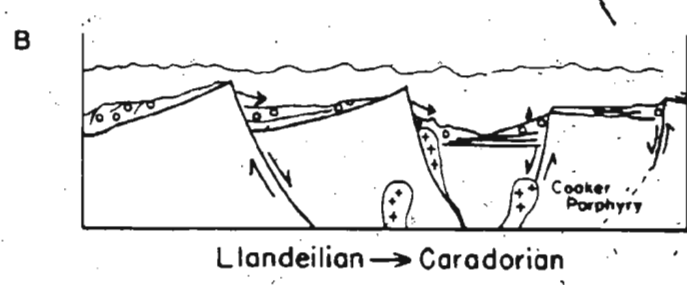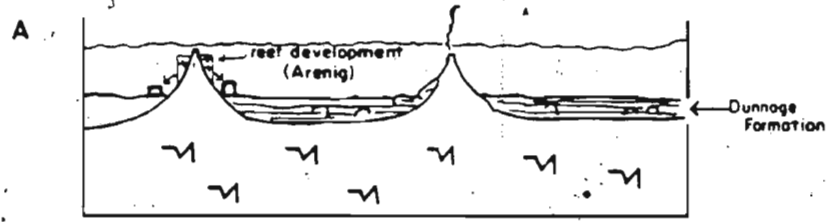
1) The Loon Bay batholiths were emplaced, accompanied and cut by associated dikes and stocks.

2) Several episodes of Acadian faulting and folding took place (for details and contrasting viewpoints, see Horne 1968, Karlstrom et al. 1982, Arnott 1983). Patterns of intrusion of the late dikes were locally controlled by shear planes related to the Reach Fault, indicating that the Reach Fault preceded the intrusion of the Late Dikes.

3) The Late Dikes were intruded in a swarm parallel to Dildo and Reach Runs, indicating that these lineaments are the expression of an earlier feature that controlled ascent of the magma, or that the Late Dikes are a manifestation of an extensional event that took place during the late Devonian.

4) The Dunnage Melange forms the core of a large anticlinorium. The late dikes parallel the axis of this anticlinorium. One dike (on Puncheon Head) is folded by this structure. An $Ar(40)/Ar(39)$ age of $375 +/- 10$ Ma has been obtained for possibly equivalent diabase dikes in the Gander Group (Reynolds and Murthy in press). This configuration suggests that extension along the northwest—southeast direction was later followed by compression in the same direction, or that the Late Dikes were intruded along tension fractures associated with the folding itself.

5.6 Summary

The sequence of events described above is summarized in Table 5.1.

Deposition of Dunnage Melange lithologies (sediments and volcanics) was followed or accompanied by block faulting and intrusion of the Coaker Porphyry during Llandeilian time, resulting in melange formation. Similar processes affected the Summerford Group. Continued substrate instability resulted in the sliding of the Dark Hole Formation over the Dunnage Melange in the late Ordovician, following intrusion of the Dildo Porphyry into that unit. Acadian events include intrusion of the Loon Bay suite, several episodes of faulting and folding, and intrusion of the Late Dikes either before or during the formation of the Dunnage Melange anticlinorium.

TABLE 5.1

Timing of Events

AGE	SEDIMENTATION	IGNEOUS ACTIVITY	STRUCTURE
Later			A Acadian
Devonian		Diabase dikes	A tectonic
			folding
			Reach Fault
		L	
	Other New	L Loon Bay	
Silurian	World Island	L plutons	
	lithologies	D	
		D	
	Sansom	D	S
Ashgill	Greywacke	D	S
	H	D	
	H	D Dildo Porphyry	S Slump
Caradoc	H Dark Hole	D	S folding
	H		BS
	DO	C	
Llandeilo	DO	C Coaker Porphyry	BS
	DO Redeposi-	C Grapnel Gabbro	BS
	DO tion of	EC	BS
	DO Dunnage	EP	BS
Llanvirn	DO Formation	EP Puncheon	BS Block
	DO as olis-	EP Diorite	BS faulting
	DO tostrome	E	BS
	DO	E	BS
Arenig	DC Carbonate	E	B
	DC breccias	E	
	D	E	
Tremadoc	D Dunnage	E Extrusive	
	D Formation	E volcanics	
	D muds	E	
Cambrian	D	B Basaltic	
		B flows	

Chapter 6

Coaker Porphyry: Petrography, Geochemistry, Petrogenesis

The mineralogical and geochemical characteristics of the Coaker Porphyry are the end result of a combination of factors: the mineralogy and geochemistry of the source, the amount of partial melting of the source, pressure, temperature, cooling history of the magma, the effects of contamination of the magma by ultramafic material, the effects of contamination of the magma by host sediments, and hydrothermal alteration. In this chapter, petrographic and geochemical data are examined to determine the effects of all these factors, and a petrogenetic model of the origin and evolution of the Coaker Porphyry is presented.

6.1 Petrography

The Coaker Porphyry includes dacites, rhyodacites, and rhyolites, composed of feldspar, quartz, and mica phenocrysts in a fine-grained quartzofeldspathic groundmass. The extrusive rock names are employed here rather than their plutonic equivalents based on the fine-grained groundmass textures of these rocks; no genetic implication of an extrusive origin is implied. Indeed, these rocks are interpreted to have intruded shallow, fluid mud (Chapter 4), and are thus transitional between extrusive and intrusive. The porphyry exhibits gradational variations in texture, mineralogy, and xenolith content. Textural variations are correlated to some extent with mode of

occurrence in the field. The petrography of the three end-member types (general, trachytic, and xenolith-rich) is summarized in table 6.1.

The most abundant, or "general type" of Coaker Porphyry occurs in massive stocks. The trachytic-textured type occurs as dikes, lobes and pillows, pillowed and flow-banded stocks, and the rare interlayered Coaker/shale form (see Chapter 4). Xenolith content of both types varies from xenolith-free Coaker Porphyry to the xenolith-rich "Causeway diorite" or "Causeway xenolith-phase" of Ray (1972). Where they occur together, the xenolith-rich units are intrusive into the xenolith-poor units.

6.1.1 Phenocrysts and implications for cooling history

Alkali feldspar phenocrysts are ubiquitous in the Coaker Porphyry, although they vary in size and abundance. They occur as single equant, euhedral crystals or as glomeroporphyritic clumps that also may include quartz. In xenolith-free Coaker Porphyry, they commonly occur in two or three distinct generations of crystal sizes. They are not zoned, although original zoning may have been obliterated by albitization. K-feldspar phenocrysts have been identified in the most felsic members of the suite; more commonly, K-feldspar is absent as a phenocryst phase. Albite and oligoclase are by far the more abundant compositions.

TABLE 6.1 Petrography of Coaker Porphyry

Type	Mineralogy	Texture	Alteration
General — most abundant type	Phenocrysts:		
	oligoclase ------	Equant, 3-10 mm, euhedral, commonly glomeropprhyritic	---- mostly fresh, some carbonate, sericite
Xenoliths absent to abundant	quartz ---------	euhedral, embayed, rounded	
	biotite ---------	microphenocrystic, subparallel align-ment, euhedral	---chlorite, car-bonate, rutile, sphene, sericite
	Groundmass: ------ quartzo-feldspathic	anhedral, equant crystals	-----partial alter-ation to seri-cite, carbonate rare prehnite
Trachytic	Phenocrysts: same as above +/-		Same as above, except that
	muscovite -------	rounded, euhedral	carbonate alter-ation may occur
Xenoliths absent to abundant	Groundmass: ------ quartzo-feldspathic	trachytic, plag. lathlike rather than equant	in discrete bands
	opaques ---------	dust dispersed in groundmass or in discrete layers	
	+/- vesicles		
Xenolith-rich (Causeway xenolith phase, Kay 1972)		seriate texture, grains fragmental	
	oligoclase to andesine ----------broken		pervasively al-tered to seri-cite, carbonate +/- prehnite
	phlogopite ----------euhedral		mostly fresh, or chlorite + rutile
	quartz ------------megacrystic		
	magnesio-hornblende --------euhedral		same as phlogo-pite
	garnet -----------euhedral, zoned		fresh

Rounded, euhedral quartz phenocrysts are common but not ubiquitous. Biotite phenocrysts are smaller than the feldspar and quartz crystals and are fluxioned around them. They commonly occur in sub-parallel alignment, particularly in trachytic-textured Coaker Porphyry.

These observations imply the following cooling history for the Coaker Porphyry. The magma cooled at depth, precipitating crystals of feldspar with or without quartz. The magma then ascended to new levels, carrying with it its phenocrysts and possibly a restite component (the glomeroporphyritic clumps?), where quartz and feldspar were joined by biotite as a crystallizing phase. The magma then ascended rapidly to shallow crustal levels (see discussion in Chapter 4), where the remaining liquid was quenched.

6.1.2 Muscovite

Euhedral crystals of muscovite, ranging in size from 1 to 8 mm across, and up to 2 mm thick, are a rare phenocryst phase occurring in some of the most felsic units of the Coaker Porphyry. The muscovite crystals are interpreted to be primary rather than secondary (sericite) because they occur singly as large, thick, euhedral crystals, they are free of inclusions of sphene, and trachytic groundmass feldspar laths are fluxioned around them. Their identity as muscovite has been established by microprobe analysis (table 6.2).

TABLE 6.2

Microprobe analyses of Coaker Porphyry minerals

Oxide (wt %)	1	2	3	4
SiO2	56.23	38.82	52.05	39.06
TiO2	0.11	3.13	0.54	0.43
Al2O3	33.98	16.09	6.12	22.41
FeO(t)	0.93	12.40	9.22	22.41
MnO	0.00	0.10	0.20	0.48
MgO	1.42	16.13	17.91	9.00
CaO	0.00	0.00	10.20	8.14
Na2O	0.06	0.38	1.04	----
K2O	8.66	8.80	0.22	----
Total	101.39	95.85	97.50	101.11

1) Ave. muscovite composition (7 micas from 2 samples)
2) Ave. phlogopite composition (12 micas from 4 samples)
3) Ave. magnesiohornblende composition (20 amphiboles from 3 samples)
4) Ave. garnet composition, sample 247-81 (89 points from 9 zoned garnets)

The muscovite phenocrysts in the Coaker Porphyry are the same size as the quartz and feldspar phenocrysts, and one muscovite crystal was observed to be partially enclosed by a feldspar crystal. This indicates that muscovite crystallization accompanied or possibly preceded crystallization of the quartz and feldspar.

The presence of primary muscovite in a hypabyssal rock is anomalous; experimental work indicates that the mineral becomes unstable at pressures below 5 kb, or that liquids in which muscovite is stable solidify at this pressure. However, primary muscovite in extrusive rhyolite has been reported by Schleicher and Lippolt (1981). They concluded that either muscovite can be stabilized at low pressures in the presence of some presently unknown phase (perhaps a fluid phase), or that the magma ascended rapidly and chilled before the muscovite could be resorbed.

6.1.3 Groundmass

The Coaker Porphyry groundmass is typically cryptofelsitic; rarely the grain-size is coarse enough to identify quartz, feldspar, and mica microscopically. The quartz and feldspar are anhedral in general-type Coaker Porphyry. This groundmass is probably devitrified glass, although the only devitrification textures to survive are fibrous chloritic rims around garnet phenocrysts in one locality. The groundmass of trachytic-textured Coaker Porphyry, as the name implies, is composed of aligned feldspar laths and mica, and anhedral quartz. Flow-banding is defined in thin-section by variations in grain-size, or opaque or carbonate content.

6.1.4 Xenoliths

Several stocks and dikes of Coaker Porphyry are charged with ultramafic and mafic xenoliths ranging in size from less than 1 mm to 30 cm in diameter, and locally comprising up to 15% of the rock fig. (6.1). More commonly, units of Coaker Porphyry contain only sparse xenoliths, usually less than one percent, and Coaker Porphyry totally lacking in xenoliths is uncommon.

The mineralogy of the xenoliths is summarized in table 6.3. The xenoliths are mostly ultramafic, but some mafic and rare trondhjemitic compositions are present as well. Trondhjemitic xenoliths do not occur intermixed with other xenolith types, but are isolated enclaves in units of Coaker Porphyry that are otherwise free of xenoliths.

The ultramafic xenoliths are mostly altered to assemblages of serpentine, carbonate, anthophyllite, and chlorite, fewer to quartz and carbonate. Chromite crystals persist in all ultramafic xenoliths, and orthopyroxene is preserved rarely as tiny patches in masses of serpentine, rendering difficult the detection of zoning in pyroxene. The mafic xenoliths are composed of magnesiohornblende and andesine.

The xenoliths are rounded, some having pronounced reaction rims and radiating textures, indicating profound disequilibrium between the xenoliths and their host magma.

Figure 6.1 Xenolith-rich Coaker Porphyry. A slab of "Causeway xenolith phase" (Kay 1976) from the type locality on Causeway Islands. Xenoliths occupy 13% of the area of the slab. Dark reaction rims around the xenoliths contain a concentration of phlogopite. Scale in cm.
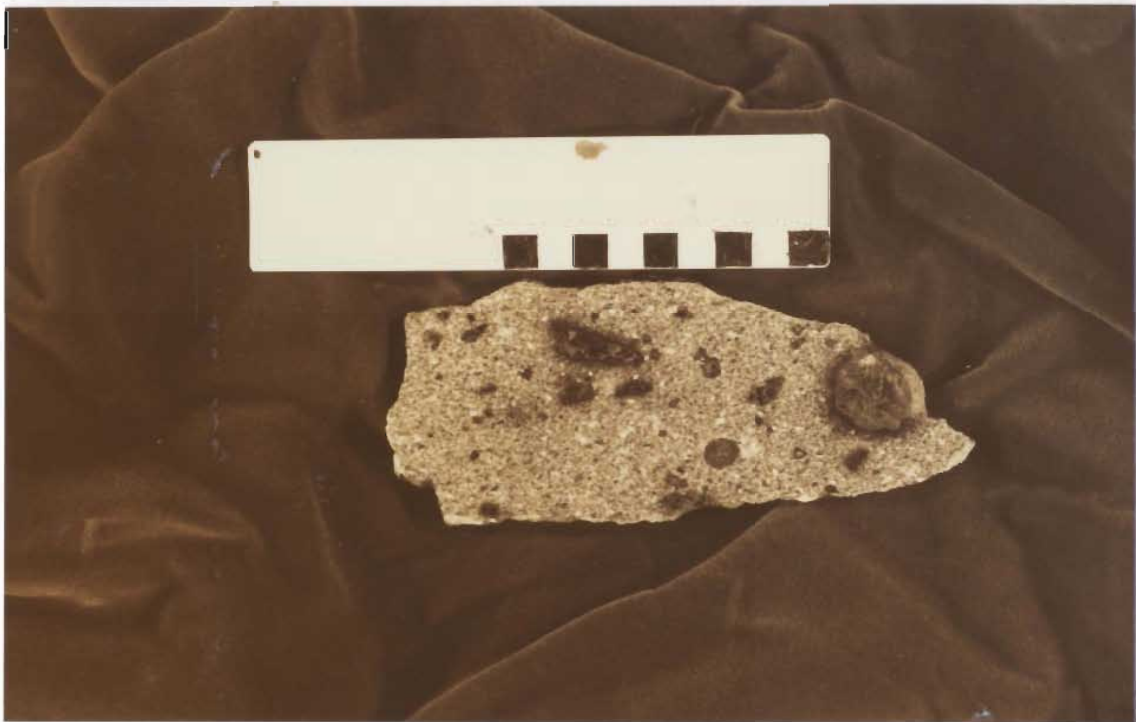
TABLE 6.3

Xenolith Types in Coaker Porphyry

1) ULTRAMAFIC ASSEMBLAGES

    -serpentine (commonly pseudomporphic after pyroxene)
    -serpentine (crenulated)
    -serpentine + chromite
    -serpentine + talc + chromite
    -serpentine + talc + phlogopite
    -serpentine + carbonate + chlorite + chromite
    -serpentine cut by and rimmed with veins of chromite and yellow
       carbonate
    -serpentine + chromite (serpentine filled with tiny inclusions of
       perovskite
    -quartz + chlorite + carbonate + chromite
    -anhedral quartz crystals dissected (as if shattered and filled)
       by veinlets of carbonate
    -chlorite + carbonate + chromite
    -quartz + carbonate + chromite + acicular opaques
    -carbonate + chromite

2) MAFIC ASSEMBLAGES

    -andesine + magnesiohornblende + phlogopite + quartz
      (coarse-grained plagioclase and fine-grained quartz
      in separated bands)
    -magnesiohornblende (euhedral, with parallel alignment)
      in fine-grained groundmass of amphibole
      + plagioclase + phlogopite + sphene + apatite
    -carbonate + chlorite
    -chlorite + carbonate + quartz + sphene surrounded by radiating
      rim of fine-grained acicular amphibole
    -prehnite + quartz + k-spar + sphene

6.1.5 Xenolith-rich Coaker Porphyry

Certain minerals and textural features occur only in xenolith-rich Coaker Porphyry and appear to be the result of reaction between the magma and the xenoliths. These minerals include phlogopite, magnesiohornblende, and garnet (table 6.2).

The golden-red phlogopite is not the pure end-member, but has an average Mg/Fe ratio of 2.31, qualifying it as phlogopite according to Deer, Howie, and Zussman (1962). Magnesiohornblende was classified according to Leake (1978). Plagioclase in these rocks is seriate, fragmental, and more altered than feldspar in xenolith-poor Coaker Porphyry. Quartz is not a common phenocryst phase in xenolith-rich Coaker Porphyry, but in one instance occurs as spectacular euhedral megacrysts up to 7 cm long. Quartz and alkali feldspar (sodic and potassic) have been detected in the groundmass.

Garnet occurs rarely in xenolith-rich Coaker Porphyry, but is not found in xenolith-free rocks. One stock on Coaker Island contains large (up to 2 cm in diameter) euhedral to subhedral garnet phenocrysts with compositions ranging from Alm(38)Py(45)Gr(17) to Alm(69)Py(13)Gr(24) (see figure 6.2). The crystals are strongly zoned and show normal, reverse and oscillatory zoning within one hand-specimen-sized sample. The assemblage of which the garnet is a part is difficult to determine because this particular rock was subject to hydrothermal alteration from which only the garnet survived in pristine condition. Assemblages of chlorite, carbonate and opaques form pseudomorphs after amphibole. Other clots of chlorite appear to

Figure 6.2 Compositions of Coaker Porphyry garnets. Garnets
display normal (towards almandine (Alm) +
spessartine (Sp)), reverse, and oscillatory zoning.
The direction of zoning from center of crystal
outwards is indicated by the direction of the
arrows. Each field encloses the compositions
measured for one garnet.
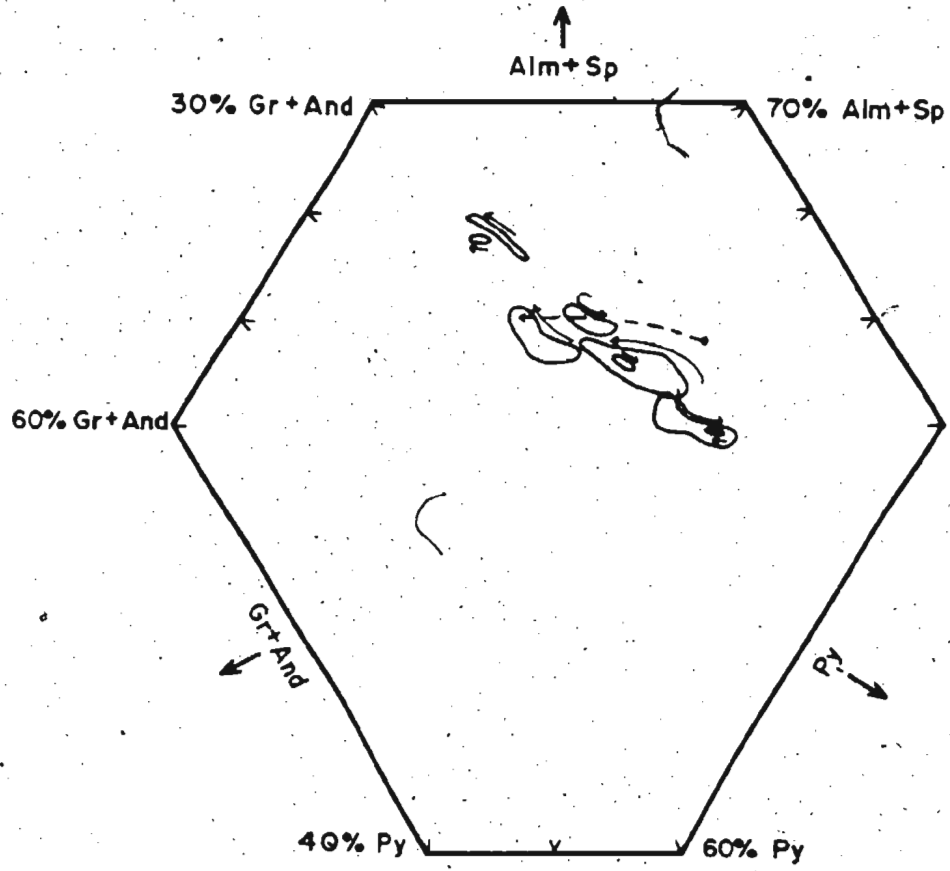
be the remains of xenoliths.

6.1.6 Hydrothermal alteration

The Coaker Porphyry was subject to mild, patchy hydrothermal alteration. This appears to have taken place during emplacement, as coeval (Grapnel Gabbro) and later (Loon Bay Granodiorite) intrusions baked the volatile alteration products out of Coaker Porphyry within their aureoles. (See section 4.6.) In uncontaminated (xenolith-free) Coaker Porphyry, biotite is invariably altered to assemblages of chlorite, carbonate, sphene, sericite, and rutile. Feldspar is albitized and sericitized. The groundmass typically contains patches of carbonate and abundant sericite.

Xenolith-rich Coaker Porphyry, on the other hand, shows a wide variation in alteration assemblages. The variation occurs on the outcrop scale, indicating that the fluids extant in the magma were extremely inhomogeneous. In the more common assemblage, phlogopite is well-preserved or slightly chloritized, prehnite is present, and the xenoliths are altered to serpentine +/- carbonate and chlorite, commonly with reaction rims of anthophyllite. In the second assemblage, mafic phases are obliterated to clots of carbonate and sphene, and the xenoliths are reduced to masses of quartz and carbonate, with only euhedral chromite crystals surviving to attest to the original ultramafic nature of these enclaves. Feldspars in both assemblages are cloudy and corroded.

These observations indicate that the fluids associated with uncontaminated Coaker Porphyry were comparitively rich in CO2 and that the reactions between the magma and the xenoliths produced H2O-rich fluids. Preliminary examinations of fluid inclusions in a quartz megacryst from xenolith-rich Coaker Porphyry have revealed that the fluid is water of low salinity containing no daughter minerals or detectable CO2 (Burry, pers. com. 1983). These findings are in accord with the experimental results obtained by Sekine and Wyllie (1982a) involving the reaction between peridotite and rhyodacitic melt. Release of this water-rich fluid during the magma-xenolith reactions was possibly responsible for producing the observed fragmentation of feldspar crystals in xenolith-rich Coaker Porphyry. Inhomogenieties in fluid distribution in the xenolith-rich phases were perhaps a function of inhomogenieties in xenolith content.

6.2 Geochemistry

Uncontaminated Coaker Porphyry consists of peraluminous rhyodacites and rhyolites, with a silica range of 64 to 76%. Major and trace element analyses and CIPW norms are given in Table 6.4 for 19 uncontaminated and 20 contaminated samples. Harker variation diagrams of major elements and selected trace elements plotted against silica are shown in figure 6.3.

The Coaker Porphyry plots in the alkali corner of the AFM diagram (fig. 6.4), in a line that terminates at the pure alkali composition, in contrast to the Loon Bay suite, which terminates against the alkali-FeO tie line. The Coaker Porphyry is calc-alkaline according

TABLE 6.4

Coaker Porphyry: Major Elements, Norms, Trace Elements

Uncontaminated by xenoliths

MAJOR ELEMENTS	50-81	53-81	58-81	87-82	88-81	89-81
$SiO2$	64.7	68.6	69.8	72.4	67.9	72.0
$TiO2$	0.40	0.29	0.29	0.07	0.30	0.12
$Al2O3$	16.8	15.0	14.9	14.6	14.7	14.1
$Fe2O3(t)$	2.61	2.29	1.85	0.59	2.31	0.56
MnO	0.04	0.04	0.05	0.05	0.04	0.04
MgO	1.26	1.40	1.07	0.25	1.44	0.31
CaO	1.74	1.24	1.37	1.01	1.22	1.03
$Na2O$	4.76	3.91	3.93	5.24	3.97	3.86
$K2O$	3.35	4.58	4.49	2.91	4.59	4.92
$P2O5$	0.12	0.10	0.08	0.06	0.10	0.02
L.O.I.	3.18	2.52	2.37	1.73	2.18	2.11
Total	98.96	99.97	100.20	98.91	98.65	99.07

NORMS

Q	18.13	23.03	24.86	28.82	22.71	28.64
OR	20.67	27.77	27.12	17.69	28.12	29.99
AB	42.05	33.95	33.99	45.63	33.95	33.69
AN	8.19	5.64	6.41	4.75	5.60	5.14
C	2.58	1.64	1.30	1.17	1.44	0.62
DI	----	----	----	----	----	----
HY	6.86	6.80	5.26	1.57	6.99	1.56
MT	0.44	0.37	0.30	0.09	0.38	0.09
IL	0.79	0.57	0.56	0.14	0.59	0.24
AP	0.29	0.24	0.19	0.14	0.24	0.05

TRACE ELEMENTS

Pb	34	41	44	48	45	34
Rb	141	206	206	116	206	144
Sr	391	293	251	110	306	232
Y	11	10	9	4	12	6
Zr	191	156	153	67	163	79
Zn	40	90	53	14	56	6
Cu	14	15	13	12	16	22
Ni	34	15	14	0	13	0
Ba	658	804	650	566	778	1087
V	19	30	30	6	32	10
Cr	26	27	18	0	18	0
La + Ce	68	60	47	21	50	20

TABLE 6.4 (continued)

Uncontaminated by xenoliths

MAJOR ELEMENTS	100-81	128-81	129-81	168-81	192-81	208-81
SiO_2	68.1	69.0	75.5	72.9	68.1	70.6
TiO_2	0.20	0.10	trace	0.08	0.33	0.17
Al_2O_3	15.0	16.9	14.6	14.9	16.5	15.4
$Fe_2O_3(t)$	2.18	2.31	0.29	0.71	2.34	1.34
MnO	0.04	0.06	0.01	0.02	0.07	0.03
MgO	1.28	0.57	0.15	0.19	1.36	0.59
CaO	1.19	0.41	0.05	0.89	2.15	0.56
Na_2O	5.02	6.83	6.15	4.46	4.33	4.19
K_2O	3.92	2.79	1.10	4.44	3.55	5.22
P_2O_5	0.08	0.07	0.06	0.00	0.03	0.00
L.O.I.	2.07	1.61	1.13	1.13	1.36	0.70
Total	99.08	100.65	99.04	99.72	100.12	98.80

NORMS

Q	18.81	15.61	35.89	27.71	21.59	23.79
OR	23.88	16.65	6.64	26.61	21.24	31.44
AB	43.79	58.35	53.15	38.28	37.10	36.14
AN	5.55	1.59	0.15	4.48	10.60	2.83
C	0.54	2.09	3.42	1.16	1.72	1.87
DI	----	----	----	----	----	----
HY	6.49	4.99	0.86	1.49	6.66	3.37
MT	0.36	0.37	0.04	0.12	0.38	0.22
IL	0.39	0.19	----	0.15	0.63	0.33
AP	0.19	0.16	0.14	----	0.07	----

TRACE ELEMENTS

Pb	43	44	55	55	38	74
Rb	98	72	73	167	163	242
Sr	142	224	44	282	356	159
Y	10	11	8	4	14	15
Zr	154	172	36	66	142	91
Zn	46	26	75	23	34	33
Cu	10	11	16	15	22	13
Ni	11	0	0	1	18	5
Ba	779	582	180	679	558	418
V	27	8	0	5	19	20
Cr	19	0	0	0	19	0
La + Ce	50	46	10	3	49	17

Table 6.4 (continued)

Uncontaminated by xenoliths

MAJOR ELEMENTS	209-81	231-81	246-81	276-81	283-81	285-81
SiO2	71.1	67.7	68.4	71.3	68.3	72.0
TiO2	0.17	0.34	0.22	0.13	0.26	0.05
Al2O3	15.0	15.9	15.8	15.2	14.6	15.1
Fe2O3(t)	1.26	2.10	1.74	1.24	2.06	0.51
MnO	0.03	0.04	0.03	0.03	0.04	0.03
MgO	0.06	1.44	0.92	0.51	1.16	0.18
CaO	0.66	1.08	1.29	1.39	1.51	1.50
Na2O	3.99	5.05	5.05	4.24	5.10	4.50
K2O	5.55	3.80	2.23	3.74	3.90	4.26
P2O5	0.02	0.08	0.06	0.10	0.07	0.01
L.O.I.	0.46	1.50	3.48	1.07	2.65	0.70
Total	98.84	99.03	99.19	98.95	99.65	98.84

NORMS

Q	24.01	18.76	26.61	28.68	18.56	26.21
OR	33.34	23.02	13.77	22.58	23.76	25.65
AB	34.32	43.81	44.65	36.65	44.49	38.80
AN	3.20	4.96	6.28	6.38	5.59	7.52
C	1.30	1.75	3.01	1.93	----	0.39
DI	----	----	----	----	1.37	----
HY	3.26	6.50	4.82	3.08	5.20	1.22
MT	0.21	0.34	0.29	0.21	0.34	0.09
IL	0.33	0.66	0.44	0.25	0.51	0.10
AP	0.05	0.19	0.15	0.24	0.17	0.02

TRACE ELEMENTS

Pb	67	35	43	47	26	71
Rb	270	110	94	159	102	193
Sr	197	219	146	303	180	279
Y	15	13	6	7	7	2
Zr	85	139	162	88	135	55
Zn	31	27	40	19	35	27
Cu	14	13	9	18	18	10
Ni	2	23	23	0	10	2
Ba	438	726	448	615	549	539
V	22	21	14	5	29	1
Cr	0	22	26	0	11	0
La + Ce	32	50	49	27	42	18

TABLE 6.4 (continued)

	Uncontam.	Contaminated by xenoliths				
MAJOR ELEMENTS	300-81	52-81	63-81	69-81	81-81	109-81
SiO2	66.4	67.9	67.8	68.1	67.5	66.2
TiO2	0.26	0.22	0.34	0.40	0.28	0.26
Al2O3	15.2	14.8	14.7	15.1	14.7	15.1
Fe2O3(t)	2.34	2.67	2.33	2.36	1.98	2.75
MnO	0.03	0.07	0.04	0.04	0.05	0.05
MgO	1.38	1.72	1.56	1.49	2.63	3.24
CaO	1.77	1.13	1.48	1.65	1.35	1.31
Na2O	4.52	3.87	3.98	4.06	4.59	4.92
K2O	2.96	4.54	4.60	4.42	3.19	3.16
P2O5	0.10	0.13	0.09	0.12	0.06	0.10
L.O.I.	3.27	2.95	2.37	2.00	2.62	2.88
Total	98.23	100.00	99.29	99.74	98.95	99.97

NORMS						
Q	22.90	22.28	21.04	21.24	21.52	16.84
OR	18.42	27.64	28.05	26.72	19.57	19.23
AB	40.28	33.74	34.75	35.15	40.32	42.88
AN	8.56	4.90	6.97	7.57	6.55	6.02
C	1.67	1.83	0.72	0.95	1.44	1.49
DI	----	----	----	----	----	----
HY	7.02	8.43	7.21	6.92	9.58	12.34
MT	0.40	0.43	0.39	0.39	0.33	0.45
IL	0.52	0.43	0.67	0.78	0.55	0.51
AP	0.24	0.31	0.22	0.28	0.14	0.24

TRACE ELEMENTS						
Pb	31	34	55	53	43	32
Rb	112	189	221	204	137	99
Sr	284	166	274	160	304	145
Y	10	12	9	12	9	9
Zr	174	163	155	154	116	115
Zn	7	55	55	73	43	43
Cu	13	11	8	12	12	11
Ni	9	20	22	13	98	100
Ba	596	713	673	578	470	558
V	23	30	34	33	39	43
Cr	7	29	33	23	156	151
La + Ce	59	59	56	48	35	37

TABLE 6.4 (continued)

Contaminated by xenoliths

MAJOR ELEMENTS	139-81	140-81	153-81	160-81	170-81	182-81
SiO_2	60.7	61.3	61.9	66.6	66.1	62.9
TiO_2	0.24	0.53	0.59	0.32	0.56	0.66
Al_2O_3	15.0	16.2	16.3	16.2	15.1	15.6
$Fe_2O_3(t)$	3.56	4.11	3.70	2.34	3.96	4.23
MnO	0.17	0.11	0.06	0.05	0.08	0.08
MgO	3.25	4.17	3.24	1.20	3.22	3.92
CaO	4.03	1.14	2.70	1.50	2.99	2.46
Na_2O	6.35	4.12	4.36	5.03	3.45	4.44
K_2O	0.16	3.70	3.22	3.64	2.10	3.16
P_2O_5	0.09	0.13	0.11	0.03	0.07	0.08
L.O.I.	5.15	3.23	2.49	2.21	1.05	1.20
Total	98.70	98.74	98.67	99.12	98.68	98.73

NORMS

Q	9.69	12.88	12.17	17.59	25.16	13.56
OR	1.01	22.89	19.78	22.20	12.71	19.55
AB	57.74	36.50	38.36	43.92	29.90	39.33
AN	12.78	5.03	13.18	7.48	14.73	12.23
C	----	3.83	1.04	1.37	1.93	0.62
DI	6.51	----	----	----	----	----
HY	11.26	16.82	13.42	6.35	13.67	12.83
MT	0.60	0.68	0.62	0.39	0.65	0.36
IL	0.49	1.05	1.17	0.63	1.09	1.31
AP	0.22	0.32	0.26	0.07	0.17	0.19

TRACE ELEMENTS

Pb	24	26	31	47	32	22
Rb	5	162	130	159	107	130
Sr	211	252	327	252	190	261
Y	12	15	13	13	14	17
Zr	131	145	149	141	142	159
Zn	38	50	57	36	76	43
Cu	22	11	16	13	9	17
Ni	66	71	97	16	78	92
Ba	104	660	546	520	369	539
V	68	73	40	15	57	56
Cr	163	140	143	4	124	129
La + Ce	42	53	42	43	41	42

Table 6.4 (continued)

Contaminated by xenoliths

MAJOR ELEMENTS	184-81	186-81	193-81	233-81	236-81	239-81
SiO2	64.9	68.6	68.6	67.5	64.0	63.3
TiO2	0.34	0.21	0.37	0.26	0.55	0.60
Al2O3	15.1	15.2	15.2	14.4	15.5	15.0
Fe2O3(t)	3.05	2.00	2.02	2.08	3.34	3.51
MnO	0.06	0.04	0.04	0.04	0.06	0.06
MgO	3.16	1.97	2.05	2.78	2.67	3.89
CaO	2.06	1.34	1.69	1.17	2.29	2.65
Na2O	4.24	4.56	4.60	4.07	4.36	4.05
K2O	3.13	3.48	3.01	3.72	2.99	3.39
P2O5	0.07	0.04	0.03	0.08	0.11	0.08
L.O.I.	2.72	1.95	1.57	2.51	3.24	2.33
Total	98.83	99.39	99.18	98.61	99.11	98.86

NORMS						
Q	18.10	22.35	23.11	22.75	17.36	13.94
OR	19.24	21.10	18.22	22.87	18.43	20.75
AB	37.33	39.60	39.88	35.84	38.48	35.50
AN	10.16	6.55	8.39	5.50	11.10	13.00
C	1.21	1.63	1.41	1.81	1.24	0.04
DI	----	----	----	----	----	----
HY	12.61	7.92	7.88	10.17	11.48	14.73
MT	0.51	0.33	0.33	0.35	0.56	0.59
IL	0.67	0.41	0.72	0.51	1.09	1.18
AP	0.17	0.10	0.07	0.19	0.27	0.19

TRACE ELEMENTS						
Pb	34	37	24	41	27	31
Rb	100	110	100	177	119	126
Sr	318	222	397	258	310	316
Y	12	9	10	8	10	9
Zr	146	132	131	113	144	136
Zn	46	40	41	42	61	55
Cu	20	13	9	17	11	12
Ni	87	55	54	97	79	130
Ba	571	507	694	529	607	515
V	42	30	32	34	49	53
Cr	102	95	92	167	125	196
La + Ce	60	44	45	41	48	43

TABLE 6.4 (continued)

Contaminated by xenoliths

MAJOR ELEMENTS	247-81	260-81	272-81
SiO2	60.8	61.0	67.1
TiO2	0.69	0.67	0.22
Al2O3	17.3	17.1	15.1
Fe2O3(t)	4.38	4.03	2.94
MnO	0.06	0.06	0.09
MgO	2.38	3.17	2.08
CaO	3.39	2.15	0.99
Na2O	5.35	5.39	3.85
K2O	1.76	2.67	2.49
P2O5	0.15	0.14	0.09
L.O.I.	3.08	2.11	3.42
Total	99.34	98.49	98.39

NORMS			
Q	10.33	8.41	29.73
OR	10.80	16.37	15.50
AB	47.03	47.32	34.31
AN	16.45	10.12	4.55
C	0.82	1.84	4.73
DI	----	----	----
HY	12.12	13.62	10.04
MT	0.72	0.66	0.49
IL	1.36	1.32	0.44
AP	0.36	0.34	0.22

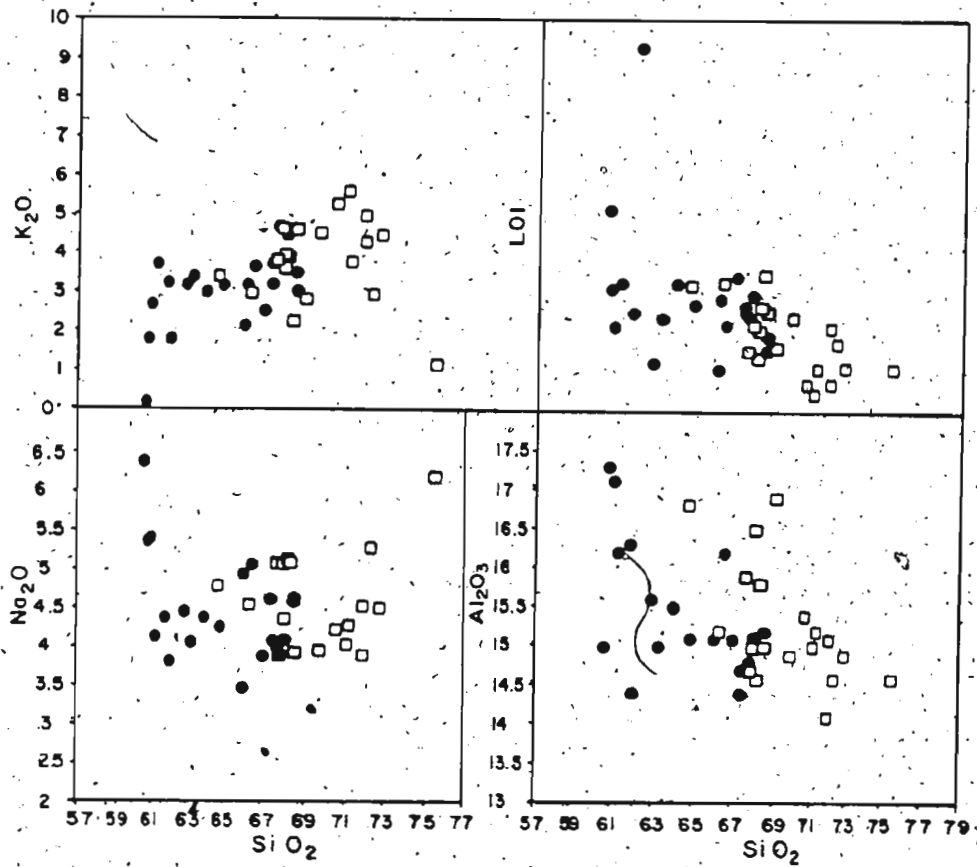| TRACE ELEMENTS			
Pb	20	20	40
Rb	71	56	97
Sr	325	300	128
Y	12	17	11
Zr	222	179	144
Zn	55	62	63
Cu	12	27	33
Ni	25	54	48
Ba	532	574	662
V	41	69	41
Cr	12	92	55
La + Ce	67	68	54

Figure 6.3 Harker variation diagrams for major and trace elements
of contaminated (•) and uncontaminated (□) Coaker
Porphyry.
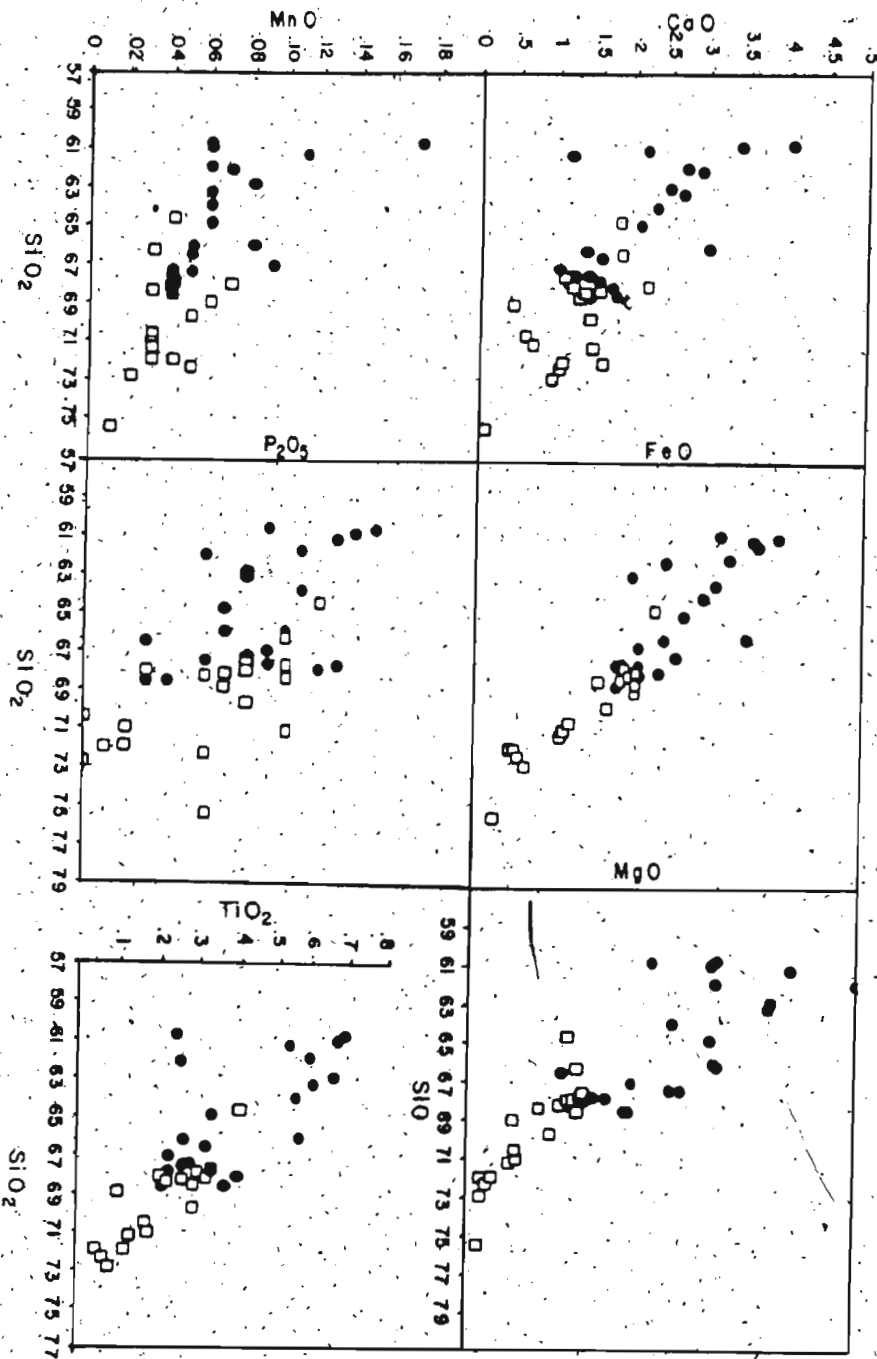
Figure 6.3 (continued)
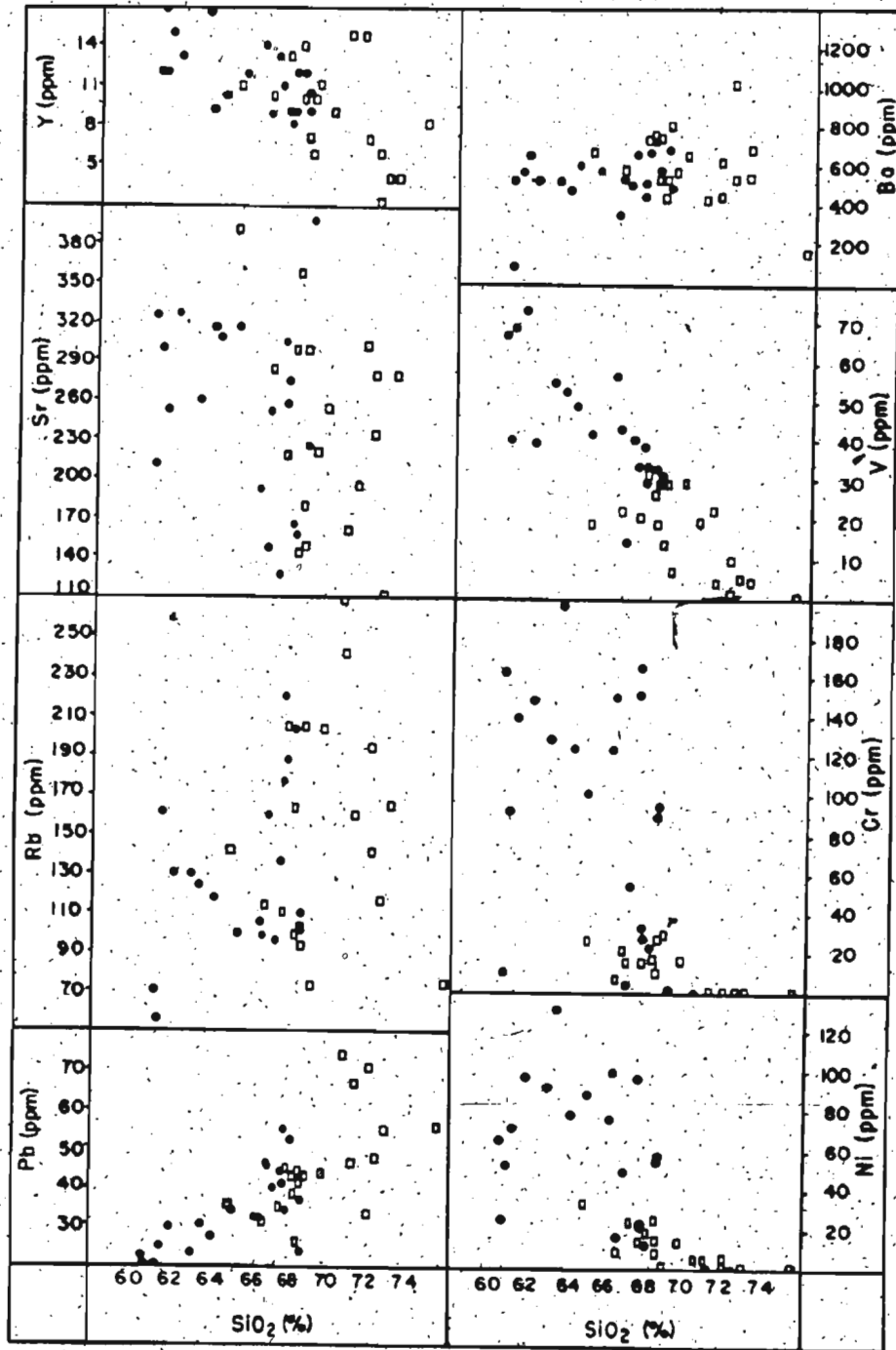
Figure 6.3 (continued)
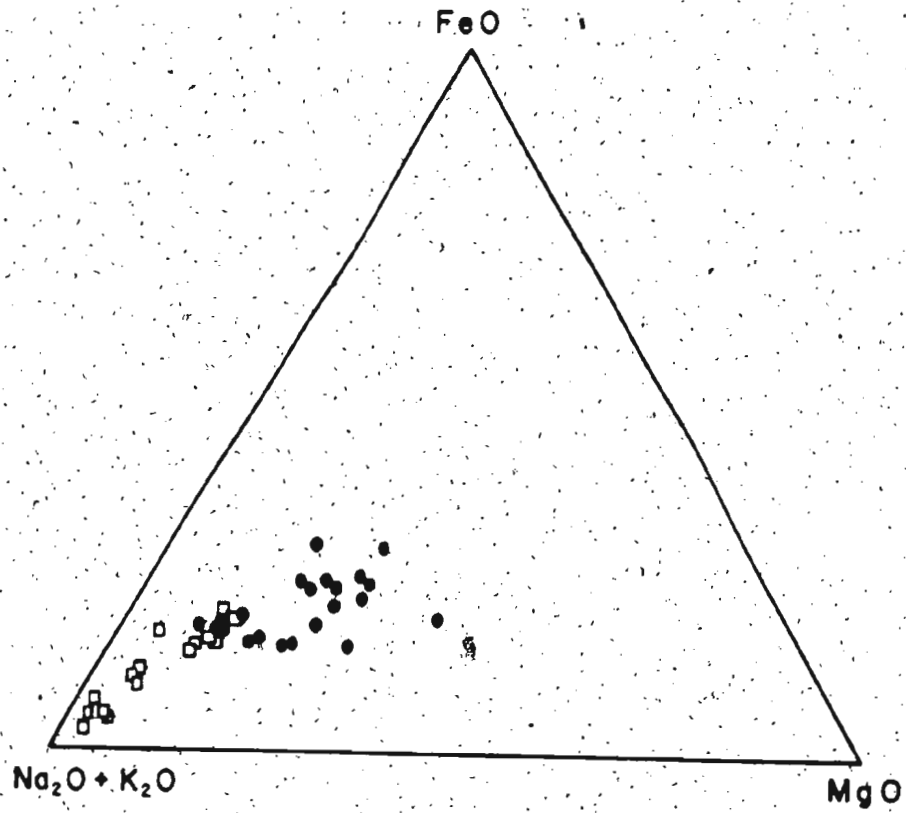
Figure 6.4 Alk-F-M diagram: Coaker Porphyry

to the discrimination diagram of Irvine and Baranger (1974), although
the application of this classification scheme to a suite of felsic
rocks with such a limited range in silica is of questionable validity.
Green (1980) has established a "silicic series" to encompass suites of
this kind.

6.2.1 Al2O3

The Coaker Porphyry is strongly peraluminous, with an average
Al2O3/(CaO+Na2O+K2O) ratio of 1.6 and an average of 1.56% normative
corundum. The only two samples analyzed which do not contain
normative corundum are among the "open system" samples discussed below
(section 6.2.2), in which secondary addition of Na2O to the rock had
occurred. The independence of normative corundum and silica (fig.
6.5a) over a silica range of 64 to 76% for uncontaminated Coaker
Porphyry, and 60 to 68% for Coaker Porphyry contaminated with
ultramafic material, indicates that the peraluminous nature of the
rock is primary, and not due to hornblende fractionation (Cawthorne
and Brown 1976), alkali leaching, or later contamination by sediments
(Huang and Wyllie 1981). One sample (BL-87-82) is from the stock on
Inspector Island associated with the interlayered mud and Coaker
Porphyry (Chapter 4), and hence is the most likely sample to display
the effects of assimilation of host sediments. It is one of the open
system samples discussed below. Its corundum content (1.17) is lower
than the average; any alumina gained from the sediment was more than
offset by alkali gain from fluid exchanges during emplacement.

Figure 6.5 A1203 saturation in Coaker Porphyry.

A. Normative corundum (Co) and diopside (Di) show
no consistent variation with Si02 content. Both
contaminated and uncontaminated Coaker Porphyry are
depicted.

B. Normative corundum increases with iron in
uncontaminated Coaker Porphyry, indicating that the
source of the magma was even richer in A1203 than
was the magma itself.
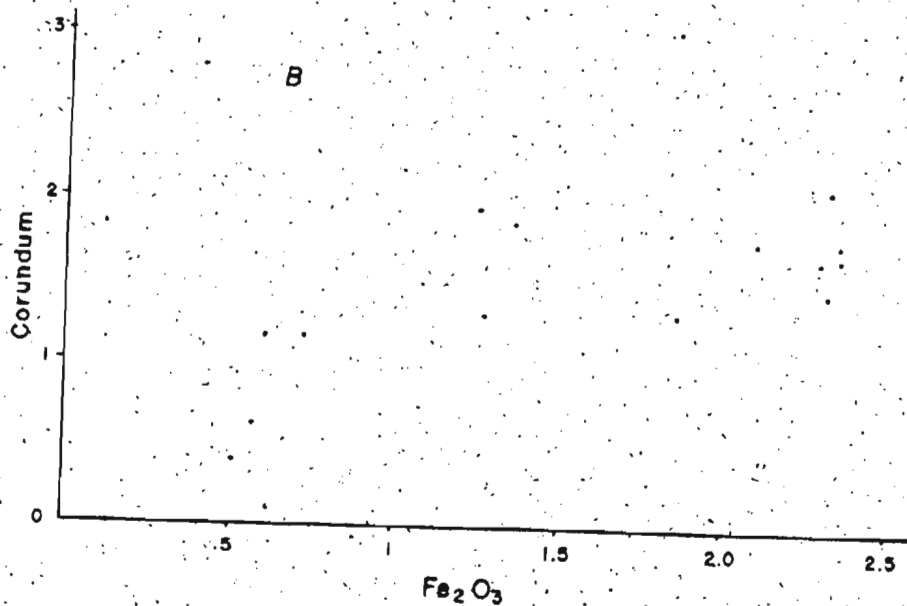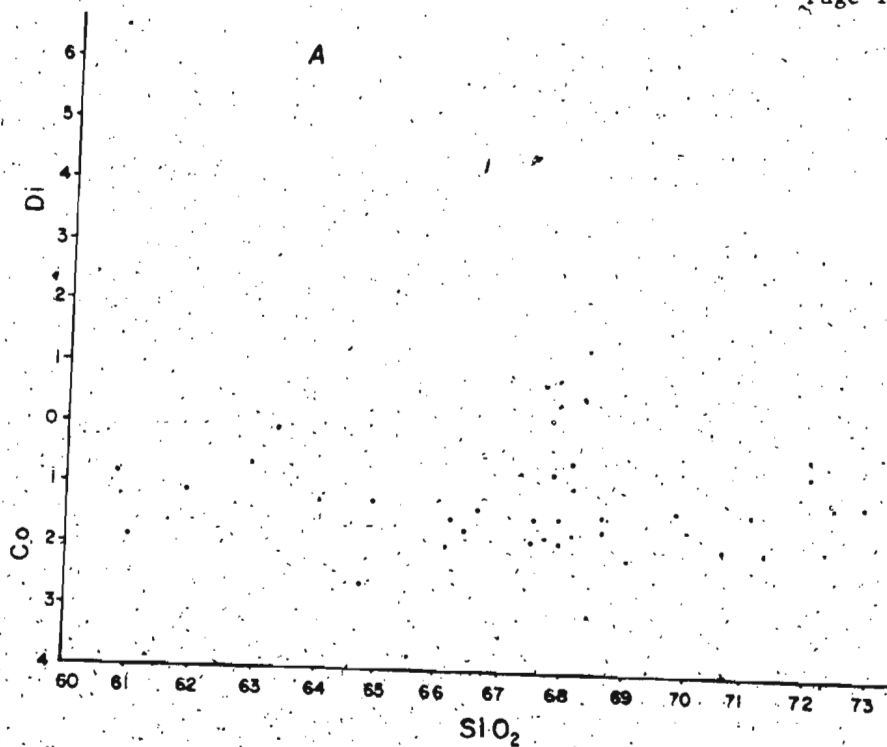
A plot of Fe2O3(t) vs normative corundum (fig. 6.5b) illustrates that corundum increases with iron, indicating that the Coaker Porphyry melt was less aluminous than its source (Wyborn et al., 1981). This trend is the opposite of that expected if the Coaker Porphyry had evolved from a metaluminous composition by amphibole fractionation, and strongly suggests that it originated by partial melting of a highly aluminous source.

6.2.2 Alkalis

Figure 6.6 is a plot of feldspar compositions obtained by microprobe analysis. Most of the feldspars have been albitized, and do not have igneous compositions. These data indicate that one of the following must have occurred:

a) Na^+ was gained,

b) K^+ and/or Ca^{++} were lost,

c) both (a) and (b) occurred,

d) a redistribution of these elements occurred within a closed system.

In case (d), K^+ and Ca^{++} would not be lost from the Coaker Porphyry, but would enter into other minerals (ie.: sericite, calcite).

An

Ab

Or
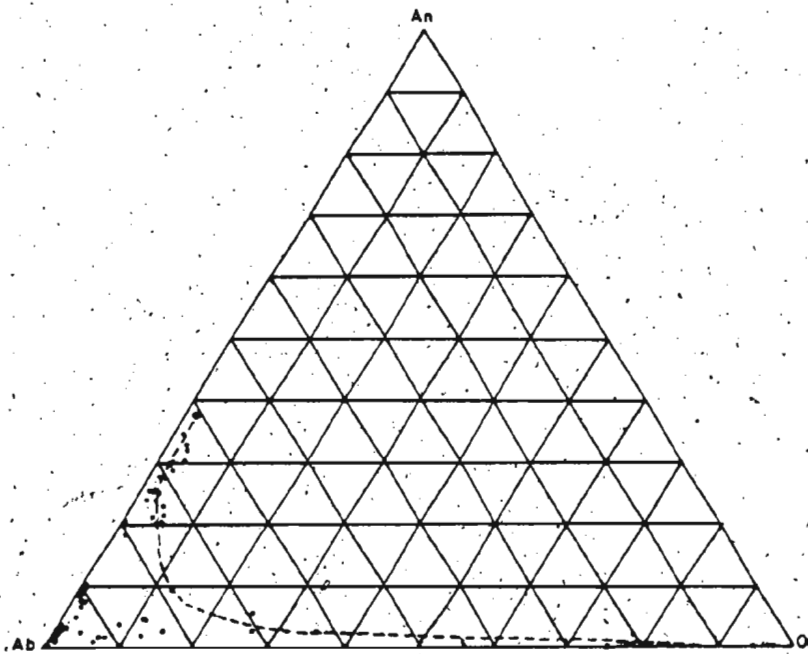
Figure 6.6 Feldspar compositions plotted from microprobe data.
Feldspars falling on the dashed line have primary
igneous composiotions, whereas those falling into the
albite corner have secondary compositions.

To test these cases, normative albite, anorthite, and orthoclase were plotted on the Ab/An/Or diagram, with the assumption that if these values plotted along a line of igneous feldspar compositions, then albitization represented a rearrangement of alkalis rather than a gain or loss of elements from the system.

Because the Coaker Porphyry has K-feldspar in the groundmass (and rarely as a phenocryst phase), a K-feldspar factor was subtracted from the normative feldspars according to the empirical equation:

$$K\text{-feldspar} = (.1)Ab + (.05)An + (.85)Or$$

This produced a normative K-feldspar having a composition similar to that obtained by microprobe analysis.

The remaining normative feldspar was recalculated to 100% and plotted on the An/Ab/Or diagram (fig. 6.7). Most of the values fell on or near an igneous composition line, indicating that albitization had occurred in an essentially closed system. However, several points did deviate from the line into the secondary albite field. These "open system" samples were identified on variation diagrams and were found to have suffered a gain in sodium, and a loss of CaO, Sr, P2O5, Rb, Cu, and K2O. K2O loss did not occur in all samples, however. Sr was removed preferentially to CaO. Other elements, including Ba and Pb, were not apparently affected.

Mass balance calculations indicate a 15% gain in albite component in the "open system" samples.
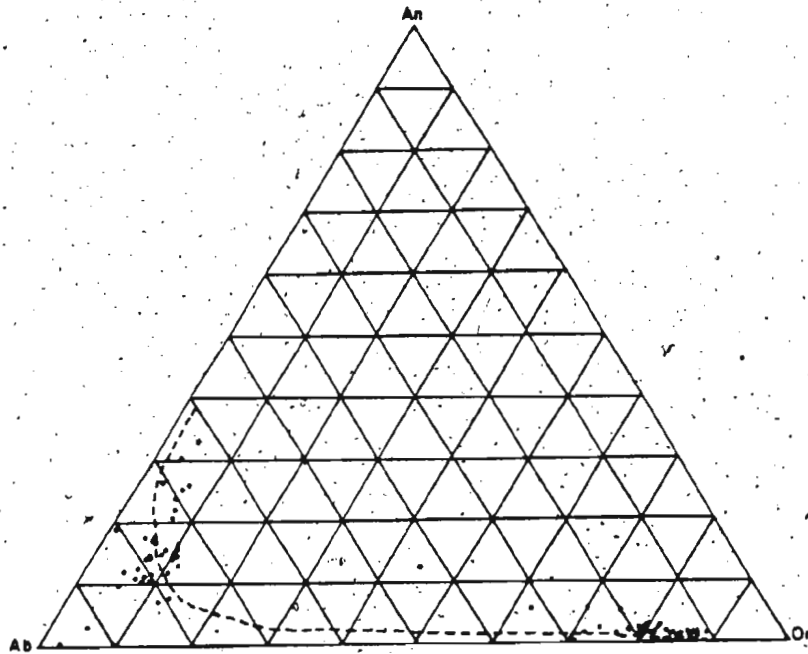
Figure 6.7 Feldspar compositions calculated from CIPW norms. Those
samples whose normative feldspars fall on or near the
line of igneous composition are interpreted to have been
altered within a closed system (without a gain or loss
of alkalis from the rock). Those falling in the albite
corner are interpreted as open system samples, to which
Na has been added and/or from which K or Ca have been lost.

6.2.3 Rare Earth Elements (REE)

Samples of Coaker Porphyry show a wide range in REE content (fig. 6.8, Table 6.5). With increasing SiO_2, REE content falls off rapidly, and the light REE (LREE) change from enriched in the more mafic samples to progressively more depleted in the more silicic rocks (fig. 6.9). The most silicic rocks have a peculiar pattern depleted in both LREE and HREE relative to the middle REE. Clearly, the REE did not behave as incompatible elements during the evolution of the Coaker Porphyry magmas.

A strong positive coorelation exists between La+Ce and Zr, and a somewhat weaken correlation between La+Ce and P_2O_5 and TiO_2, as illustrated by the variation diagrams in fig. 6.9. Similarly positive correlations exist between Y, which behaves like the HREE, and Zr, P_2O_5, and TiO_2 (fig. 6.10). These results indicate that REE content in the Coaker Porphyry was controlled by the accessory phases zircon, sphene or rutile, and apatite.

The REE pattern of the more mafic samples of Coaker Porphyry has LREE strongly fractionated relative to HREE, indicating that the HREE were retained by garnet or hornblende, either as a fractionating or a residual phase.

Eu anomalies are small and inconsistent. Most phases interacting with a granitic magma (hornblende, garnet, plagioclase, K-feldspar, etc.) result in either a positive or a negative Eu anomaly. Petrographic and geochemical results, and mass balance calculations (discussed below), indicate that several phases are involved which
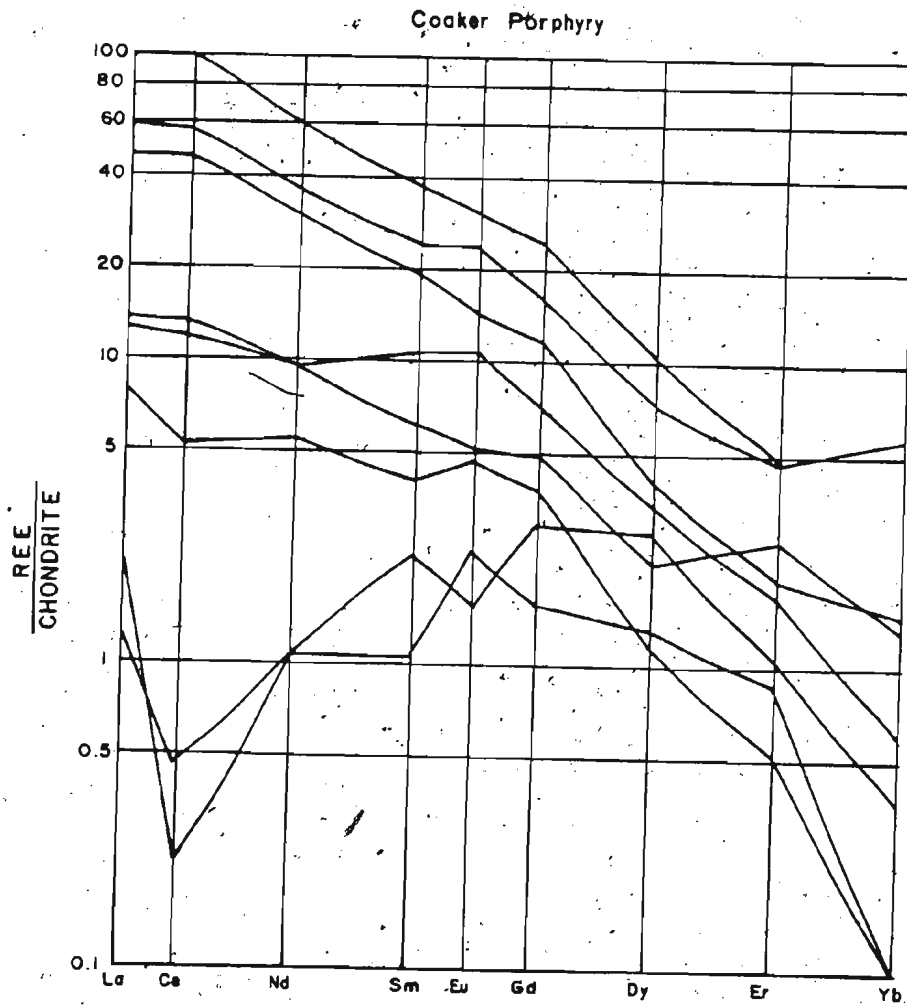
Figure 6.8 REE/Chondrite: Coaker Porphyry

TABLE 6.5

Rare Earth Elements: Coaker Porphyry

Element (ppm)	87-82	89-81	129-81	239-81	247-81	260-81	276-81	285-81
La	2.50	3.99	0.39	14.96	31.64	18.54	4.28	0.67
Ce	4.32	9.74	0.38	38.15	80.45	46.40	10.80	0.19
Nd	3.32	5.62	0.64	17.94	36.26	21.44	5.65	0.69
Sm	0.79	1.22	0.45	3.79	7.32	4.73	2.13	0.20
Eu	0.34	0.37	0.11	1.03	2.23	1.70	0.76	0.17
Gd	0.98	1.23	0.75	2.97	6.28	3.90	1.76	0.41
Dy	0.38	0.70	0.88	1.32	3.30	2.34	1.20	0.42
Er	0.11	2.55	0.22	0.42	1.04	1.01	0.35	0.19
Yb	0.00	0.28	0.08	0.31	0.00	1.18	0.12	0.00

Chondrite Norm.

	87-82	89-81	129-81	239-81	247-81	260-81	276-81	285-81
La	7.94	12.66	1.25	47.50	100.45	58.84	13.59	2.13
Ce	5.31	11.98	0.47	46.93	98.95	57.07	13.28	0.24
Nd	5.56	9.41	1.08	30.05	60.73	35.91	9.46	1.16
Sm	4.01	6.20	2.26	19.24	37.17	24.00	10.83	1.03
Eu	4.72	5.15	1.54	14.30	30.94	23.52	10.57	2.36
Gd	3.80	4.76	2.90	11.49	24.25	15.08	6.81	1.59
Dy	1.17	2.17	2.72	4.05	10.16	7.21	3.70	1.31
Er	0.53	2.55	1.04	1.95	4.87	4.75	1.64	0.89
Yb	0.00	1.36	0.37	1.49	0.00	5.68	0.58	0.00
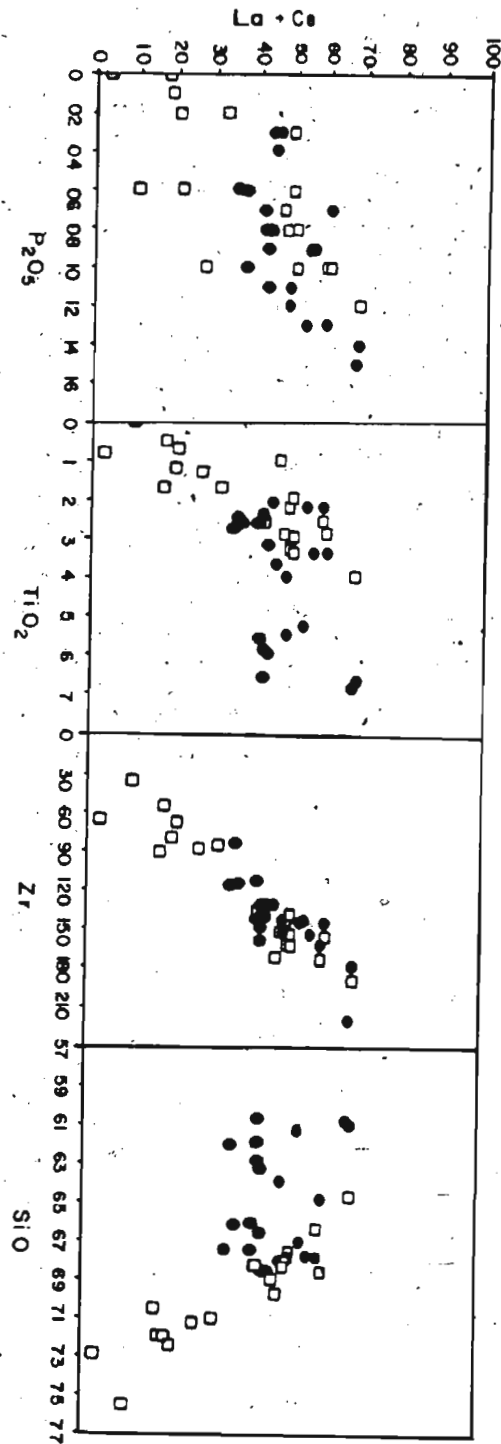
Figure 6.9 Light REE (La + Ce) versus P2O5, TiO2, Zr and SiO2..
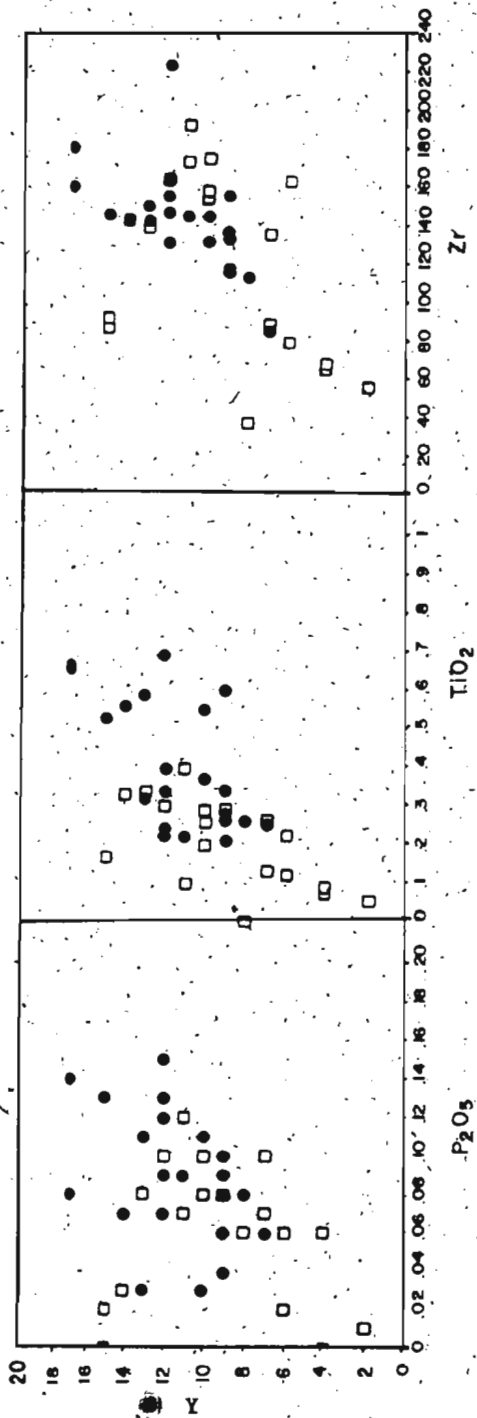
Figure 6.10 Y versus P2O5, T1O2 and Zr

combine to nullify each other's effects on Eu content (see Hanson 1978).

6.2.4 Zirconium

Zr solubility in peraluminous melts is extremely low; approximately 60 ppm Zr would be needed to saturate the magma (Watson 1979). Zr solubility is inversely related to $Al_2O_3/(Na_2O+K_2O)$, and is lowered still further by the presence of Fe and Ca. It is independent of SiO_2 content or Na_2O/K_2O ratio.

Partial melting of a zircon-bearing source produces initial liquids that are saturated in Zr, and zircon persists as a residual phase that buffers Zr content in the melt. Zr content should therefore remain constant over a wide range of percentages of partial melting (Watson 1979).

Zr content in the Coaker Porphyry is inversely proportional to SiO_2 (fig. 6.11), and ranges from 191 ppm to 36 ppm. Zr contents greater than 60 ppm reflect the presence of extra zircon, of either a primary cumulate origin, or of a xenocrystic origin. The relationship with SiO_2 is not a result of partial melting or solubility effects. Nor do Zr contents or SiO_2 show a correlation with alteration. The relationship must therefore reflect fractionation of crystal phases from the melt or addition of crystal phases to the melt.
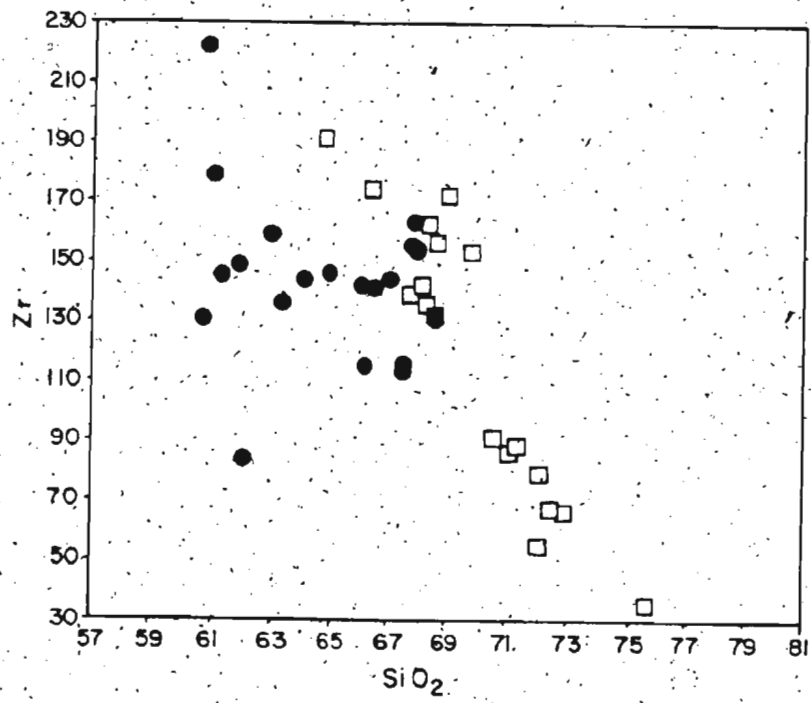
Figure 6.11 Zr versus SiO2,

Settling and accumulation of minute zircon crystals in a siliceous magma is unlikely, particularly in view of the Coaker Porphyry's proven ability to carry large ultramafic xenoliths. The observed Zr behavior in the Coaker Porphyry could be the result of one or both of the following:

1) Zircons trapped in phenocrysts (biotite, plagioclase, quartz), were concentrated by differentiation; flow differentiation and filter pressing are more common mechanisms of differentiation of felsic magmas than is crystal settling (Burnham and Ohmoto 1981).

2) Zirconium content, as well as the concentrations of the other elements, is a function of the amount of restite contained in the magma (White and Chappel 1977), the most siliceous Coaker Porphyry being the purest sample of the liquid.

With the possible exception of glomeroporphyritic clumps of feldspar, there are no obvious restite materials or minerals (ilmenite, cordierite, almanidine, sillimanite, pyroxene) in the Coaker Porphyry. (Evidence is presented below that the ultramafic xenoliths do not represent samples of the source of the Coaker Porphyry, and that the garnets are products of the reaction between the magma and the ultramafics). Therefore, explanation (1) is preferred. The silicic Coaker Porphyry samples are those from which the phenocryst phases have been removed, and the mafic samples are those in which phenocrysts were concentrated. The implication, then, is that the mafic samples contain more phenocrysts, and the felsic samples fewer, than actually crystallized from their particular liquid.

compositions.

6.2.5 Other Trace Elements

Rb and Pb increase with both K_2O and SiO_2, and show a strong positive correlation with each other, indicating that Rb, Pb, and K_2O were all incompatible elements that became concentrated in the residual liquid (fig. 6.12). The K/Rb ratio decreases slightly as Rb increases, indicative of biotite fractionation (Harris et al. 1983) (fig. 6.13).

The Rb/Sr ratio increases, and the Sr/Ba ratio decreases, with increasing SiO_2 (fig. 6.14), both of which are indicative of plagioclase fractionation (Hanson 1978). A decrease in the Rb/Sr ratio with increasing Sr (fig. 6.13) is consistent with both plagioclase and biotite fractionation (Harris et al. 1983).

Cu shows no correlation with SiO_2, Zn, Pb, or $Fe_2O_3(t)$. Zinc and lead are also independent, the former substituting for iron in mafic minerals (biotite), and the latter concentrating in residual liquids. These observations, and the absence of a sulfide phase such as pyrite in the Coaker Porphyry, indicate that S was probably of little importance as a component of fluid or phenocryst phases.
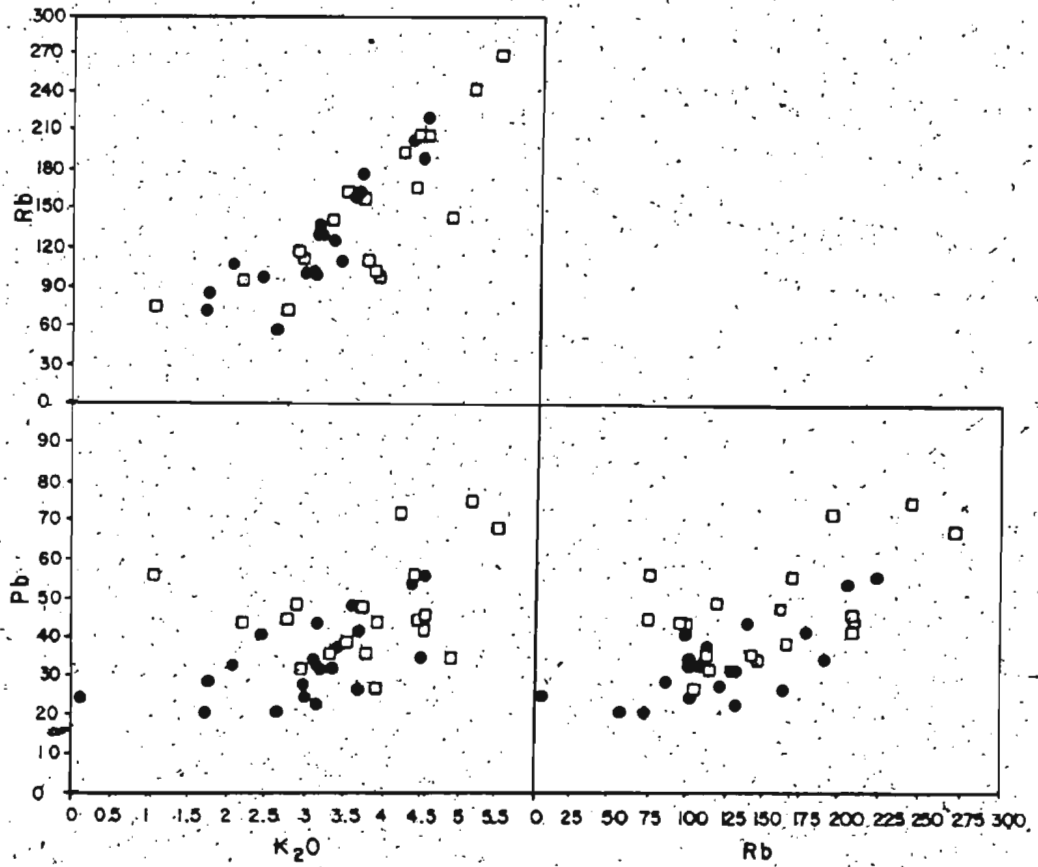
Figure 6.12 Correlations among the incompatible elements Rb, Pb and K2O.
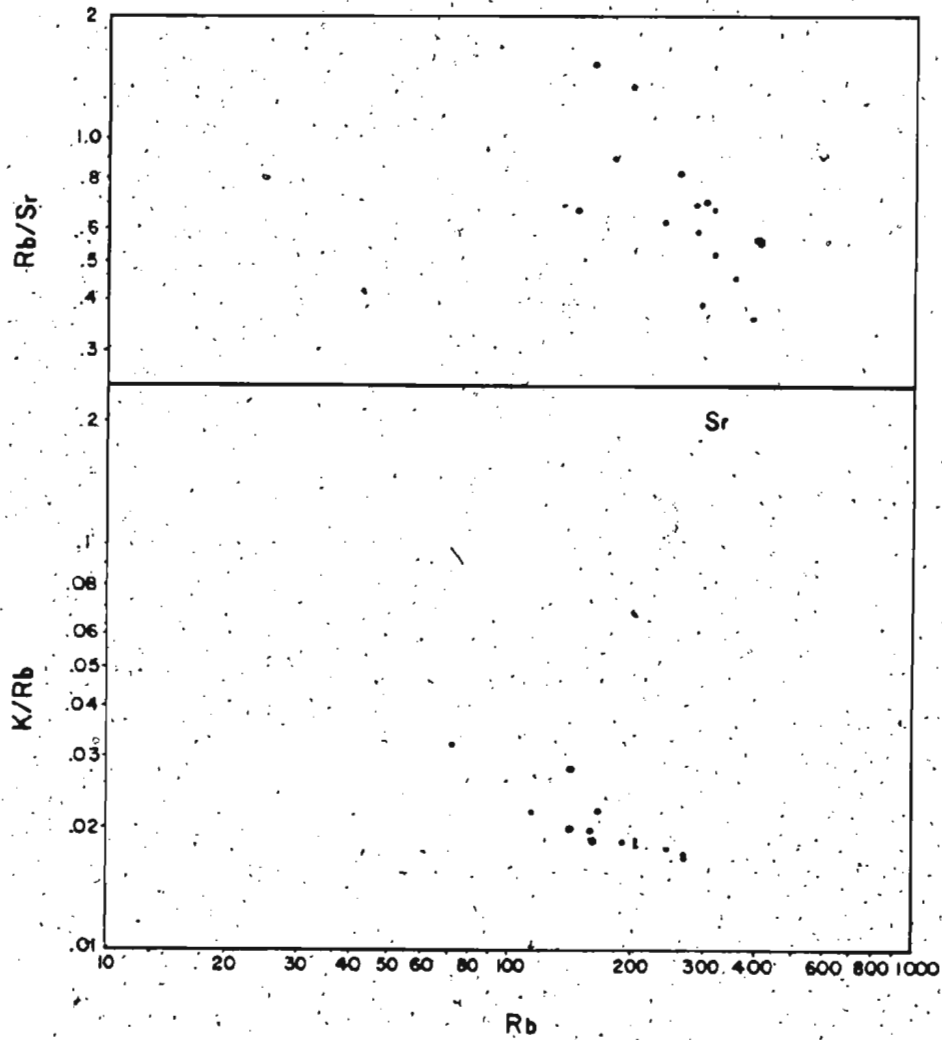
Figure 6.13 Rb/Sr versus Sr and K/Rb versus Rb. Data plotted are from closed-system, uncontaminated Coaker Porphyry.
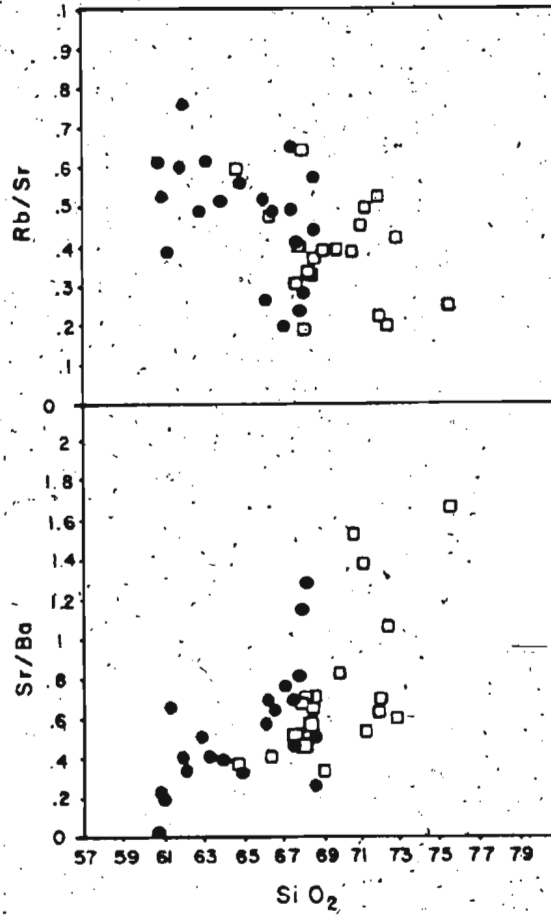
Figure 6.14 Sr/Ba and Rb/Sr versus SiO2.

6.3 Effects of contamination of the magma by ultramafic xenoliths

The mineralogical and textural effects of the interaction between the ultramafic xenoliths and their host magma are discussed in sections 6.1.4 through 6.1.6. The effects of the xenoliths on the chemistry of the Coaker Porphyry can be seen in fig. 6.3., where the compositions of contaminated and uncontaminated samples are plotted in a series of variation diagrams, and in Table 6.4, where the average compositions of the contaminated and uncontaminated samples are given. Predictably, the contaminated samples are enriched in $Fe_2O_3(t)$, MgO, CaO, TiO_2, V, Cr, and Ni, and are depleted in SiO_2, Na_2O, K_2O, Rb, and Pb, relative to the uncontaminated magmas.

The contaminated samples that were analyzed were those containing relatively few xenoliths, and xenoliths were removed from the sample where possible. However, because of the small size of some xenoliths, complete removal was impossible. The analyses reflect the contributions of Coaker Porphyry, minerals resulting from the xenolith-magma reaction, and small xenoliths. Mass balance calculations indicate that 10 to 20% ultramafic components were incorporated into the samples. None of the samples analyzed has a silica content of less than 60%.

6.3.1   Comparisons   with   the   experimental   system
KAlSiO4-Mg2SiO4-SiO2-H2O

Sekine and Wyllie (1982a and b) investigated the system
KAlSiO4-Mg2SiO4-SiO2-H2O at pressures between 20 and 30 kbar. They
found that the interaction between hydrous silicic liquid and
peridotite resulted in the precipitation of three mineral assemblages:
phlogopite (Ph), phlogopite + quartz (Qz), and phlogopite + enstatite
(En), accompanied by the evolution of H2O (V). The three critical
reactions occurring in the system are (1) the quaternary eutectic
reaction Ph + Sanidine (Or) + Qz + V = L at 680 C, (2) the peritectic
reaction Ph + Qz + V = En + L at 750 C, and (3) the peritectic
reaction Ph + En + V = Fo + L at 1,130 C.

The assemblages preserved by quenching of the contaminated Coaker
Porphyry are Ph + L and Ph + Qz + L. The presence of quartz
megacrysts in the latter case indicates precipitation in the Qz + L
field prior to the precipitation of phlogopite. No enstatite (opx)
has been observed as a phenocryst phase in contaminated Coaker
Porphyry, suggesting, in light of the experimental results , that the
temperatures of hybridization were low (lower than 750 C in the
H2O-saturated experimental system - fig. 6.15).

Hornblende is present as a phenocryst phase in contaminated
Coaker Porphyry, but does not appear in any of the systems
investigated by Sekine and Wyllie (1982a,b,c). These systems include
KAlSiO4-Mg2SiO4-SiO2-H2O +/- CaO, Na2O, and Al2O3, and an experiment
involving natural granite and natural peridotite. Their experiments

Figure 6.15 Mg_2SiO_4 – $KAlSiO_4$ – SiO_2 phase diagram after Sekine and Wyllie (1982a) showing possible reaction paths for two Coaker Porphyry liquids (LA and LB). LA: L1A is pure liquid or liquid + k-spar. It reacts with peridotite (P), moving towards the P composition until it reaches composition L2A. At this point, phlogopite begins to precipitate. The magma is quenched at point L3A, leaving Coaker Porphyry groundmass + phlogopite +/- k-spar.

LB: L1B consists of liquid + quartz. It reacts with peridotite (P), moving towards the P composition until it reaches composition L2B, where phlogopite joins quartz as a crystallizing phase. Quenching at point L3B gives rise to a L (Coaker Porphyry groundmass) + Qz + Phlog composition.

Mg_2SiO_4

FO

P

−700°C

20−30 KBAR
H_2O− SATURATED

En

Fo+En+Ph

Ph

En+Ph+Qz

Ph+Or+L

Ph+L

Ph+Qz+L

L3A L3B

L2B

KAISiO₄

Or

L2A LIA

LIB

SiO_2
Qz

① Or+L
② L
③ Qz+L
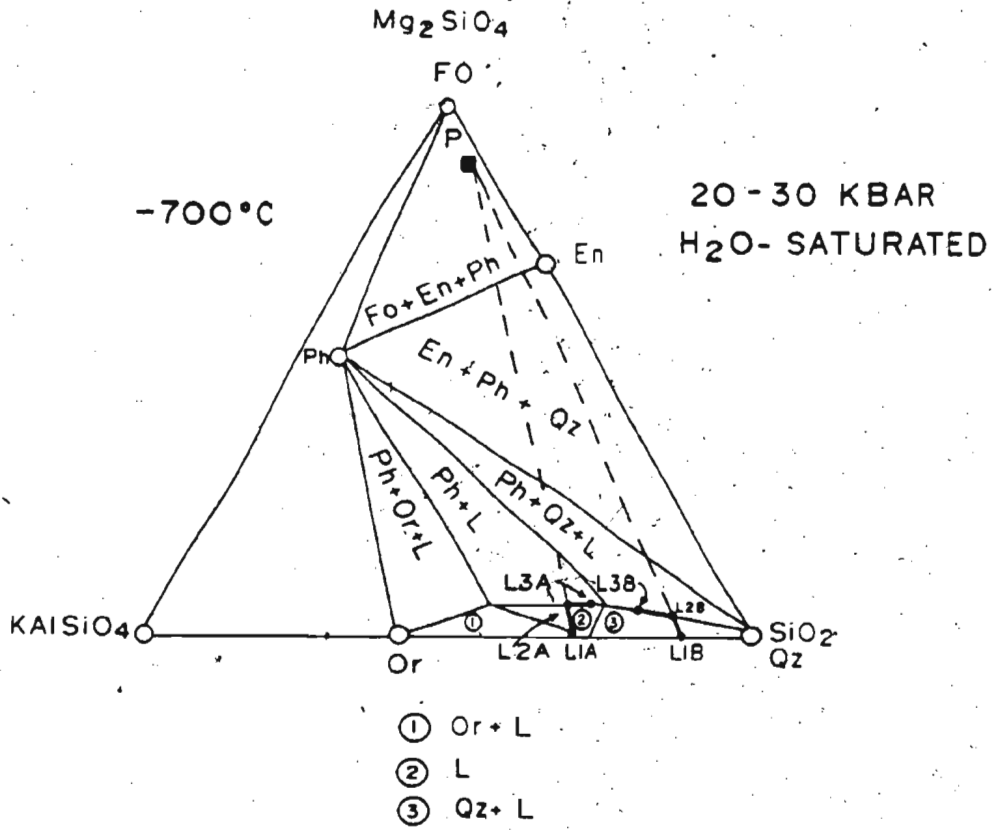
were conducted at 20 to 30 kbar, above the stability range of hornblende. The hybridization between the Coaker Porphyry and its xenoliths must have occurred or continued below this pressure. The invariant point for reactions (1) and (2) above occur at about 0.5 kbar (Sekine and Wyllie 1982a), indicating a minimum pressure of 0.5 kbar for the production of phlogopite. The absence of opx phenocrysts in the contaminated Coaker Porphyry suggests that the pressure was probably somewhat higher than the minimum.

Sekine and Wyllie (1982b) have determined that a garnet solid solution rich in pyrope component is produced in the system $CaAl_2Si_2O_8$-$KAlSiO_4$-Mg_2SiO_4-SiO_2-H_2O at high (30 kbar) pressure by the reaction (4) Opx + L = Py-rich garnet +Qz + V. The garnets in the Coaker Porphyry contain a large almandine component (but very low spessartine), but are unusually rich in Py and Gr for igneous garnets from felsic rocks. They correspond roughly to the compositions obtained by Green and Ringwood (1972) by crystallization of a garnetiferous rhyolite at 18 kbar pressure under hydrous conditions (fig. 6.2). Phase relationships determined by Green and Ringwood (1972) indicate that garnet is a liquidus phase in systems with high H_2O, and quartz in systems with low H_2O. Interestingly, Green and Ringwood (1972) were unable to reproduce experimentally the Alm-rich garnets more commonly found in natural systems. The occurrence of this garnet in the Coaker Porphyry indicates hybridization at pressures in the upper part of the hornblende stability range.

Table 6.2 gives the average composition of the garnet from the Coaker Porphyry, The composition of the rock in which the garnet occurs is given in Table 6.4. If the rock composition is assumed to correspond with the liquid coexisting with the garnet, the calculated K(d) is large, indicating a low temperature below 900 C according to Green (1977).

6.3.2 Mineral compositions – experimental and natural

Table 6.6 compares the chemistry of Coaker Porphyry garnets, phlogopite, and magnesiohornblende to garnets, phlogopite, and clinopyroxene obtained by the experimental mixing of a natural granite and peridotite (Sekine and Wyllie 1982c), and to phlogopite, magnesiohornblende, and clinopyroxene from a xenolith-bearing rhyodacite associated with the New England Batholith, Australia (Flood et al. 1977).

The experimentally derived minerals were obtained at 30 kbar pressure from a mixture of 90% granite with 10% peridotite; temperatures were 830 C for phlogopite, 850 C and 900 C for the clinopyroxene, and 900 C for the garnet (Sekine and Wyllie 1982c).

The New England rhyodacite contains xenoliths of orthopyroxene, clinopyroxene, and plagioclase, and combinations thereof, which are partially to totally replaced by magnesiohornblende and/or biotite. The magma contains phenocrysts of quartz, andesine, biotite, magnesiohornblende, clinopyroxene, rare orthopyroxene, K-feldspar, and magnetite in a quartzofeldspathic groundmass (Flood et al. 1977).

.TABLE 6.6

Comparisons of Mineral Compositions from Contaminated Coaker Porphyry,
New England Batholith, and Experimental Results

Oxide (wt. %)	Phlogopite (Ave. C.P.)	Phlogopite (Ave. 4 Ml)	Biotite (N.E.)
SiO2	38.82	45.2	36.52
TiO2	3.13	1.1	5.07
Al2O3	16.09	16.3	13.49
FeO(t)	12.40	3.81	18.97
MnO	0.10	----	0.17
MgO	16.13	20.6	11.00
CaO	0.00	0.0	0.14
Na2O	0.38	0.0	0.28
K2O	8.80	9.56	8.82
Total	95.85	96.65	94.46

Oxide (wt %)	Hornblende (Ave. CP)	Hornblende (N.E.)	Clinopyroxene (N.E.)	Clinopyroxene (Ave. 6 Ml)
SiO2	52.05	46.33	52.65	55.3
TiO2	0.54	1.49	----	---
Al2O3	6.12	8.03	0.90	8.78
FeO(t)	9.22	16.51	11.90	3.48
MnO	0.20	0.49	0.74	----
MgO	17.91	12.13	12.21	11.3
CaO	10.20	10.42	21.13	14.1
Na2O	1.04	1.24	0.33	5.12
K2O	0.22	0.84	----	---
Total	97.50	97.48	99.86	98.99

Garnets

Oxide (wt %)	CP (High Mg)	CP (High Ca)	CP (High Fe)	Ml
SiO2	39.91	38.00	38.03	42.1
TiO2	0.22	0.15	0.55	0.0
Al2O3	22.75	21.93	21.94	23.3
FeO(t)	19.12	24.81	26.10	11.0
MnO	0.41	0.46	0.78	0.32
MgO	12.12	5.75	3.91	17.9
CaO	6.52	9.72	9.98	5.18
Cr2O3	0.02	0.02	0.00	0.65
Total	101.07	100.84	101.34	100.45

The experimentally obtained garnets are richer in MgO and poorer in FeO, CaO, and TiO2 than even the most Py-rich garnet of the Coaker Porphyry. Similarly, the experimental phlogopite is richer in MgO and SiO2, and poorer in FeO and TiO2 than the Coaker Porphyry phlogopite. The New England biotite has even lower SiO2 and MgO and higher FeO and TiO2 than the Coaker Porphyry phlogopite, and is also lower in Al2O3 than the two phlogopites.

The New England magnesiohornblende, like the biotite, is poorer in SiO2 and MgO, and richer in FeO and TiO2 than its Coaker Porphyry equivalent.

The Coaker Porphyry magnesiohornblende is similar in composition to the experimentally obtained clinopyroxene, except that the latter has a large jadeite component in the pyroxenes, and hence is enriched in Na and Al. Jadeite was a component of the original peridotite used in the experiment. The New England clinopyroxene, predictably, is lower in MgO and higher in FeO than the experimental clinopyroxene; it also lacks the jadeite component.

The observed differences between the three groups of minerals is most likely a function of the composition of the material contaminating the magma. The experimental contaminant was a partially hydrated peridotite mylonite of mantle derivation. The Coaker Porphyry was contaminated with gabbroic as well as ultramafic material, contributing a larger amount of FeO, TiO2, and CaO than would have been available from peridotite alone. The xenoliths of the New England rhyodacite are from a cumulate gabbro or an anhydrous

residuum from a partial melting event (Flood et al. 1977), accounting

for the even greater FeO and TiO2 in these minerals. Other

differences, such as variations in CaO, SiO2, and Al2O3, are probably

governed by factors such as partition coefficients among other phases

present (such as orthopyroxene, magnetite), pressure, temperature, and

P(H2O).

6.4 Rb/Sr Isotopic Geochemistry

Data and statistics for the Rb/Sr isotopic compositions for eight

samples are given in Table 6.7. One of these points, that for the

garnetiferous Coaker Porphyry, was a large distance off the isochron

and was removed from the calculations. Removal of other single points

from the calculation did not affect to any great extent the slope or

intercept of the isochron. Three of these samples were afterwards

determined to have been albitized; however, the albitization event is

the same age as the magmatic event, and a net loss of Rb and Sr from

the system occurred.

The Sr(87)/Sr(86) vs Rb(87)/Sr(86) diagram yields an age of 445.3

+/- 8.2 Ma for the Coaker Porphyry, and an initial Sr(87)/Sr(86) ratio

of .71033 +/- .00018 (fig. 6.16). Initial ratios higher than .706

are indicative of a sedimentary source for the magma (White and

Chappel 1977).

TABLE 6.7

Rb-Sr Data for Coaker Porphyry

Rb(87)/Sr(86)	STD DEV	Sr(87)/Sr(86)	STD DEV
4.634780	0.046348	0.739876	0.000116
1.507680	0.015077	0.718945	0.000440
2.020390	0.020204	0.722900	0.000117
2.337370	0.023374	0.723564	0.000829
3.050980	0.030510	0.729054	0.000164
1.779620	0.017796	0.721608	0.000021
1.988540	0.019885	0.723408	0.000033
0.533070	0.005331	0.713695	0.000057

Intercept	0.710329 +/- 0.000183
Slope	0.006343 +/- 0.000117
Age (Million years)	445.268027 +/- 8.161694
Covariance	-0.000000
Correlation Coefficient	-0.812794
Chi-squared	29.132593
Chi-squared	
Degrees of Freedom	4.855432
Degrees of Freedom	6
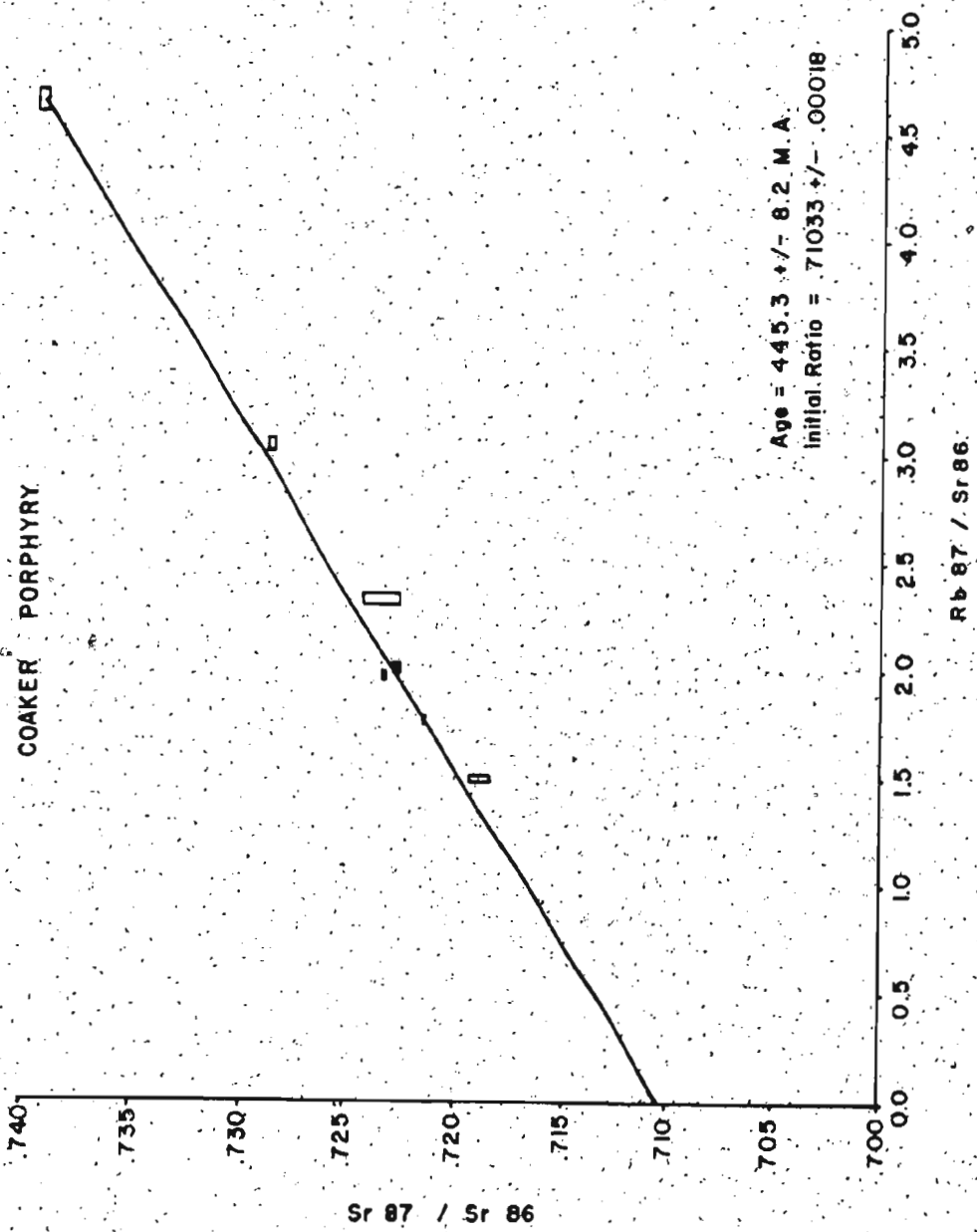
Figure 6.16 . Whole-rock Rb/Sr isochron: Coaker Porphyry.

6.5 The source of the Coaker Porphyry

Potential sources from which the Coaker Porphyry might have been derived include:

1) the mantle

2) metavolcanics, (amphibolite)

3) sediments, metasediments

Three factors support a volcanic or mantle source for the Coaker Porphyry. These are:

1) the occurrence of the Coaker Porphyry in the oceanic Dunnage Zone,

2) the presence of ultramafic xenoliths in the Coaker Porphyry, which, according to White and Chappel (1977), would most likely be samples of the source of the magma, and

3) high $Na2O$, which is characteristic of a magma derived from a source that has not undergone a surficial weathering cycle (Chappel and White (1974).

However, several factors indicate that the Coaker Porphyry arose from a sedimentary rather than an igneous source:

1) limited $SiO2$ range (from 64 to 76%) is characteristic of S-type (sediment-derived) felsic suites (Chappel and White 1974, Hine et al 1978),

2) the high Sr(87)/Sr(86) ratio of 0.71033 +/- .00018 precludes a mantle origin for the Coaker Porphyry unless considerable contamination by crustal material is invoked. The low scatter of points on the isochron strongly suggests that such contamination is unlikely.

3) the presence of primary igneous muscovite is characteristic of S-type magmas.

4) the corundum-normative character of the Coaker Porphyry indicates that the Coaker Porphyry evolved from a highly aluminous source. Hornblende fractionation is not indicated in the evolution of the magma (See section 6.2.1.)

5) On the pseudophase diagram (Al-Na-K)-Ca-(Fe2+Mg) (fig. 6.17), the Coaker Porphyry plots exclusively in the biotite-cordierite-plagioclase field, a characteristic of S-type magmas (White and Chappel 1977, Hine et al. 1978).

6) The high Na2O content of the Coaker Porphyry has been demonstrated (sec.6.2.2) to be due to albitization and is not a primary feature.

Finally, several factors suggest that the ultramafic and mafic xenoliths in the Coaker Porphyry represent material incorporated during ascent and are not samples of the source. Firstly, the ultramafic xenoliths have textural features (radiating internal structure, reaction rims) that indicate that a profound disequilibrium existed between the xenoliths and the host magma, and that they
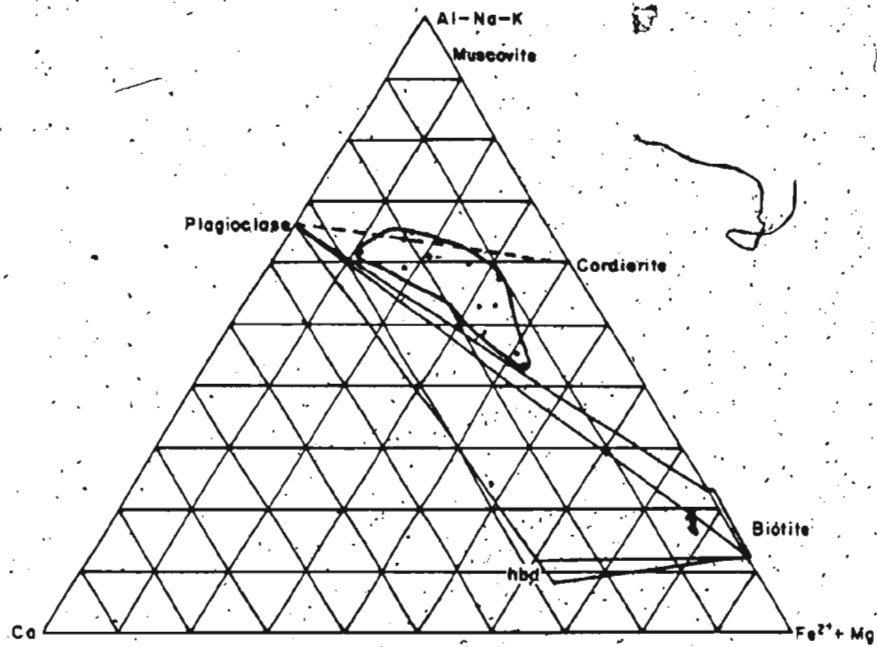
Figure 6.17 Pseudophase diagram of system $(Al-Na-K)-Ca-(Fe^{2+}+Mg)$ after Hine et al. 1978. Closed-system, uncontaminated Coaker Porphyry plots in the plagioclase - biotite - cordierite field, a characteristic of S-type magmas.

reacted vigorously with one another (section 6.4). The absence of hornblende phenocrysts and other minerals associated with the xenoliths from uncontaminated Coaker Porphyry cannot be explained by selective removal of these phases from the magma; they must have appeared in contaminated magmas as a result of the contamination. Disequilibrium between host magma and xenoliths is not characteristic of enclaves of restitic or congeneric origin (Didier 1973).

Secondly, to obtain a peraluminous magma by partial melting of a hydrous peridotite would necessitate melting at pressures of less than 20 kbar. Temperatures at depths corresponding to these pressures would have to be anomolously high to melt the peridotite (Cawthorne et al. 1975).

Thirdly, the absence of mafic and intermediate rocks in the Coaker Porphyry suite is inconsistent with an origin by fractionation of a mafic parent magma derived from a mantle source. Furthermore, the presence of large, dense ultramafic xenoliths in the felsic members of this hypothetical suite of mantle-derived magmas is inconsistent with a fractional crystallization model.

The bulk of the evidence indicates that the Coaker Porphyry originated by the partial melting of a sedimentary or metasedimentary source.

The Coaker Porphyry was intruded at very shallow crustal levels (less than 2 km depth - see Chapter 4). A granitic magma that is saturated with water cannot ascend to pressures less than 2 kbar without quenching due to the negative slope of the water-saturated

granite solidus surface. That the Coaker Porphyry magma was relatively dry is consistent with its shallow level of emplacement and the scarcity of vescicles.

Initiation of partial melting of a sedimentary or metasedimentary source involves the presence of water, either as a fluid phase or structurally bound in hydrated minerals. Melting in the second case involves the dehydration of these minerals (Huang and Wyllie 1973; Winkler 1976). A silicate liquid need not be saturated in H_2O to precipitate muscovite or biotite; the initial liquid could have a very low (less than 0.5%) water content (Huang and Wyllie 1981). Because the amount of water that is soluble in a silicic liquid decreases with decreasing pressure, a melt formed by the dehydration of muscovite (yielding >8% H_2O in the melt) would become water-saturated and solidify before attaining shallow crustal levels (Clemens and Wall 1981). A higher temperature melt containing less water would result from the dehydration of biotite (Clemens and Wall 1981, Winkler 1976). Therefore, metasediment containing biotite but no free water or muscovite is indicated as a source for the Coaker Porphyry.

The following reactions involve the dehydration-melting of biotite:

(1) biotite + sillimanite + 2 quartz -> K-spar (component in melt) + almandine + H_2O (Winkler 1976)

(2) Al-rich biotite + quartz -> K-spar component + gedrite + H2O (Winkler 1976)

(3) Mg-rich biotite + plagioclase + quartz -> K-spar + Ab component + hornblende +/- ilmenite (if Fe and Ti high) (Winkler 1976)

(4) biotite + plagioclase + quartz -> hornblende + k-spar + sphene (Busch et al. 1974)

(5) biotite + sillimanite + quartz + feldspars -> garnet + melt + K-spar +/- vapor + cordierite (Clemens and Wall 1981)

(6) biotite + quartz + feldspar -> opx + melt +/- feldspars, garnet + cordierite (Clemens and Wall 1981)

Mass-balance calculations give the best least squares fit for the following reaction to produce Coaker Porphyry plus a residuum:

26.05% quartz + 35.37% biotite + 36.15% plagioclase + 2.43% sillimanite -> 72.88% Coaker Porphyry melt + 14.54% almandine + 5.79% anorthite + 5.39% hypersthene + 0.9% ilmenite + 0.5% K-feldspar.

Partial melting of a biotite-rich source rarely results in the complete consumption of all the biotite in the source (Winkler 1976). Therefore, biotite is another probable residual phase in the above system. Anorthite in the residuum reflects the Ca enrichment that occurs in the source as a function of removal of a melt phase. The calculated source material contains 17.10% Al_2O_3, consistent with the observations (section 6.3 above) that the Coaker Porphyry melt arose from a source more aluminous than itself.

6.6 Summary

The Coaker Porphyry is a peraluminous S-type rhyodacite that formed from partial melting by dehydration reactions of biotite in an aluminous metasedimentary source. The resulting dry silicic magma ascended to shallow crustal levels, precipitating sodic plagioclase, quartz, and biotite en route, and muscovite and K-feldspar in the more felsic fractions. It encountered and reacted with ultramafic and mafic material to produce phlogopite, magnesio-hornblende, and garnet. These reactions took place at around 18 kbar pressure and at temperatures below 900 C, indicating that the Coaker Porphyry arose from great depths (50 km). Effects of contamination of the magma by host sediments are not detectable. Hydrothermal alteration occurring penecontemporaneously with emplacement resulted in the addition of albite component to some samples, and the rearrangement of alkalis within others.

Chapter 7

The Loon Bay Suite and Dildo Porphyry

Based upon field relations, the Dildo Porphyry and the Loon Bay suite were regarded as two physically distinct suites of rocks. However, the two groups are petrographically and chemically indistinguishible from one another. Both groups of rocks range from andesitic to rhyolitic, although the range of the plutonic members is considerably more limited (tonalitic to granodioritic). The Dildo Porphyry and the Loon Bay suites are therefore treated together in the following discussion.

7.1 Petrography

Petrographically, the fine-grained rocks fall into three textural/mineralogical groups:

1) a mafic group, corresponding to those samples having a silica content of less than approximately 65%. These rocks are characterized by an intersertal groundmass texture.

2) a cryptofelsitic group, corresponding approximately to silica contents of greater than 65% and less than 70%. These rocks have a cryptofelsitic groundmass, commonly with granophyric spherulites.

3) a granophyric group, corresponding approximately to silica contents of greater than 70%. These rocks have a granophyric groundmass or a cryptofelsitic groundmass containing abundant spherulites of granophyre.

The coarse-grained Loon Bay plutonic rocks range from granodioritic to tonalitic (Floran 1971). They belong to the group of hornblende-biotite granites that typify the Dunnage Zone (Strong 1981).

The petrography of the Loon Bay/ Dildo Porphyry (LB/DP) suite is summarized in Table 7.1.

7.1.1 Granophyre

The most felsic members of the LB/DP suite are characterized by abundant granophyre in the groundmass. The granophyre takes the form of spherulites, many of which are cored by grains of quartz, or less commonly, feldspar. Some samples contain granophyric phenocrysts. Granophyre becomes less abundant in the less silicic members of the suite, although intersertal granophyre is common in the mafic group.

Myrmekite occurs around the edges of plagioclase megacrysts in the coarse-grained Loon Bay granodiorites.

Also of note is the occurrence of secondary granophyre in the groundmass of Coaker Porphyry within the aureoles of Loon Bay plutons. Granophyre does not occur in Coaker Porphyry outside the aureoles.

TABLE 7.1

Petrography of Dildo Porphyry and Loon Bay Suite

Rock Type	Phenocrysts	Groundmass
Silicic DP (> 70% SiO2)	quartz (euhedral) alkali feldspar (sericitized) +/- biotite (altered to chlorite or car- bonate + sphene) +/- granophyre	Cryptofeldspathic, commonly with granophyric spherules +/- plagioclase laths +/- epidote accessory apatite
Intermediate DP (64 to 70% SiO2)	alkali feldspar (sericitized) +/- amphibole (most commonly chlorite or carbonate + sphene pseudomorph) +/- biotite (altered to chlorite or car- bonate + sphene) +/- quartz +/- opaques (pyrite, magnetite)	cryptofeldspathic +/- opaques +/- granophyre +/- chlorite +/- epidote +/- biotite accessory apatite
Mafic DP (< 64% SiO2)	plagioclase (sericitized) chlorite +/- biotite +/- quartz +/- opaques (pyrite, magnetite)	diabasic with abundant opaques, chlorite +/- epidote +/- amphibole +/- interstitial quartz, granophyre accessory apatite
Loon Bay plutonic suite	quartz oligoclase with myrmekitic rims	biotite, hornblende, quartz, oligoclase, interstitial alkali feldspar, zircon, sphene apatite

Three mechanisms proposed to give rise to granophyric texture (Smith 1974) are:

1) devitrification,

2) metasomatism and

3) primary crystallization of a fluid-rich eutectic melt.

Myrmekite is generally regarded (see Smith 1974, Hughes 1982) as being distinct from granophyre, having a different origin. Yet several of the mechanisms proposed for myrmekite formation are similar to those proposed for granophyre formation (Phillips 1972), and Hibbard (1978) regards the distinction between granophyre and myrmekite as artificial. He proposes an origin by pressure quenching of eutectic liquids on a microscopic scale as the origin for both phenomena.

Although devitrification of a glassy groundmass is not a likely mechanism for the formation of the myrmekite in the coarse-grained Loon Bay granodiorite, it is possible that the granophyre in the groundmasses of the fine-grained LB/DP rocks and the baked Coaker Porphyry originated in this way. Whereas primary crystallization of a fluid-rich eutectic melt (by pressure quenching or otherwise) is a probable origin for the granophyre and myrmekite in the Loon Bay granodiorite and the fine-grained LB/DP suite, it is not a possible mechanism for producing the granophyre in baked Coaker Porphyry. Metasomatism is a mechanism that cannot be discounted in any of the three cases.

7.1.2 Inclusions

The coarse-grained Loon Bay granodiorite is characterized by abundant enclaves that locally comprise up to 50% of the rock (Floran 1971). These enclaves are composed of the same minerals as the host rock, but with a higher proportion of hornblende and a more calcic plagioclase (Heyl 1935). They are poorer in quartz, and many are practically devoid of K-feldspar (Floran 1971). They are rounded in shape, and are generally about 10 cm across. Their assimilation by the host magma varies; some inclusions are distinct from the surrounding material, others appear as vague "ghostlike" impressions (Floran 1971). Mafic schlieren are also characteristic of the Loon Bay granodiorites.

Floran (1971) suggested that the inclusions are assimilated country rock; however several factors indicate that they are congeneric inclusions (Didier 1973): (1) their concentration in the central parts of the batholith (Floran 1971), (2) their rounded shape, (3) their diffuse contacts, and (4) they share a common mineral suite with the host magma.

Enclaves in fine-grained LB/DP rocks are rare, and were only observed in two instances. One is a mafic sample containing xenoliths that appear to be simply coarser-grained samples of their host, except that they contain corroded chromite crystals. The other is a felsic stock on Fish Head containing xenoliths that resemble very fresh samples of the marginal phases of the Loon Bay granodiorites (deformed, fine-grained, with large zoned feldspars rimmed with

myrmekite).

7.1.3 Alteration

Whereas the coarse-grained Loon Bay Granodiorite samples are relatively fresh, the fine-grained rocks of the DP/LB suite are universally highly altered. Mafic phases are reduced to assemblages (commonly pseudomorphic after mica or amphibole) of chlorite + carbonate + sphene +/- epidote, rutile, sericite, stilpnomelane. Feldspars are sericitized (and/or epidotized) and in some cases are rendered opaque by alteration. These rocks are far more thoroughly metasomatized than is characteristic of the Coaker Porphyry.

7.2 Geochemistry

The LB/DP suite encompasses samples with a range in silica of 55 to 82%, from andesitic to rhyolitic compositions (Table 7.2). This is a far greater range than that of the Coaker Porphyry, which is comprised only of rhyodacites and rhyolites. The LB/DP rocks are also more mafic than Coaker porphyry samples of equivalent SiO_2%. Whereas the Coaker Porphyry can best be described as belonging to the silicic series of Green (1980), the LB/DP suite is distinctly calc-alkaline (fig. 7.1, 7.2).

TABLE 7.2

Loon Bay/ Dildo Porphyry:
Major Elements, Norms, Trace Elements

Loon Bay Granodiorite

MAJOR ELEMENTS	23-80	30-80	35-80	37-80	41-80	42-80
SiO2	70.4	62.5	71.4	70.7	69.2	69.4
TiO2	0.37	0.77	0.40	0.40	0.46	0.34
Al2O3	14.9	16.8	15.2	15.7	15.5	15.2
Fe2O3(t)	3.12	5.59	2.78	2.78	2.63	2.75
MnO	0.08	0.10	0.06	0.06	0.07	0.06
MgO	1.27	3.01	1.05	1.03	1.05	1.08
CaO	3.13	5.40	2.30	2.76	2.28	2.21
Na2O	3.99	4.30	4.08	4.07	4.03	4.06
K2O	2.72	1.46	2.66	2.81	3.30	3.04
P2O5	0.09	0.20	0.12	0.08	0.11	0.09
L.O.I.	0.37	0.55	0.51	0.68	0.79	1.02
Total	100.34	100.68	100.56	101.07	99.42	99.25

NORMS						
Q	26.47	13.66	29.62	27.24	25.78	26.80
OR	16.08	8.62	15.71	16.54	19.77	18.29
AB	33.77	36.34	34.51	34.31	34.57	34.97
AN	14.72	22.20	10.62	13.12	10.74	10.56
C	----	----	1.71	1.13	1.44	1.45
DI	0.19	2.69	----	----	----	----
HY	7.51	13.68	6.34	6.27	6.13	6.61
MT	0.35	0.88	0.45	0.45	0.43	0.44
IL	0.70	1.46	0.76	0.76	0.89	0.66
AP	0.21	0.46	0.28	0.18	0.26	0.21

TRACE ELEMENTS						
Pb	10	6	11	16	10	9
Rb	76	35	65	61	74	77
Sr	240	431	249	270	279	327
Y	23	21	20	20	21	15
Zr	118	126	120	126	115	118
Zn	39	67	40	34	40	37
Cu	12	29	15	16	20	12
Ni	3	22	3	2	1	2
Ba	417	300	505	561	542	761
V	52	123	44	39	48	52
Cr	1	41	0	0	0	2
La + Ce	45	47	42	49	52	68

TABLE 7.2 (continued)

Loon Bay
Granodiorite / Silicic LB/DP

MAJOR ELEMENTS	45-80	24-80	26-82	28-82	57-82	59-82
SiO2	62.9	76.7	72.9	79.8	75.8	76.0
TiO2	0.71	0.03	0.03	0.09	trace	trace
Al2O3	16.1	12.7	13.6	12.5	12.7	12.8
Fe2O3(t)	5.11	0.47	0.61	0.51	0.51	0.80
MnO	0.12	0.02	0.07	0.02	0.02	0.03
MgO	2.82	0.01	0.36	0.18	0.05	0.02
CaO	4.22	0.50	1.25	0.38	0.37	0.44
Na2O	3.83	3.44	7.60	3.79	3.78	3.86
K2O	1.96	5.13	0.05	1.70	4.38	4.40
P2O5	0.24	0.04	0.10	0.05	0.04	0.04
L.O.I.	1.48	0.31	2.04	1.50	0.81	0.87
Total	99.49	99.35	98.61	100.52	98.46	99.26

NORMS

	45-80	24-80	26-82	28-82	57-82	59-82
Q	17.74	36.11	26.60	50.50	36.79	35.84
OR	11.82	30.60	0.31	10.15	26.51	26.43
AB	33.07	29.38	66.59	32.39	32.76	33.20
AN	19.76	2.24	2.95	1.57	1.61	1.95
C	0.59	0.68	----	3.89	1.19	1.00
DI	----	----	2.32	----	----	----
HY	14.25	0.73	0.82	1.12	0.96	1.36
MT	0.83	0.10	0.11	0.09	0.09	0.13
IL	1.38	0.06	0.06	0.17	----	----
AP	0.57	0.09	0.24	0.12	0.09	0.09

TRACE ELEMENTS

	45-80	24-80	26-82	28-82	57-82	59-82
Pb	5	32	0	3	23	20
Rb	54	92	2	46	105	111
Sr	425	22	206	58	39	40
Y	21	26	15	10	35	34
Zr	146	81	107	76	51	56
Zn	60	9	24	19	14	30
Cu	28	18	18	16	14	9
Ni	15	0	0	0	0	0
Ba	486	82	120	492	499	440
V	122	1	4	4	0	3
Cr	32	0	0	0	0	0
La + Ce	53	37	23	62	35	39

Table 7.2 (continued)

Silicic LB/DP

MAJOR ELEMENTS	70-82	73-82	91-82	96-82	97-82	201-81
SiO2	81.7	73.6	70.1	77.1	72.3	75.9
TiO2	0.06	0.23	0.26	0.06	0.17	0.03
Al2O3	10.2	13.9	13.9	13.1	14.1	13.5
Fe2O3(t)	0.49	1.65	1.96	0.58	1.65	0.90
MnO	0.03	0.04	0.06	0.03	0.03	0.04
MgO	0.11	0.75	1.02	0.19	0.44	0.21
CaO	0.77	1.18	2.37	0.58	2.05	0.90
Na2O	3.63	4.06	4.08	4.11	3.83	4.58
K2O	1.45	3.33	2.15	3.29	2.19	2.39
P2O5	0.04	0.08	0.11	0.02	0.05	0.00
L.O.I.	1.34	1.20	4.32	1.27	2.90	0.78
Total	99.82	100.02	100.33	100.33	99.71	99.23

NORMS						
Q	53.82	33.19	31.90	39.11	36.85	37.82
OR	8.70	19.91	13.23	19.63	13.37	14.35
AB	31.19	34.76	35.96	35.11	33.48	39.36
AN	3.61	5.40	11.50	2.77	10.17	4.54
C	1.38	1.68	0.85	1.79	1.88	1.77
DI	----	----	----	----	----	----
HY	1.01	4.16	5.45	1.35	3.53	1.96
MT	0.07	0.26	0.33	0.09	0.27	0.15
IL	0.12	0.44	0.51	0.12	0.33	0.06
AP	0.09	0.19	0.27	0.05	0.12	----

TRACE ELEMENTS						
Pb	121	32	8	14	8	21
Rb	33	52	61	77	67	46
Sr	99	158	239	72	165	142
Y	17	14	13	14	9	29
Zr	80	84	98	65	112	68
Zn	93	32	33	15	31	17
Cu	11	17	29	17	15	10
Ni	0	2	6	0	0	1
Ba	376	631	418	929	398	486
V	6	32	35	0	17	1
Cr	0	1	3	0	0	0
La + Ce	34	34	29	37	42	44

TABLE 7.2 (continued)

Silicic   Intermediate

MAJOR ELEMENTS	207-81	32-82	46-82	60-82	63-82	67-82
SiO2	77.7	69.1	67.1	65.3	64.7	68.9
TiO2	trace	0.43	0.29	0.11	0.51	0.43
Al2O3	12.9	14.6	16.7	14.5	15.2	14.9
Fe2O3(t)	0.90	3.54	2.46	2.71	4.29	2.61
MnO	0.03	0.06	0.06	0.06	0.07	0.04
MgO	0.02	1.70	1.22	1.39	2.02	1.17
CaO	0.36	2.78	2.98	3.56	3.47	2.96
Na2O	3.89	4.61	4.98	4.05	4.33	4.10
K2O	4.45	1.77	1.60	2.11	2.02	2.14
P2O5	0.00	0.18	0.03	0.08	0.16	0.02
L.O.I.	0.41	1.96	1.98	6.02	3.07	1.68
Total	100.66	100.73	99.40	99.89	99.84	98.95

NORMS

Q	36.49	25.63	22.92	24.24	19.75	28.06
OR	26.23	10.59	9.71	13.28	12.34	13.00
AB	32.83	39.49	43.26	36.51	37.86	35.67
AN	1.78	12.77	14.97	16.14	16.61	14.96
C	1.03	0.48	1.47	----	----	0.52
DI	----	----	----	1.76	0.08	----
HY	1.49	9.21	6.64	7.19	11.27	6.48
MT	0.14	0.57	0.40	0.46	0.70	0.43
IL	----	0.83	0.57	0.22	1.00	0.84
AP	----	0.42	0.07	0.20	0.38	0.05

TRACE ELEMENTS

Pb	18	5	5	11	4	9
Rb	123	27	35	60	39	49
Sr	21	380	671	290	291	353
Y	37	10	5	14	22	11
Zr	60	158	89	120	183	130
Zn	23	48	46	36	61	46
Cu	13	13	20	29	16	18
Ni	0	9	0	3	13	7
Ba	421	582	447	431	626	551
V	2	63	43	61	93	44
Cr	0	14	0	9	15	3
La + Ce	40	64	26	37	55	36

TABLE 7.2 (continued)

Intermediate

MAJOR ELEMENTS	72-82	75-82	81-82	85-82	86-82	93-82
SiO2	68.9	66.1	66.3	69.6	68.2	69.9
TiO2	0.04	0.56	0.23	0.29	0.20	0.31
Al2O3	15.2	15.2	14.6	14.1	14.1	15.1
Fe2O3(t)	3.45	3.82	2.99	2.29	2.32	2.65
MnO	0.07	0.07	0.06	0.06	0.06	0.05
MgO	0.90	2.38	1.21	1.44	1.24	1.33
CaO	2.76	3.78	2.73	2.00	2.38	1.86
Na2O	4.26	4.01	4.36	4.01	4.29	4.30
K2O	2.59	2.00	2.18	1.88	1.80	2.21
P2O5	0.16	0.15	0.13	0.10	0.11	0.12
L.O.I.	1.05	2.06	4.49	4.12	4.40	2.50
Total	99.84	100.13	99.28	99.89	99.10	100.33

NORMS						
Q	24.94	22.04	24.61	32.13	29.77	29.77
OR	15.49	12.05	13.59	11.52	11.23	13.35
AB	37.34	34.60	38.92	35.17	38.33	37.19
AN	12.80	17.91	13.39	9.61	11.71	8.63
C	0.60	----	0.44	2.15	1.09	2.60
DI	----	0.17	----	----	----	----
HY	7.12	11.16	7.76	8.12	6.80	7.14
MT	0.56	0.62	0.50	0.50	0.40	0.43
IL	0.77	1.08	0.46	0.57	0.40	0.60
AP	0.38	0.35	0.32	0.24	0.27	0.28

TRACE ELEMENTS						
Pb	12	16	8	7	5	11
Rb	60	47	62	56	48	68
Sr	307	404	200	339	280	307
Y	34	14	22	17	15	13
Zr	206	123	133	118	109	120
Zn	53	51	43	32	28	48
Cu	11	27	19	24	17	24
Ni	2	14	4	11	9	12
Ba	576	525	440	397	311	695
V	36	88	51	46	50	55
Cr	0	29	0	11	6	17
La + Ce	50	35	32	36	37	28

Table 7.2 (continued)

	Intermediate			/	Mafic	
MAJOR ELEMENTS	94-82	95-82	98-82	31-82	34-82	36-82
SiO2	64.5	67.8	64.5	63.0	63.0	55.1
TiO2	0.63	0.20	0.43	0.62	0.69	0.43
Al2O3	15.0	14.6	15.1	14.3	15.1	14.3
Fe2O3(t)	3.84	2.54	4.02	4.26	5.16	5.16
MnO	0.06	0.05	0.06	0.06	0.07	0.09
MgO	2.24	1.38	2.25	2.60	3.40	3.23
CaO	3.06	2.94	3.37	2.98	2.63	5.02
Na2O	4.08	3.92	3.99	4.78	4.84	3.98
K2O	2.36	2.04	1.70	1.17	1.70	1.59
P2O5	0.06	0.07	0.18	0.12	0.19	0.26
L.O.I.	3.26	3.81	4.48	5.24	3.54	10.59
Total	99.09	98.35	100.28	99.13	100.32	99.45

NORMS

Q	20.59	28.63	22.69	19.40	15.51	10.53
OR	14.55	12.62	10.49	7.36	10.38	10.57
AB	36.03	34.72	35.24	43.08	42.32	37.90
AN	15.53	14.79	17.26	14.91	12.20	18.52
C	0.33	0.80	0.66	0.04	1.00	----
DI	----	----	----	----	----	6.25
HY	11.04	7.45	11.71	12.92	15.93	13.70
MT	0.64	0.42	0.67	0.73	0.85	0.93
IL	1.12	0.40	0.85	1.25	1.35	0.92
AP	0.14	0.17	0.44	0.30	0.45	0.68

TRACE ELEMENTS

Pb	7	11	0	4	0	5
Rb	53	60	42	31	24	40
Sr	284	246	313	300	638	292
Y	15	14	18	18	20	22
Zr	125	114	150	137	147	146
Zn	52	45	52	52	64	55
Cu	23	21	22	28	28	39
Ni	16	14	18	39	28	25
Ba	941	526	478	287	540	301
V	91	56	93	89	122	115
Cr	35	19	21	71	65	49
La + Ce	41	31	42	38	49	52

TABLE 7.2 (continued)

Mafic

MAJOR ELEMENTS	61-82	68-82	74-82	76-82	90-82	92-82
SiO2	60.6	58.9	57.0	59.1	60.1	58.6
TiO2	0.26	0.73	0.98	0.74	0.55	0.93
Al2O3	14.6	14.9	15.7	14.8	15.1	15.3
Fe2O3(t)	4.98	5.79	6.96	5.49	5.40	6.09
MnO	0.08	0.09	0.11	0.10	0.09	0.09
MgO	3.80	3.77	3.54	3.81	2.65	3.91
CaO	3.86	5.09	6.19	4.79	3.56	4.82
Na2O	3.83	4.11	3.83	3.79	4.01	3.99
K2O	1.67	1.69	1.72	1.74	1.98	1.92
P2O5	0.19	0.35	0.29	0.30	0.26	0.22
L.O.I.	6.46	3.79	2.85	4.64	5.90	3.39
Total	100.33	99.21	99.17	99.30	99.60	99.26

NORMS

	61-82	68-82	74-82	76-82	90-82	92-82
Q	16.20	11.51	8.26	13.39	15.89	10.20
OR	10.51	10.47	10.53	10.86	12.49	11.83
AB	34.52	36.45	33.65	33.88	36.21	35.22
AN	18.87	18.04	21.35	19.26	17.04	18.95
C	----	----	----	----	0.54	----
DI	0.17	4.96	7.10	3.10	----	3.70
HY	17.88	15.67	15.30	16.37	15.16	16.72
MT	0.85	0.97	1.16	0.92	0.91	1.01
IL	0.53	1.45	1.93	1.48	1.11	1.84
AP	0.47	0.85	0.70	0.73	0.64	0.53

TRACE ELEMENTS

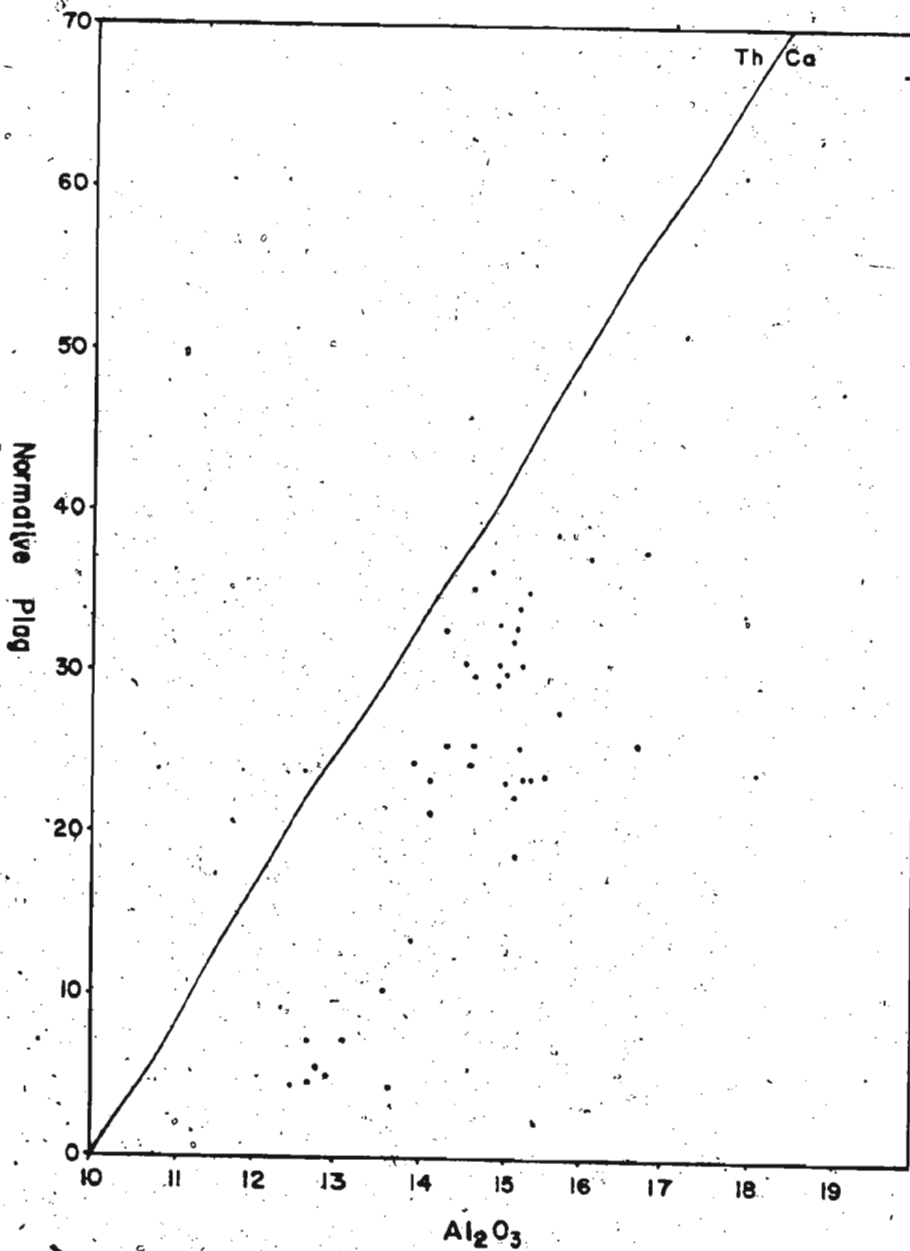|	61-82	68-82	74-82	76-82	90-82	92-82
Pb	2	4	4	6	5	8
Rb	48	31	46	37	49	30
Sr	345	589	602	509	251	586
Y	20	24	27	20	28	23
Zr	131	167	179	147	202	148
Zn	56	69	79	68	79	61
Cu	21	25	15	24	14	20
Ni	48	33	25	54	15	43
Ba	428	514	523	504	433	997
V	105	135	162	124	118	122
Cr	106	58	10	84	5	59
La + Ce	42	59	57	51	50	55

Figure 7.1 Normative plagioclase vs Al2O3: Loon Bay/ Dildo Porphyry suite, after Irvine and Baragar 1974. The rocks plot in the clac-alkaline field.
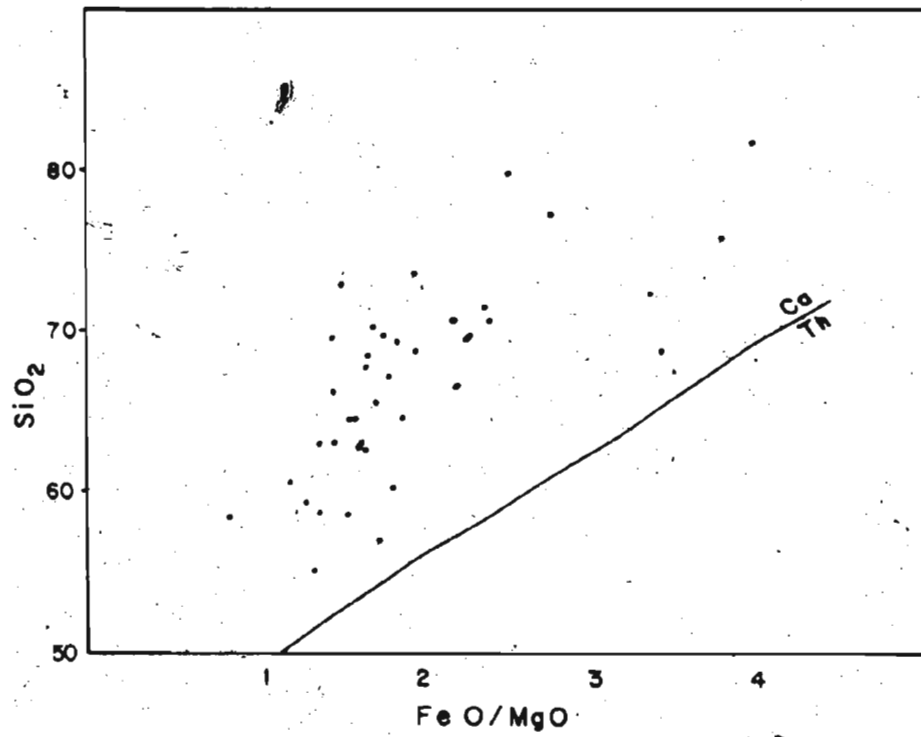
Figure 7.2   SiO2 versus FeO/MgO, after Irvine and Baragar 1974. The
rocks plot exclusively in the calc-alkaline (Ca) field.

7.2.1 Al2O3

Like the Coaker Porphyry, the LB/DP suite is essentially peraluminous. However, the LB/DP rocks become progressively less corundum normative with decreasing SiO2, and the mafic members of the suite are diopside normative (fig. 7.3). This trend, combined with a negative correlation between normative corundum and iron (fig. 7.4), strongly indicates that the Loon Bay suite evolved from a metaluminous to a peraluminous composition, a trend which, in calc-alkaline magmas, has been convincingly linked to hornblende fractionation (Cawthorne et al. 1975, Cawthorne et al. 1976).

7.2.2 Other major elements

The trends exhibited by some of the major elements, element ratios, and trace elements reflect the textural changes in the groundmass discussed above, in that inflections occur in variation diagrams corresponding to approximately 63% and 72% SiO2. Fig. 7.5 illustrates several Harker diagrams.

The mafic samples show a decrease in CaO, Ca/Mg and Ca/Fe, and a constant K/Mg ratio up to 63% SiO2. For greater silica values, CaO decreases at a lower rate, and the Ca/Mg, Ca/Fe, and K/Mg ratios increase, the last dramatically. At the same time, FeO and TiO2 contents decrease at a steady rate throughout this silica range and show no inflection, although MgO appears to increase slightly in the mafic range. These results indicate that plagioclase was a major fractionating phase in the mafic rocks. The constant K/Mg ratio for
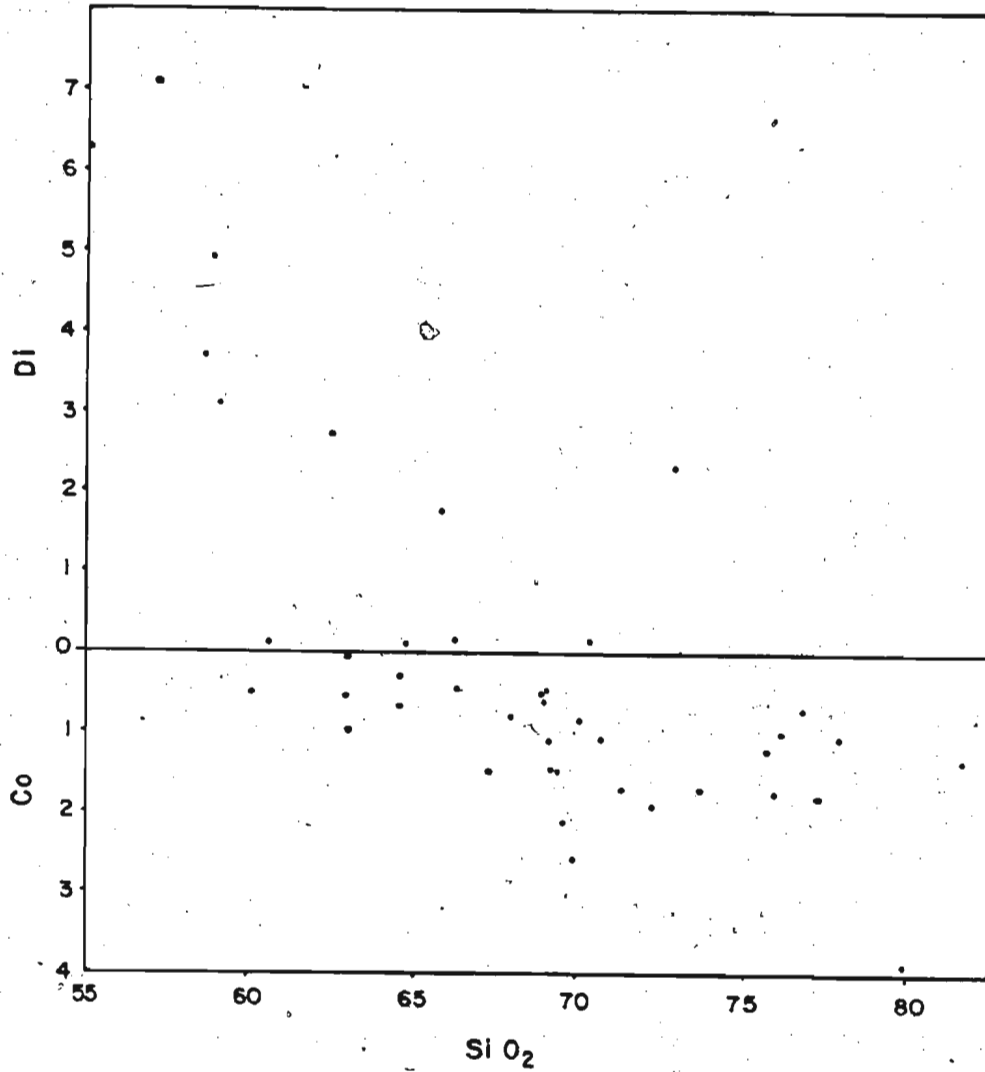
Figure 7.3 Normative corundum (Co) or diopside (Di) versus SiO2. The suite becomes increasingly corundum normative with increasing SiO2, indicating hornblende as a fractionating phase.
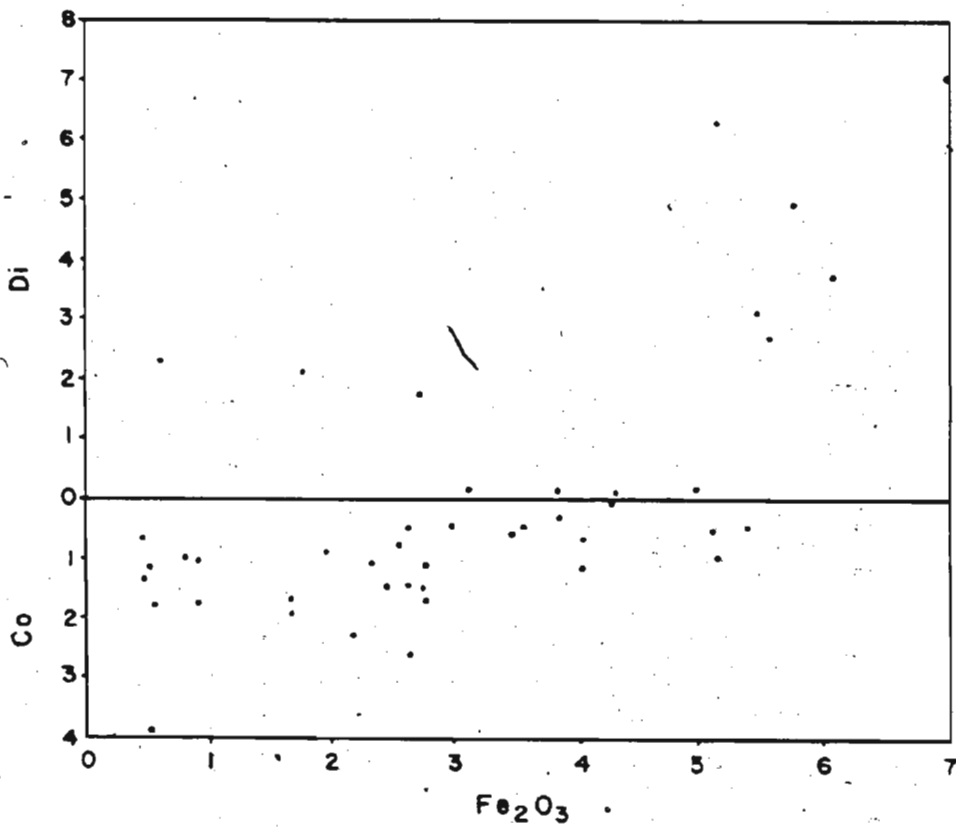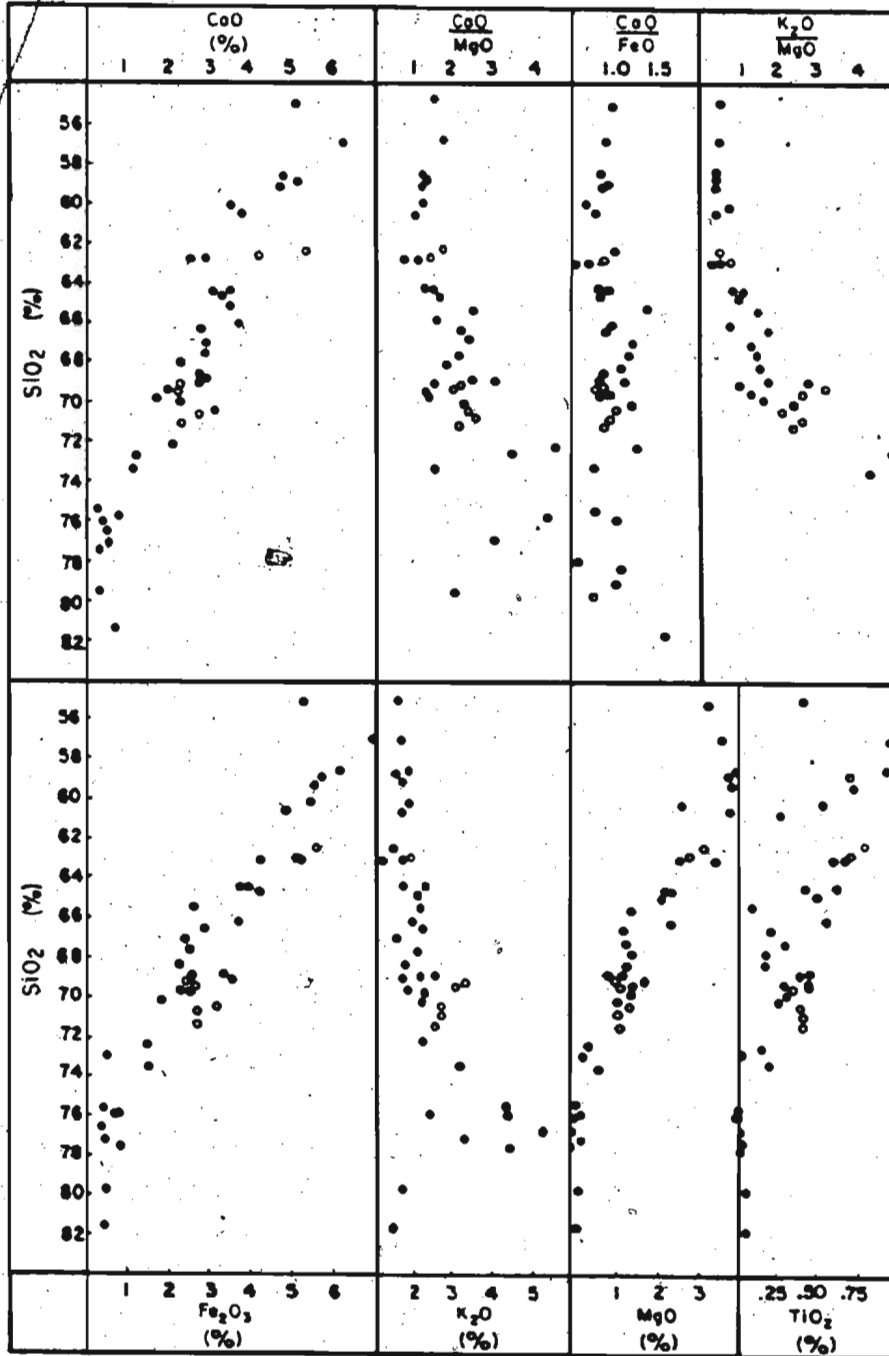
Figure 7.4 Normative corundum (Co) or diopside (Di) versus Fe2O3.
The trend indicates that the suite evolved from a
metaluminous source.

Figure 7.5 Harker variation diagrams, major elements: Loon

Bay granodiorite (•) and Dildo Porphyry (•).

the mafic samples and the trends shown by MgO and K2O vs SiO2 indicate that these elements were not being removed from the melt at this stage, although FeO and TiO2 were decreasing. This trend is consistent with the fractionation of small amounts of titanomagnetite. At 63% SiO2, a ferromagnesian mineral appeared on the liquidus, and removed FeO, MgO, and TiO2 relative to CaO and K2O. This pattern is consistent with the fractionation of both hornblende and biotite, as indicated by petrographic observations.

The second inflection at about 72% SiO2 corresponds petrographically with the development of a predominantly granophryic groundmass texture and the virtual absence of mafic mineral phases. It is marked geochemically by the levelling off of FeO, MgO, TiO2, and CaO at extremely low concentrations, and the abrupt increase in K2O. Trace element patterns, which are even more marked, are discussed below. These trends indicate that these high-SiO2 samples are residual liquids from which almost all ferromagnesian minerals have been extracted, that they are the extreme end products of differentiation.

On the AFM plot (fig. 7.6), the LB/DP suite follows a calc-alkaline trend that terminates on the A-F sideline, indicating that hornblende was a fractionating phase in the differentiation of the magma (Strong and Dickson 1978).
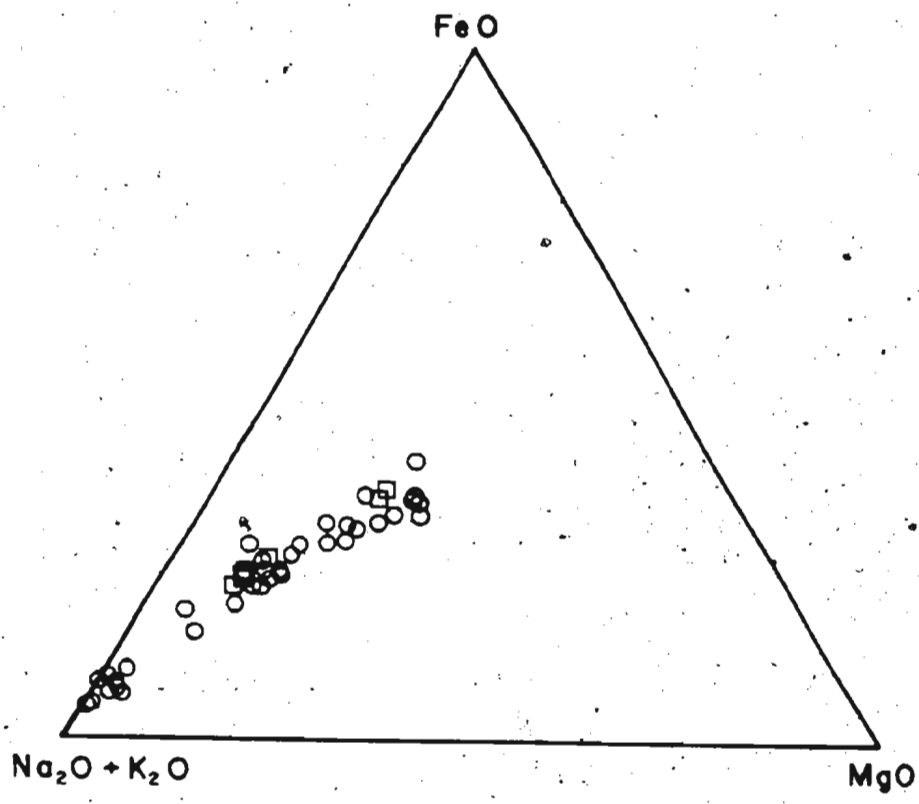
Figure 7.6 Alk-F-M plot: Loon Bay granodiorite (□) and Dildo
Porphyry (o).

7.2.3 Trace elements

The trace elements mimic the trends shown by the major elements (fig. 7.7). Ni and Cr have high but erratic values in the mafic samples, and drop off sharply above 63% SiO2, following MgO. The Sr trend imitates CaO. V and Zn follow iron.

Rb and Pb increase gradually with SiO2 up to about 71%, then increase dramatically.

Rb/Sr ratio increases, and the Sr/Ba ratio decreases, with increasing SiO2 (fig. 7.8), both of which are indicative of plagioclase fractionation (Hanson 1978). A K/Rb ratio that decreases and then levels out with increasing Rb is consistent with biotite fractionation followed by hornblende and plagioclase fractionation. An increase in the K/Ba ratio with SiO2 also indicates biotite fractionation, although early removal of biotite is not consistent with other element trends or with petrographic observations.

Cu appears to decline slightly with SiO2 and shows a weak positive correlation with Ni (fig. 7.9), indicating that fractionation of a minor sulfide phase may have been involved in the differentiation of the magma.

The LB/DP suite is more mafic than the Coaker Porphyry, with higher FeO, MgO, TiO2, V, Zn and Cu at equivalent SiO2. The Coaker Porphyry is noticeably richer in Pb and Rb than the LB/DP suite (fig. 7.10); when plotted against SiO2, the fields for these two suites do not overlap.
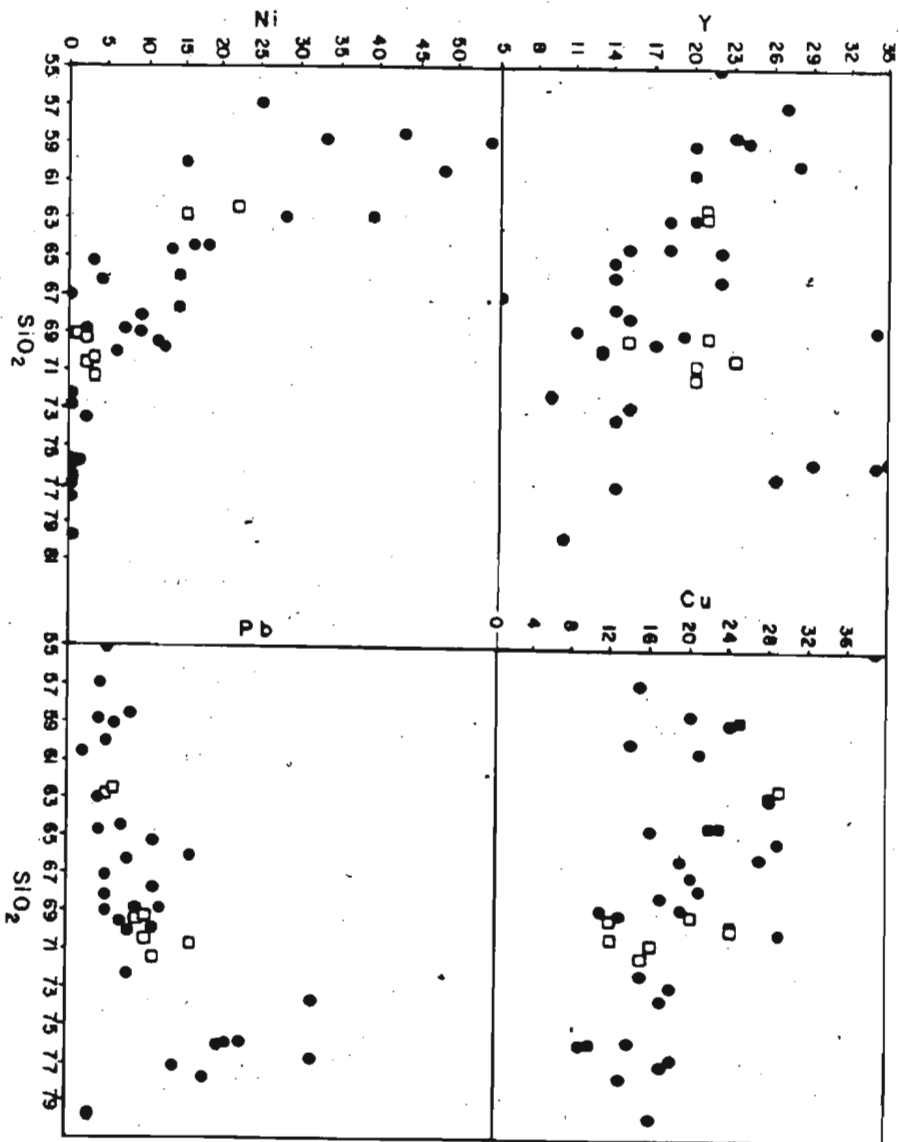
Figure 7.7 Harker variation diagrams, trace elements.
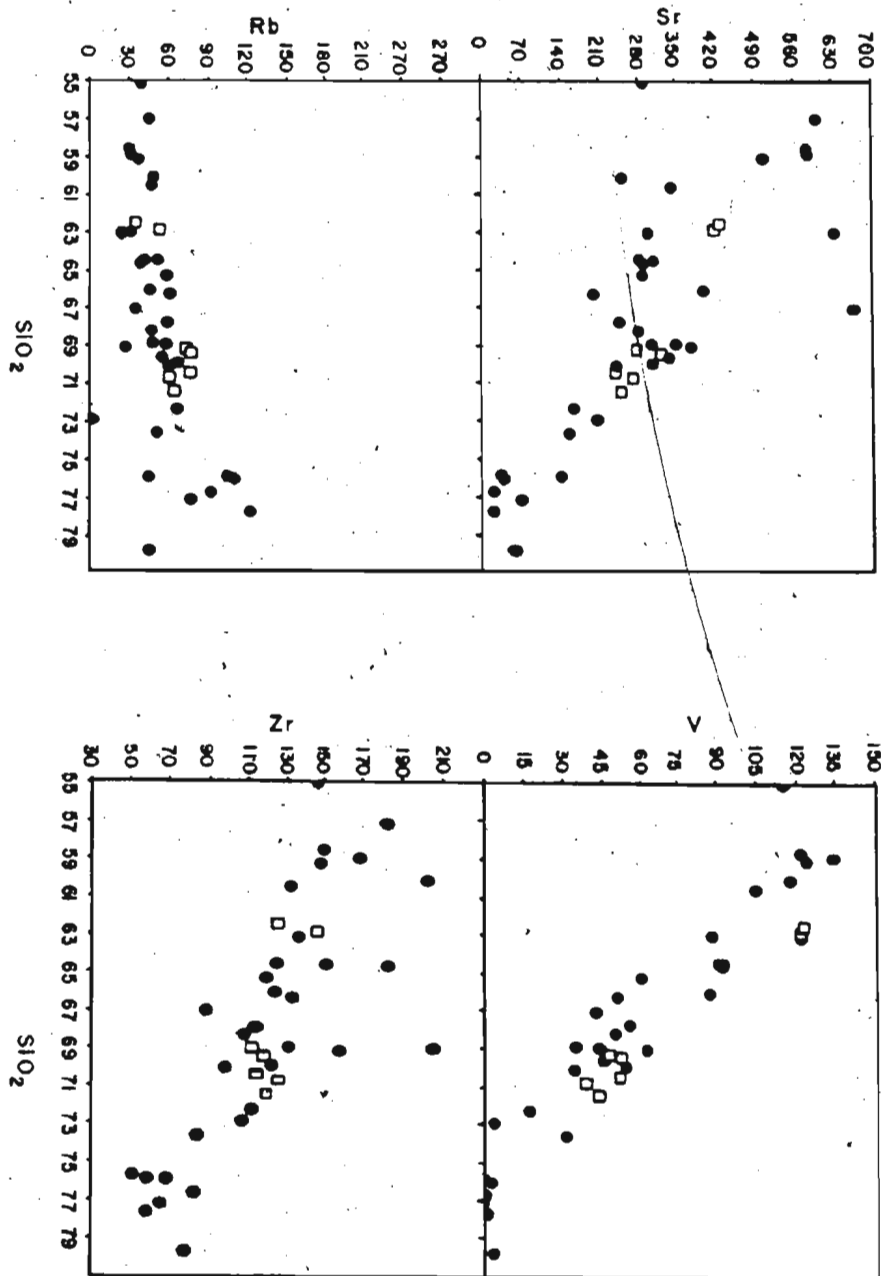
Figure 7.7 (continued)
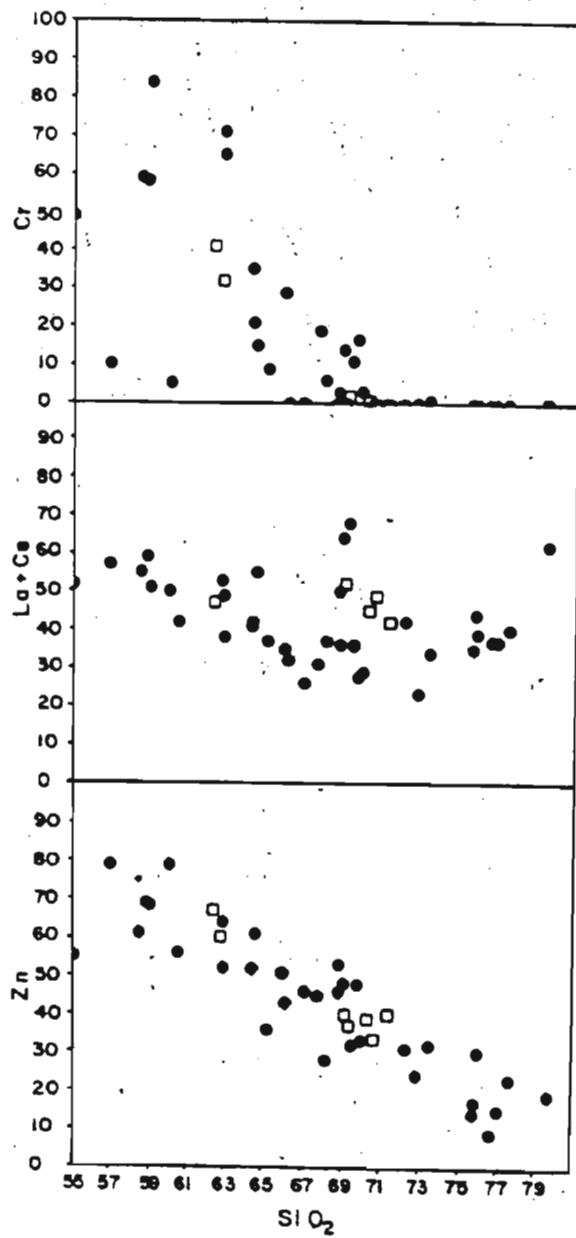
Figure 7.7 (continued)
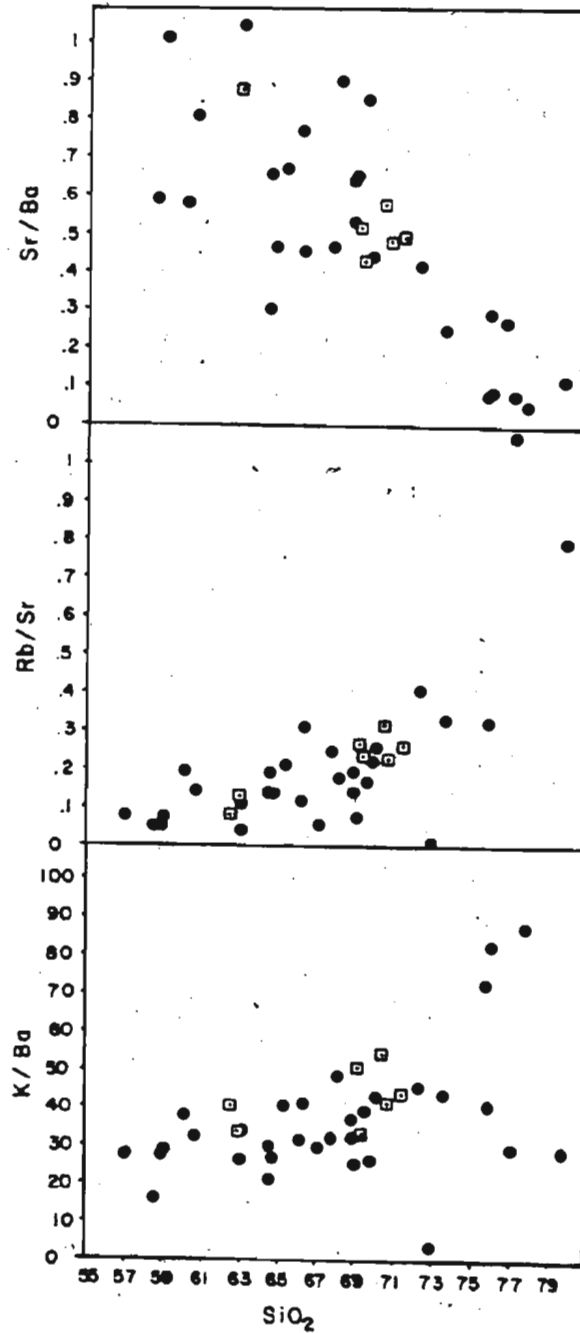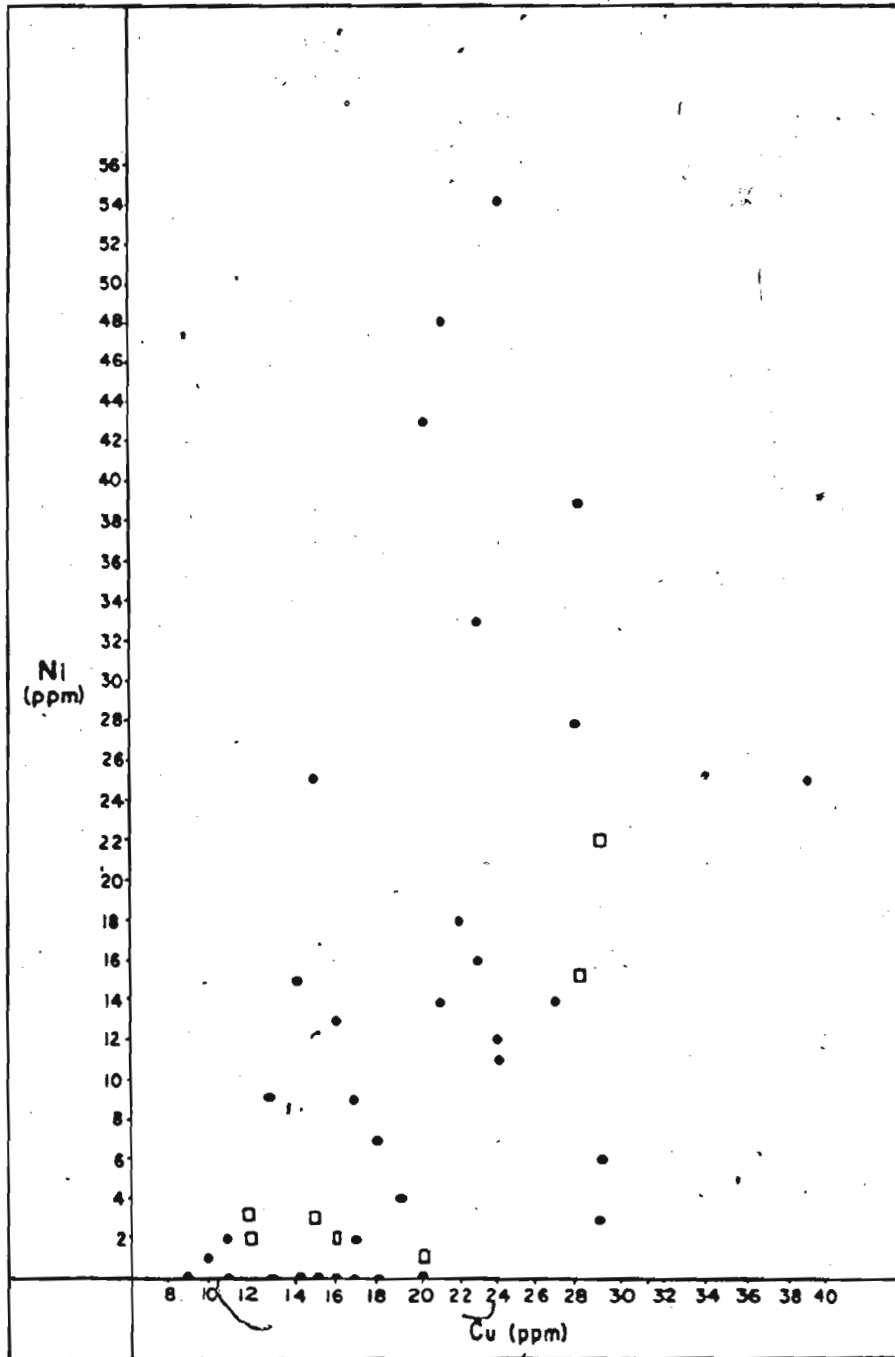
Figure 7.8 K/Ba, Rb/Sr and Sr/Ba versus SiO2.

Figure 7.9   Cu versus Ni
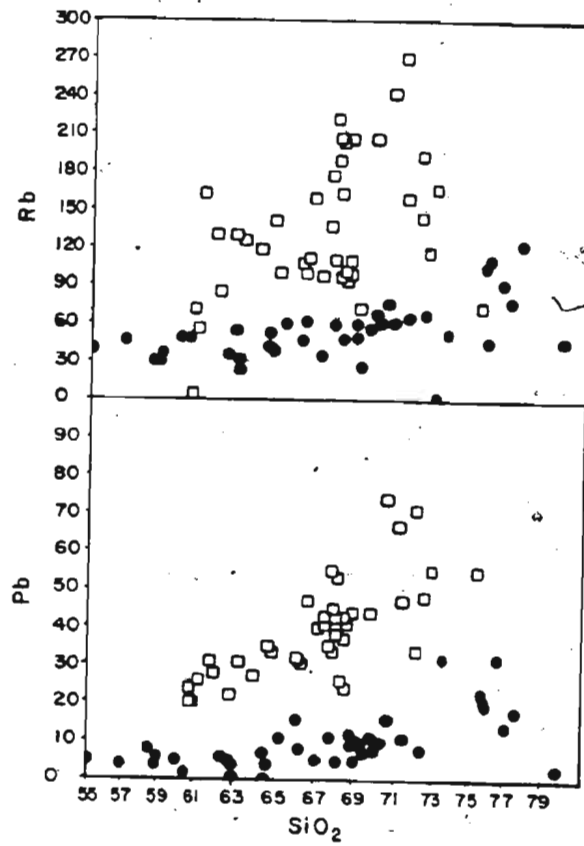
Figure 7.10   A comparison between Coaker Porphyry (□) and Loon Bay/
Dildo Porphyry (•) contents of RB and Pb versus Si02.

7.2.4 REE

La + Ce and Y both show a V-shaped trend when plotted against G SiO2, in which they decline gradually, and then increase rapidly in the most silicic samples. These elements correlate weakly with Zr, TiO2, and P2O5 over most of their range, but are decoupled at high SiO2 values (fig. 7.11).

Chondrite-normalized values of REE from twelve LB/DP samples ranging from 55 to 82% SiO2 (fig. 7.12, table 7.3) show remarkably little variation in pattern. All are strongly LREE-enriched, and most have small positive Eu anomalies. This pattern could result from hornblende, garnet, and/or zircon as a residual or fractionating phase.

7.3 The source of the LB/DP suite

Several factors indicate that the LB/DP suite had a mantle or igneous source, arising either directly from partial melting or by fractionation of a more mafic parent magma. These factors include:

1) the presence of hornblende, and evidence that hornblende fractionation played a major role in the evolution of the magma,

2) the plotting of the LB/DP suite in the I-type granitic field on the pseudophase diagram (Al-Na-K)-Ca-(Fe2+Mg) (fig. 7.13) (White and Chapel 1977, Hine et al. 1978),
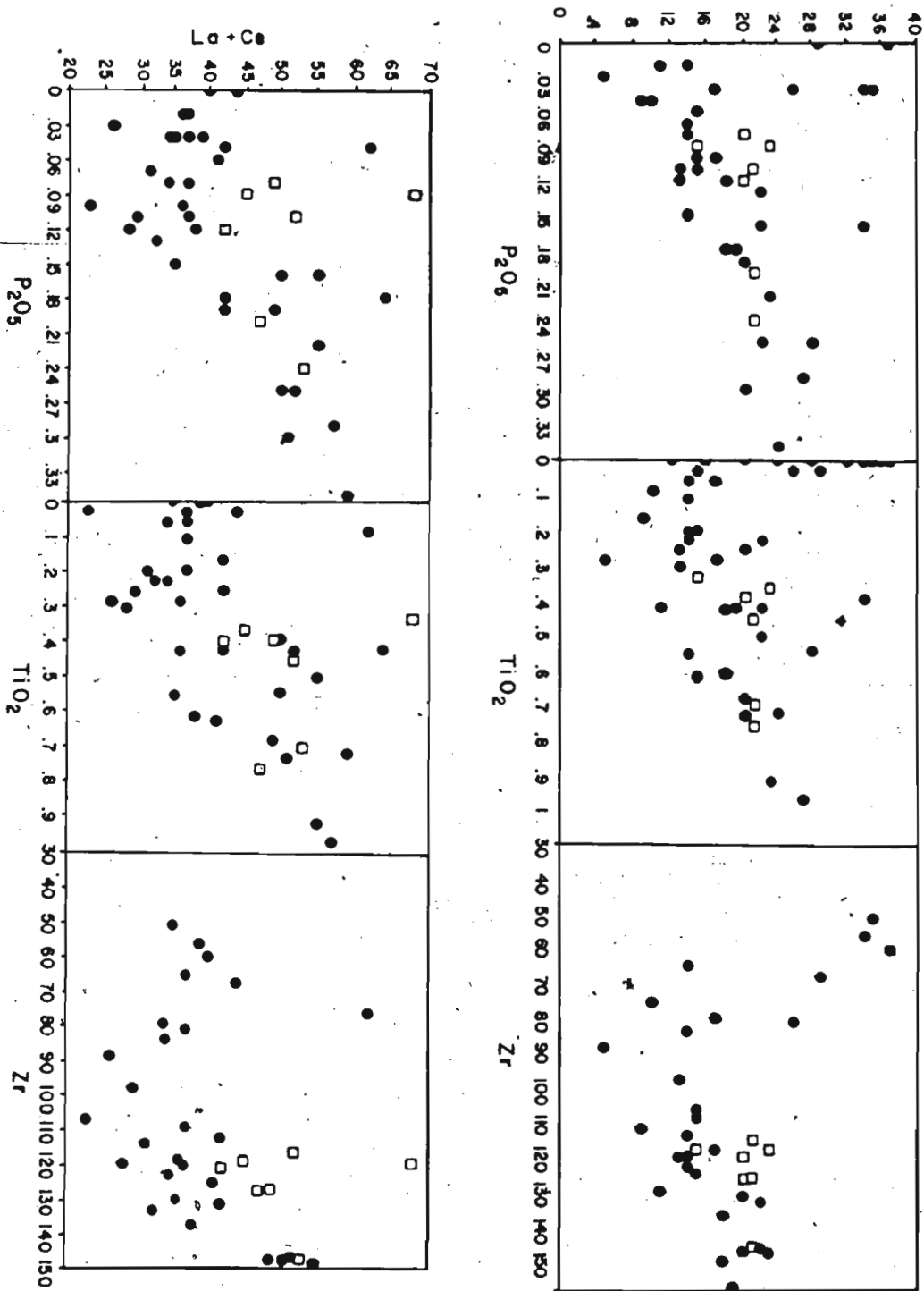
Figure 7.11 Y and La + ce versus P2O5, TiO2 and Zr.
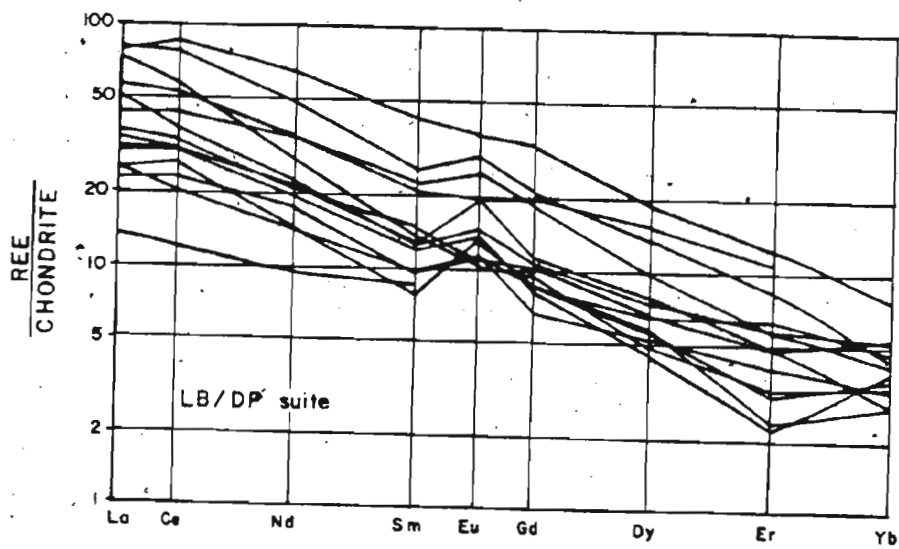
Figure 7.12 REE/Chondrite: Loon Bay/Dildo Porphyry suite

TABLE 7.3

Rare Earth Elements: LB/DP suite

Element (ppm)	26-82	32-82	36-82	60-82	67-82	70-82	72-82
La	7.66	26.18	17.69	15.76	7.42	11.48	13.58
Ce	16.94	66.12	43.09	31.60	19.07	27.07	36.42
Nd	8.38	29.18	21.25	13.86	10.55	12.48	21.14
Sm	1.93	5.31	4.41	2.44	1.86	2.90	4.05
Eu	0.83	2.16	1.76	1.41	0.81	0.78	1.39
Gd	2.16	5.48	4.78	2.87	2.31	2.69	5.03
Dy	1.80	4.41	3.12	2.54	1.89	2.36	4.91
Er	0.65	1.80	1.23	1.03	0.50	1.21	2.29
Yb	0.74	0.89	0.87	0.57	0.58	1.09	0.40

Chondrite Norm.

	26-82	32-82	36-82	60-82	67-82	70-82	72-82
La	24.32	83.13	56.17	50.04	23.54	36.45	43.11
Ce	20.84	81.33	53.01	38.87	23.46	33.30	44.79
Nd	14.04	48.87	35.59	23.22	17.67	20.91	35.41
Sm	9.82	26.96	22.37	12.40	9.45	14.72	20.55
Eu	11.48	29.88	24.44	19.52	11.18	10.87	19.30
Gd	8.33	21.17	18.44	11.10	8.91	10.38	19.42
Dy	5.44	13.56	9.60	7.83	5.81	7.25	15.09
Er	3.04	8.45	5.77	4.82	2.34	5.69	10.77
Yb	3.54	4.29	4.19	2.74	2.78	5.25	1.91

TABLE 7.3 (continued)

Elements (ppm)	73-82	74-82	85-82	86-82	89-82	93-82	97-82
La	4.06	25.53	11.50	10.37	23.31	8.06	4.22
Ce	9.68	70.76	25.51	24.70	48.55	21.73	9.76
Nd	6.31	39.12	12.43	11.88	16.51	8.58	5.53
Sm	1.54	8.36	2.54	2.36	2.71	1.74	1.69
Eu	0.21	2.63	1.05	0.99	0.73	0.94	0.84
Gd	1.66	8.56	2.64	2.13	2.42	2.12	1.73
Dy	1.11	6.21	2.09	2.08	1.54	1.46	1.65
Er	0.36	2.67	1.00	1.33	0.70	0.45	0.84
Yb	0.00	1.80	1.11	1.00	0.69	0.77	0.68

Chondrite Norm.

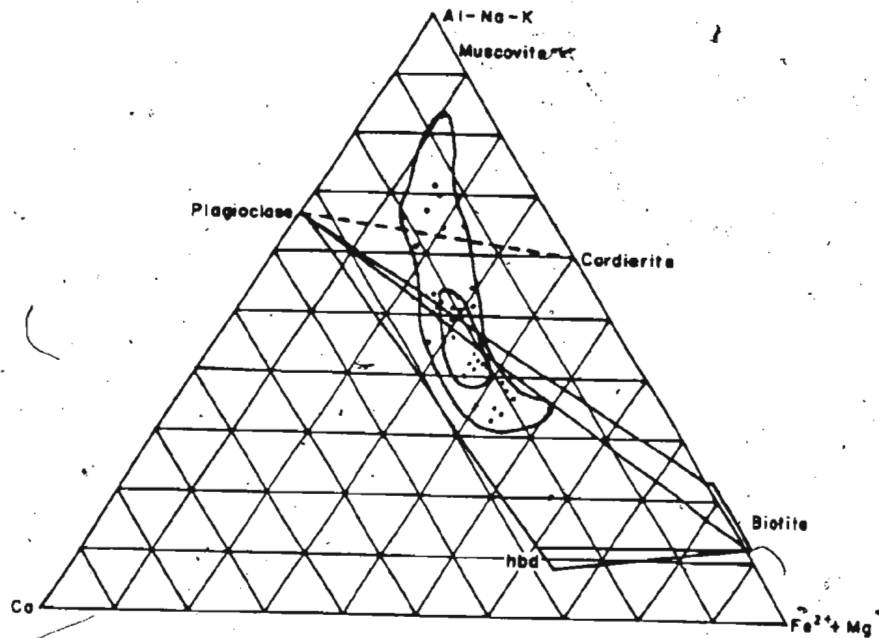|	73-82	74-82	85-82	86-82	89-82	93-82	97-82
La	12.89	81.04	36.50	32.93	73.99	25.60	13.41
Ce	11.91	87.03	31.38	30.38	59.72	26.73	12.00
Nd	10.57	65.54	20.82	19.89	27.66	14.37	9.26
Sm	7.79	42.45	12.89	11.99	13.77	8.85	8.56
Eu	2.89	36.41	14.60	13.67	10.09	13.00	11.59
Gd	6.41	33.06	10.19	8.24	9.35	8.19	6.69
Dy	3.40	19.11	6.42	6.39	4.75	4.50	5.06
Er	1.67	12.55	4.70	6.23	3.27	2.12	3.94
Yb	0.00	8.64	5.34	4.80	3.31	3.70	3.27

Figure 7.13 Pseudophase diagram of system (Al–Na–K)–Ca–(Fe^{2+}+Mg) after Hine et al. 1978. LB/DP samples range from metaluminous to peraluminous as is typical of calc-alkaline I-type magmas. The smaller field encloses Loon Bay samples, the larger Dildo Porphyry.

3) the wide range in composition from andesitic to rhyolitic,

4) the low values of Pb and Rb,

5) the high initial values of Cr and Ni,

6) the occurrence of magnetite and sphene.

The most voluminous composition within the range encompassed by this suite is the tonalite-granodiorite of the plutonic Loon Bay batholiths. No rocks more mafic than andesitic are included. These factors indicate that the LB/DP suite did not evolve from a mafic parent by fractional crystallization, but that the primary magma was an intermediate silicic magma such as a tonalite or quartz diorite. The andesitic stocks and dikes within this suite probably represent cumulate-rich phases that emerged in small quantities from the lower or outer parts of the magma chamber. That such a congeneric mafic magma existed is attested to by the presence of the mafic inclusions in the Loon Bay batholiths. The relatively high quantities of Ni (up to 60 ppm) and Cr (up to 100 ppm) in the andesitic samples suggest that these compositions were not derived from a $\rangle$ basalt by crystallization of a MgO-rich phase such as olivine or orthopyroxene. The rhyolitic end of the suite represents fluid-rich residual liquids of a eutectic composition, possessing a relatively high concentration of incompatible elements.

7.4 Summary

The Loon Bay/ Dildo Porphyry suite is a calc-alcalic suite consisting of tonalite-granodiorite batholiths and small stocks and dikes of andesitic through rhyolitic composition. Partial melting of a metavolcanic or contaminated mantle source gave rise to an intermediate silicic magma that fractionated/ plagioclase, magnetite, hornblende and biotite to produce the observed compositional range. Peraluminous compositions evolved from metaluminous magmas by hornblende fractionation. This is in contrast to the Coaker Porphyry which has a primary peraluminous compostion. The LB/DP suite also differs from the Coaker Porphyry by its higher concentrations of compatible elements, and lower incompatible elements, most notably Pb and Rb. The most important distinction between the two igneous units is that the Coaker Porphyry is an S-type granitic rock (derived from a sedimentary source), and the LB/DP suite is I-type (derived from an igneous source).

Chapter 8

The Mafic Intrusions

The mafic intrusions in the Dunnage Melange include the pre-Caradocian New Bay Gabbro, Puncheon Diorite, and Grapnel Gabbro, and the Devonian diabase dikes. Of these, the diabase dikes are the most voluminous within the Dunnage Melange, but clearly post-date melange formation (Chapter 4, 5). The other three mafic units are volumetrically minor compared to the silicic rocks discussed earlier (Chapters 6 and 7), although dikes of the New Bay Gabbro are abundant in the southwest portion of the Dunnage Melange where the Coaker Porphyry is absent.

8.1 Petrography

The petrography of these rocks is summarized in Table 8.1.

8.1.1 The Puncheon Diorite

The Puncheon Diorite stocks have coarse-grained, relatively felsic interiors, and finer-grained, mafic outer rims, the latter characterized by schlieren and mafic cognate inclusions. Kay (1976) and Jacobi and Schweikert (1976) attributed these features to crystal settling and accumulation around the outer portions of the stock. However, these mafic rims are characterized by subophitic groundmass textures rather than cumulate textures, and are finer-grained than the

TABLE 8.1 Petrography of the Mafic Intrusions

Rock Type	Phenocrysts	Groundmass
New Bay Gabbro	Plagioclase Augite	Subophitic texture plagioclase, augite, hypersthene, opaques, interstitial quartz and alkali feldspar
Puncheon Diorite	Augite Plagioclase	Medium to coarse Subophitic to intergranular augite, serpentine, opaques, plagioclase, interstitial quartz, alkali feldspar, and granophyre
Grapnel Gabbro	Augite (commonly glomeroporphyritic) (Ultramafic xenoliths)	Coarse subophitic texture plagioclase, augite, opaques, hypersthene, interstitial quartz, alkali feldspar
Diabase dikes	Plagioclase	Fine to medium grained Intergranular to subophitic plagioclase, augite, hypersthene, opaques, interstitial quartz, granophyre

center of the stock. Naney and Swanson (1980) have suggested that
such differentiation could occur as a result of suppression of
plagioclase crystallization by Fe and Mg in the melt. The cooler
outer part of the stock would solidify first and would be more mafic
due to exclusion of the felsic components, which would be concentrated
in the interior of the stock. The grain size difference is simply a
reflection of the rate of cooling in the inner and outer parts of the
stock.

Cognate inclusions and schlieren, according to Didier (1973), are
samples of relatively mafic material from the chilled margin of the
body that were incorporated into the magma as a result of magmatic
processes such as convection. Schlieren are inclusions that have been
extremely attenuated by these processes. Another possible mechanism
of incorporation of inclusions and attentuation to produce schlieren
might be high-temperature subsolidus strain, for example, by shear
stresses on the stock during or shortly after its emplacement.

The Puncheon Diorite differs from the other mafic intrusions in
its lack of orthopyroxene, although masses of serpentine may be
replacement products of orthopyroxene. Plagioclase and augite are its
phenocryst phases.

8.1.2 Grapnel Gabbro

The Grapnel Gabbro differs from the other mafic intrusions in
that augite is its sole phenocryst phase, and it contains primary
phlogopite and amphibole, and ultramafic xenoliths. The phlogopite

and amphibole occur most commonly in association with the augite phenocrysts. Xenoliths are small and sparse, and resemble those found in the Coaker Porphyry.

8.2 Geochemistry

The four mafic rock types all plot in the sub-alkaline, tholeiitic fields of the discrimination diagrams of Irvine and Baragar (1971) and Miyashiro (1975) (fig. 8.1), and occupy the within-plate tholeiite fields of Pearce and Cann (1973) and Pearce and Norry (1979) (fig. 8.2). The REE patterns (fig. 8.3) are enriched in light relative to heavy REE and have negligible Eu anomalies. These factors indicate that the mafic intrusions arose from an undepleted mantle source in an extensional tectonic setting. Geochemical analyses are given in Tables 8.2 and 8.3.

8.2.1 Relationship to the silicic rocks

A silica gap of 10% separates the most siliceous of the mafic rocks from the uncontaminated Coaker Porphyry. A smaller gap (1%) separates the mafic rocks from the andesitic members of the Loon., Bay/ Dildo Porphyry suite; however the former are tholeiites and the latter is calc-alkaline. Therefore, the mafic and silicic rocks in the area do not appear to be genetically related.

The possibility was examined that the Grapnel Gabbro, with its ultramafic xenoliths, phlogopite and magnesiohornblende, might be a result of the reaction between small amounts of Coaker Poprhyry magma

Figure 8.1 Discimination diagrams showing subalkaline
tholeiitic behaviour of the mafic intrusions.

A. The negative slope of the trend of SiO2
vs FeO/MgO for the mafic intrusions indicates that
they are tholeiitic rather than calc-alkalic
(Miyashiro 1975).

B. The mafic intrusions plot in the
subalkaline field of the alkalis vs SiO2 diagram of
Irvine and Baragar (1971).

A
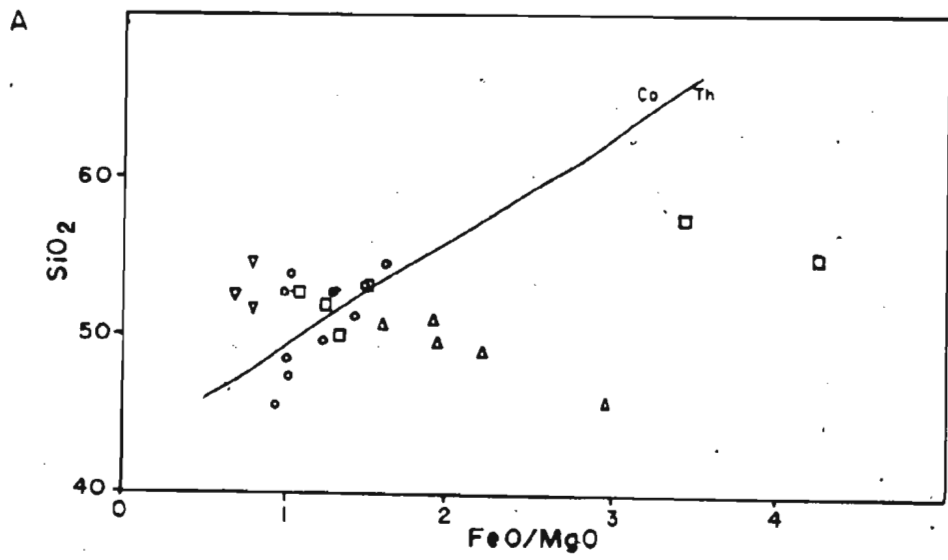
○ DIABASE   △ NEW BAY GABBRO

□ PUNCHEON   ▽ GRAPNEL GABBRO

B

A

A=LKT
B=OFB
C=CAP
D=WPB

○ DIABASE	△ NEW BAY GABBRO
□ PUNCHEON DIORITE	▽ GRAPNEL GABBRO
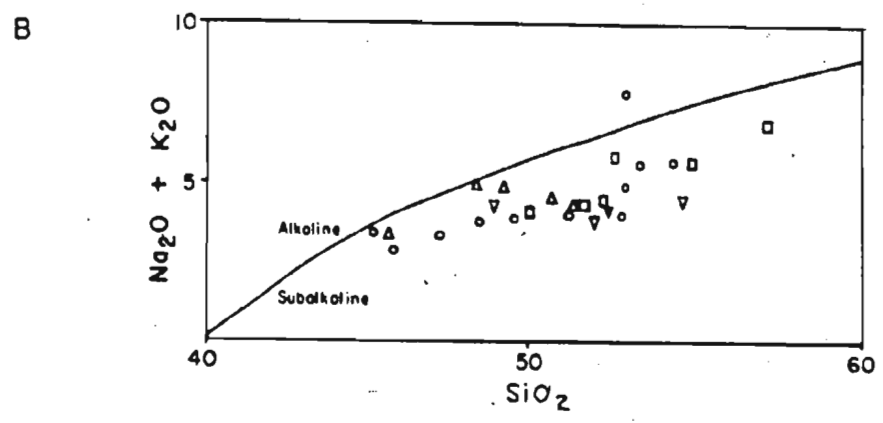
Figure 8.2a   After Pearce and Cann 1973. ♯ = Low K tholeiites;
         B = ocean floor basalts; C = calc-alkaline basalts;
         D = within plate basalts.

Figure 8.2b   After Pearce and Norry 1979. Fields shown include ⌐
within - plate basalts.

Figure 8.3   REE/Chondrite: Mafic intrusions. NBG.= New Bay Gabbro
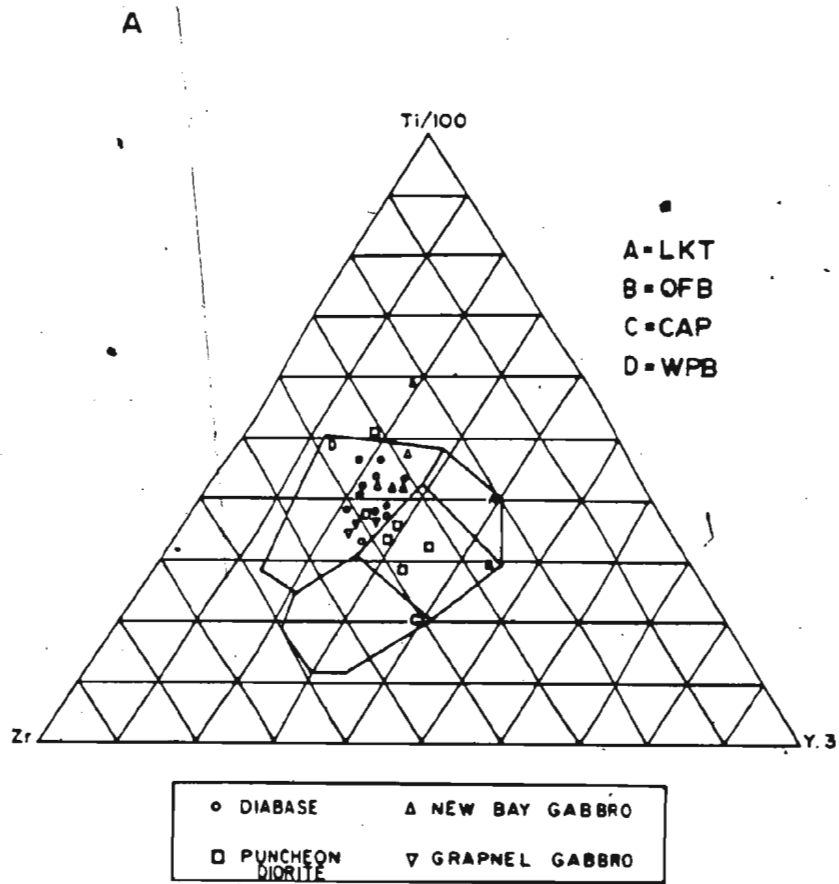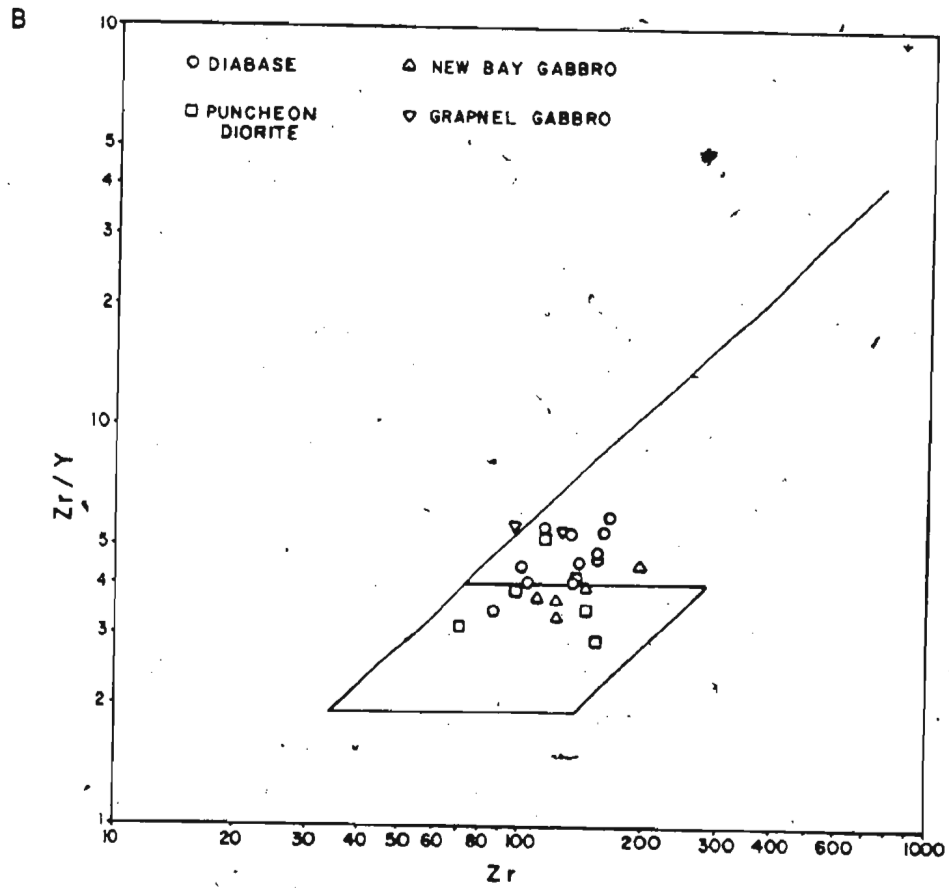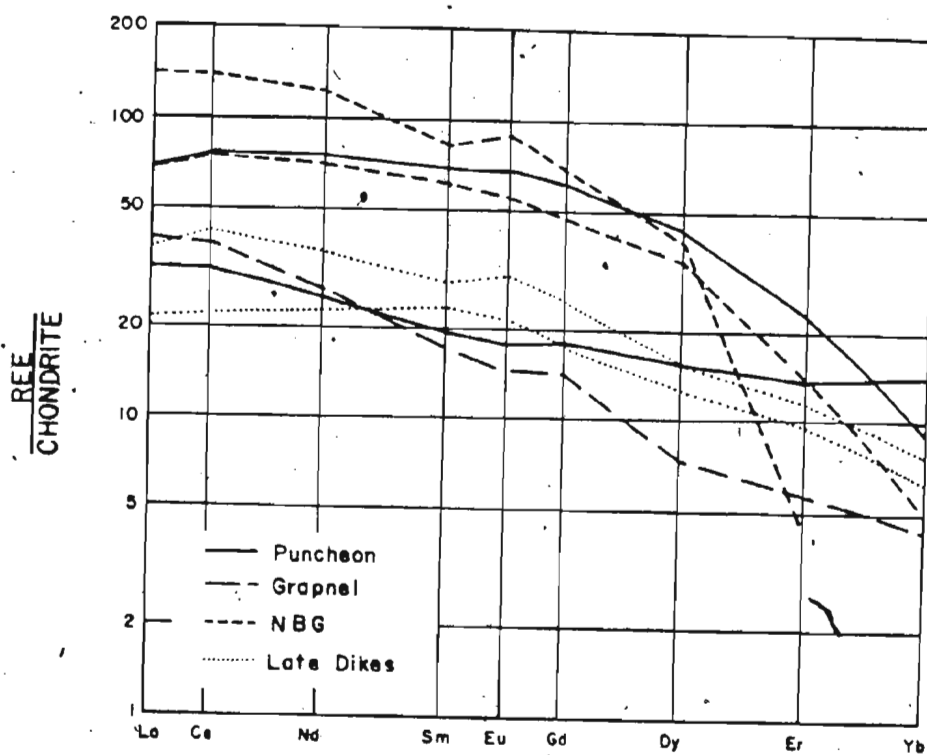
TABLE 8.2

Mafic Rocks: Major Elements, Norms, Trace Elements

Puncheon Diorite

MAJOR ELEMENTS	50-82	221-81	222-81	223-81	226-81	232-81
SiO2	51.9	57.3	55.0	50.0	53.0	52.4
TiO2	1.10	1.26	1.24	1.14	1.05	0.88
Al2O3	16.1	18.4	18.2	15.3	17.2	16.4
Fe2O3(t)	9.16	6.95	7.36	10.99	7.35	8.71
MnO	0.17	0.12	0.12	0.19	0.13	0.16
MgO	6.51	1.79	1.55	7.30	4.36	6.57
CaO	7.64	5.12	7.01	8.03	6.54	8.12
Na2O	3.46	4.13	3.82	3.27	3.95	2.87
K2O	0.99	2.58	1.89	0.88	1.98	1.38
P2O5	0.21	0.14	0.21	0.07	0.12	0.08
L.O.I.	1.91	1.75	2.62	3.02	3.97	2.38
Total	99.15	99.54	99.02	100.19	99.65	99.86

NORMS

Q	----	6.35	6.08	----	----	0.91
OR	6.02	15.59	11.59	5.35	12.23	8.37
AB	30.01	35.74	33.53	28.48	34.93	24.13
AN	26.20	24.59	27.94	25.18	24.41	28.92
DI	9.33	0.38	5.72	12.63	7.16	9.73
HY	21.77	13.46	10.97	12.59	16.46	24.61
OL	2.42	----	----	11.58	1.21	----
MT	1.51	1.13	1.22	1.81	1.23	1.43
IL	2.15	2.45	2.44	2.23	2.08	1.71
AP	0.50	0.33	0.50	0.17	0.29	0.19

TRACE ELEMENTS

Rb	58	115	90	41	88	65
Sr	277	329	234	255	317	210
Y	53	41	33	22	21	25
Zr	154	147	135	70	113	98
Nb	7	4	7	5	8	6
Zn	82	63	68	83	81	89
Cu	53	38	35	43	7	44
Ni	52	0	5	26	10	49
V	198	123	138	227	167	181
Cr	131	0	0	124	6	162

TABLE 8.2 (continued)

Grapnel Gabbro

MAJOR ELEMENTS	18-82	19-82	36-82
SiO2	54.2	52.3	51.7
TiO2	0.74	0.60	0.77
Al2O3	14.5	14.2	14.1
Fe2O3(t)	7.29	8.25	7.69
MnO	0.19	0.16	0.18
MgO	8.76	10.90	9.55
CaO	5.30	6.55	6.60
Na2O	2.43	2.14	2.02
K2O	2.46	1.87	1.84
P2O5	0.14	0.16	0.18
L.O.I.	3.08	3.20	5.46
Total	99.09	100.33	100.09

NORMS			
Q	2.88	----	1.80
OR	15.14	11.39	11.49
AB	21.42	18.66	18.06
AN	22.28	24.34	25.33
DI	3.36	6.52	6.48
HY	31.92	33.74	33.54
OL	----	2.58	----
MT	1.21	1.21	1.30
IL	1.46	1.17	1.55
AP	0.34	0.38	0.44

TRACE ELEMENTS			
Rb	104	86	68
Sr	245	259	216
Y	23	17	22
Zr	126	96	101
Nb	8	6	7
Zn	119	74	66
Cu	35	49	18
Ni	174	257	215
V	158	164	219
Cr	400	579	583

Table 8.2 (continued)

New Bay Gabbro

MAJOR ELEMENTS	41-82	43-82	77-82	79-82	100-82
SiO2	48.9	50.3	50.8	45.7	49.4
TiO2	1.73	1.30	1.71	2.82	2.12
Al2O3	15.8	15.4	13.4	11.8	15.0
Fe2O3(t)	12.08	11.04	12.50	18.90	12.00
MnO	0.19	0.17	0.20	0.26	0.19
MgO	4.89	5.95	5.81	5.71	5.52
CaO	8.26	9.77	9.76	8.96	7.88
Na2O	3.23	3.01	2.78	2.32	3.52
K2O	1.08	0.90	0.76	0.77	0.82
P2O5	0.24	0.16	0.20	0.28	0.45
L.O.I.	2.46	1.70	1.80	1.84	1.87
Total	98.86	99.70	99.72	99.36	98.77

NORMS

Q	----	----	0.52	----	----
OR	6.62	5.43	4.59	4.67	5.00
AB	28.35	25.99	24.02	20.13	30.74
AN	26.37	26.38	22.30	20.01	23.43
DI	12.12	18.23	21.47	19.99	11.53
HY	12.63	12.77	21.27	13.73	15.82
OL	7.92	6.51	----	12.23	6.28
MT	2.00	1.79	2.04	3.09	1.98
IL	3.41	2.52	3.32	5.49	4.16
AP	0.58	0.38	0.47	0.66	1.08

TRACE ELEMENTS

Rb	41	22	33	27	
Sr	384	296	266	413	
Y	33	36	36	43	
Zr	121	144	122	197	
Nb	14	14	13	11	
Zn	90	87	127	95	
Cu	65	84	74	17	
Ni	19	24	11	35	
V	297	303	770	318	
Cr	0	8	0	38	

TABLE 8.2 (continued)

Diabase dikes

MAJOR ELEMENTS	65-81	71-81	123-81	126-81	127-81	155-81
SiO_2	52.7	49.2	54.5	52.5	47.3	53.5
TiO_2	1.12	1.76	1.17	1.17	1.19	1.41
Al_2O_3	14.8	16.5	15.3	17.6	15.1	14.3
$Fe_2O_3(t)$	9.05	9.56	9.14	7.63	8.28	7.20
MnO	0.15	0.17	0.13	0.14	0.16	0.11
MgO	8.21	6.90	4.93	5.20	7.30	6.13
CaO	7.10	6.64	2.98	4.40	7.86	5.81
Na_2O	3.42	2.99	5.33	4.84	1.96	3.64
K_2O	0.54	1.00	0.33	2.79	1.06	1.78
P_2O_5	0.10	0.26	0.16	0.21	0.19	0.27
L.O.I.	2.16	4.09	5.42	3.33	8.11	5.18
Total	99.35	99.07	99.39	99.81	98.51	99.33

NORMS

Q	0.34	-----	3.28	-----	6.93	-----
OR	3.28	6.22	2.07	17.09	6.55	11.96
AB	29.78	26.64	47.84	40.00	17.35	35.02
AN	24.11	30.16	14.57	18.72	30.62	19.81
DI	9.33	2.24	1.21	2.04	7.22	8.92
HY	29.24	26.76	26.68	-----	27.12	8.55
OL	-----	2.23	-----	16.76	-----	10.69
MT	1.49	1.60	1.60	1.26	1.38	1.30
IL	2.19	3.52	2.36	2.30	2.36	3.04
AP	0.24	0.63	0.39	0.50	0.46	0.71

TRACE ELEMENTS

Rb	21	29	6	55	33	34
Sr	257	426	322	457	451	466
Y	25	29	30	32	20	24
Zr	104	160	140	158	113	133
Nb	7	11	8	6	10	14
Zn	75	79	113	62	61	65
Cu	30	21	21	17	36	43
Ni	104	59	4	20	91	90
V	154	237	294	195	226	165
Cr	330	40	30	85	249	206

TABLE 8.2 (continued)

Diabase dikes

MAJOR ELEMENTS	169-81	227-81	263-81	306-81
SiO2	48.2	51.2	45.2	53.0
TiO2	1.62	1.85	1.10	1.34
Al2O3	15.7	15.8	14.2	15.7
Fe2O3(t)	9.33	9.52	8.79	8.90
MnO	0.16	0.18	0.24	0.16
MgO	8.28	5.89	8.47	5.23
CaO	7.54	6.71	7.42	7.27
Na2O	2.65	2.86	1.79	4.22
K2O	1.13	0.95	1.40	0.75
P2O5	0.32	0.20	0.11	0.16
L.O.I.	4.43	4.45	11.22	3.20
Total	99.36	99.61	99.94	99.93

NORMS

Q	2.35	4.06	----	0.16
OR	6.66	5.90	9.32	4.58
AB	22.37	25.43	17.07	36.92
AN	27.54	28.87	29.96	22.41
DI	6.26	3.90	8.72	11.37
HY	29.52	26.07	23.86	20.07
OL	----	----	6.84	----
MT	1.49	1.60	1.59	1.47
IL	3.07	3.69	2.35	2.63
AP	0.74	0.49	0.29	0.38

TRACE ELEMENTS

Rb	31	29	57	24
Sr	417	309	211	444
Y	28	33	25	33
Zr	168	155	86	133
Nb	11	10	5	5
Zn	77	63	57	65
Cu	45	41	37	25
Ni	154	77	148	8
V	222	234	209	223
Cr	43	121	294	36

TABLE 8.3

Rare Earth Elements: Mafic Intrusions

Element (ppm)	New Bay 77-82	Gabbro 79-82	Diabase 65-81	Dike 306-81	Grapnel 19-82	Gabbro 50-82	Puncheon Diorite 221-81
La	44.44	21.53	6.81	11.80	12.57	21.94	9.89
Ce	115.27	60.50	18.06	34.08	31.34	60.76	25.23
Nd	74.42	41.82	13.76	21.43	16.50	45.83	14.99
Sm	16.57	11.98	4.64	5.70	3.50	13.65	3.79
Eu	6.45	4.00	1.58	2.13	1.05	13.65	1.30
Gd	17.81	12.08	4.56	6.28	3.64	15.94	4.76
Dy	13.03	11.18	4.19	5.13	2.42	13.99	5.07
Er	0.93	3.04	2.08	2.50	1.22	4.32	2.89
Yb	0.00	1.04	1.32	1.65	0.89	1.93	3.04

Chondrite Norm.

Element							
La	141.08	68.35	21.62	37.45	39.90	69.64	31.40
Ce	141.78	74.42	22.21	41.92	38.55	74.74	31.04
Nd	124.66	70.04	23.04	35.89	27.65	76.77	25.10
Sm	84.12	60.79	23.54	28.91	17.79	69.31	19.22
Eu	89.39	55.34	21.92	29.52	14.48	69.29	17.94
Gd	68.76	46.63	17.60	24.23	14.06	61.59	18.39
Dy	40.09	34.41	12.88	15.79	7.45	43.06	15.61
Er	4.37	14.27	9.75	11.74	5.74	20.26	13.59
Yb	0.00	4.99	6.35	7.94	4.30	9.28	14.63

and large amounts of peridotite. However, several factors indicate
that this was not the mechanism of formation of the Grapnel Gabbro:
(1) A silica gap of 6% exists between the Grapnel Gabbro and the
contaminated Coaker Porphyry. One would expect to find intermediate
values as a result of the mixing of a complete range of ratios of
magma and peridotite between the two extremes. (2) Mass balance
calculations indicate that the Grapnel Gabbro is not equivalent to any
combination of Coaker Porphyry and peridotite. (3) Sekine and Wyllie
(1982c) found experimentally that the product of the reaction between
the silicic magma and peridotite is a quartz-rich rock. Although the
Grapnel Gabbro contains interstitial quartz and granophyre in its
groundmass, normative quartz is low or absent.

8.2.2 Relationships among the mafic rocks

Although the pre-Caradocian mafic intrusions are all tholeiites
with similar trace element contents and behavior, they are
distinguished from one another on the basis of their distribution in
the field area, their mineralogy, and their major element
geochemistry. Commonly their fields do not overlap on variation
diagrams. These differences are probably the result of local
inhomogeneities in the mantle source, contamination, varying extents
of differentiation, or even escape of the magma from different levels
of the same magma chamber. Similar variations are observed in samples
from small areas along mid-ocean ridges (see Wood et al. 1979), or
even from one dredge haul (Miyashiro et al 1973).

Volcanic blocks from the Dunnage Melange and volcanic units of the Summerford Group are also tholeiitic to alkalic and plot in fields of within-plate basalts on discrimination diagrams (Hibbard 1976, Wasowski 1983).

8.2.3 Devonian diabase dikes

Geochemical data are available for Devonian dikes from the northeastern Gander Zone (Jayasinghe 1978) and from the South Lake Igneous Complex in the central Dunnage Zone (Lorenz and Fountain 1982). The former are distinctly alkalic, and the latter show a transitional tholeiitic - alkalic chracter, whereas those intruding the Dunnage Melange are tholeiitic. Their chemistry reflects variation in the mantle source across the orogen, although they most probably arose in response to the same tensional event.

8.3 Interpretation

The "within-plate" character of the mafic rocks of the Dunnage Melange is a reflection of their origin from an undepleted mantle source in an extensional environment. Continental rifting, which is an early or incipient stage of ocean formation, produces basalts of this affinity. Whereas the mafic rocks of the Dunnage Melange are not continental rift basalts, their regional setting is compatible with their having formed in an environment of incipient rifting in a back-arc position. Their chemistry is inconsistent with an origin in a compressional tectonic environment such as island arc or fore arc.

8.4 Summary

The Puncheon Diorite, New Bay Gabbro, and Grapnel Gabbro are tholeiites originating from incipient rifting in a back-arc basin environment. They are not genetically related to the silicic rocks in the field area, nor is the Grapnel Gabbro the result of the reaction between Coaker Porphyry and large amounts of peridotite. The Devonian diabase dikes are less alkalic than those from the Gander Zone or central Dunnage Zone, reflecting differences in the mantle source across the orogen.

Chapter 9.

Conclusions .

The Dunnage Melange and its intrusions were part of a complex and dynamic igneous, sedimentary and tectonic system, the local history of which was characterized by penecontemporaneous sedimentation, block faulting, olistostrome deposition, intrusion, and sediment slumping and sliding in Ordocician time (Chapter 5). The earliest intrusions are mafic tholeiites with a chemistry indicative of a tensional rather than a compressional environment, interpreted to be related to back-arc basinal rifting (Chapter 8). The Dunnage Formation was then intruded, penecontempoeaneously with sedimentation and melange formation (Chapter 4), by a suite of silicic rocks that have a sedimentary source, yet contain abundant ultramafic xenoliths (Chapter 6). These intrusions were followed closely in time by a calc-alkaline suite that was derived from an igneous or mantle source (Chapter 7).

The exact time at which melange formation began is unknown; we only know the ages of some of the lithologies involved, and the time at which melange formation abated (Caradocian). The Coaker Porphyry is interpreted to have intruded in the late stages of melange formation during Lladeilian time, indicating that disruption began prior to this (Chapters 4,5).

The age of the Dunnage Melange corresponds to the time during which the destruction of the ancient continental margin of North America was occurring. The foundering of the continental margin and the influx of flysch from the east began in Arenigian time (Stevens 1970; Williams 1980). This flysch heralded the approach of the allochthonous slices that were stacked from east to west and emplaced on the continental margin by Caradocian time (Stevens 1970; Williams 1975; 1980). Thus, by Arenigian time, collision of the volcanic arc with the North American continent had not only begun, but had progressed to the extent that ophiolite was uplifted and was contributing to the flysch. The emplacement of ophiolites onto the continental margin during Llandvirnian-Caradocian time (Stevens 1970) places the leading edge of the continental margin, with its apron of sediments, well down the subduction zone by Caradocian time. Voluminous quantities of trondhjemite, tonalite and granodiorite containing zircons with Grenvillian cores, occurring along the western margin of the Dunnage Zone, are interpreted by G. Dunning (pers. com. 1983) to be the result of melting of subducted Grenvillian basement or sediments derived from it. The Coaker Porphyry is interpreted here to be the result of melting of sedimentary material associated with the subducted leading edge of the continental margin.

It is proposed that large quantities of this magma (as well as the material from melting of Grenvillian basement) permeated and reacted with the overlying mantle. The Coaker Porphyry represents a minute sample of this magma that reached the surface, facilitated by the local occurrence of block faulting. The magma carried with it

samples of the ultramafic material through which it passed, and with which it reacted.

The Loon Bay/Dildo Porphyry suite is interpreted here to be the result of partial melting of the hybrid mantle produced by the reaction between the rhyodacitic melts and peridotite. A mantle source with crustal contamination has been proposed for this suite by Strong and Dickson (1978). Wyllie and Sekine (1982) and Sekine and Wyllie (1982) had postulated that such a hybrid mantle, produced by the mechanism described here, is the source of andesites and the calc-alkaline suite.

In summary, the Coaker Porphyry arose from the partial melting of sediments from the leading edge of the subducted continental margin of North America during the final stages of subduction. It intruded the unconsolidated muds of the Dunnage Melange, its ascent facilitated by block faulting. This last, along with the intrusion of rift-related tholeiites and the instability expressed by olistostrome deposition and slumping, is an expression of the extensional environment that locally prevailed up to middle Ordovician time, probably in a back-arc setting. A siliceous calc-alkaline suite, the Loon Bay granodiorites and the Dildo Porphyry, intruded the region as part of the later Acadian orogeny, arising from mantle contaminated by large quantities of Coaker-type magmas.

Figure 9.1 Tectonic setting of the Dunnage Melange and its
intrusions.

A. The Dunnage Formation forms in a back-arc
basinal environment.

B. The closing of Iapetus involves the overriding
of the North American continental margin by the
island arc. Extensive partial melting of subducted
sediments and continental crust produce voluminous
quantities of S-type magmas. Most of the magma
remains in the mantle wedge, where it reacts with
mantle peridotite and solidifies. Only minor
amounts reach shallow levels (the Coaker Porphyry).

C. Partial melting of the contaminated mantle
wedge gives rise to silicic calc-alkaline magmas
(Loon Bay/Dildo Porhyry suite).

A

Dunnage Formation

Tremadoc

B

Dunnage Melange

C C ↑ C C ↑ C C
C C C C ↑ C C C +
C C C C C
C C C C

Mantle

S-type
magmas
(Cooker)

Llandeilo

C

C

↑ C ↑ C C ↑ C
↑ C ↑ C ↑ C ↑ C

Calc-alkaline
magmas
(LB/DP suite)

contaminated mantle

Silurian
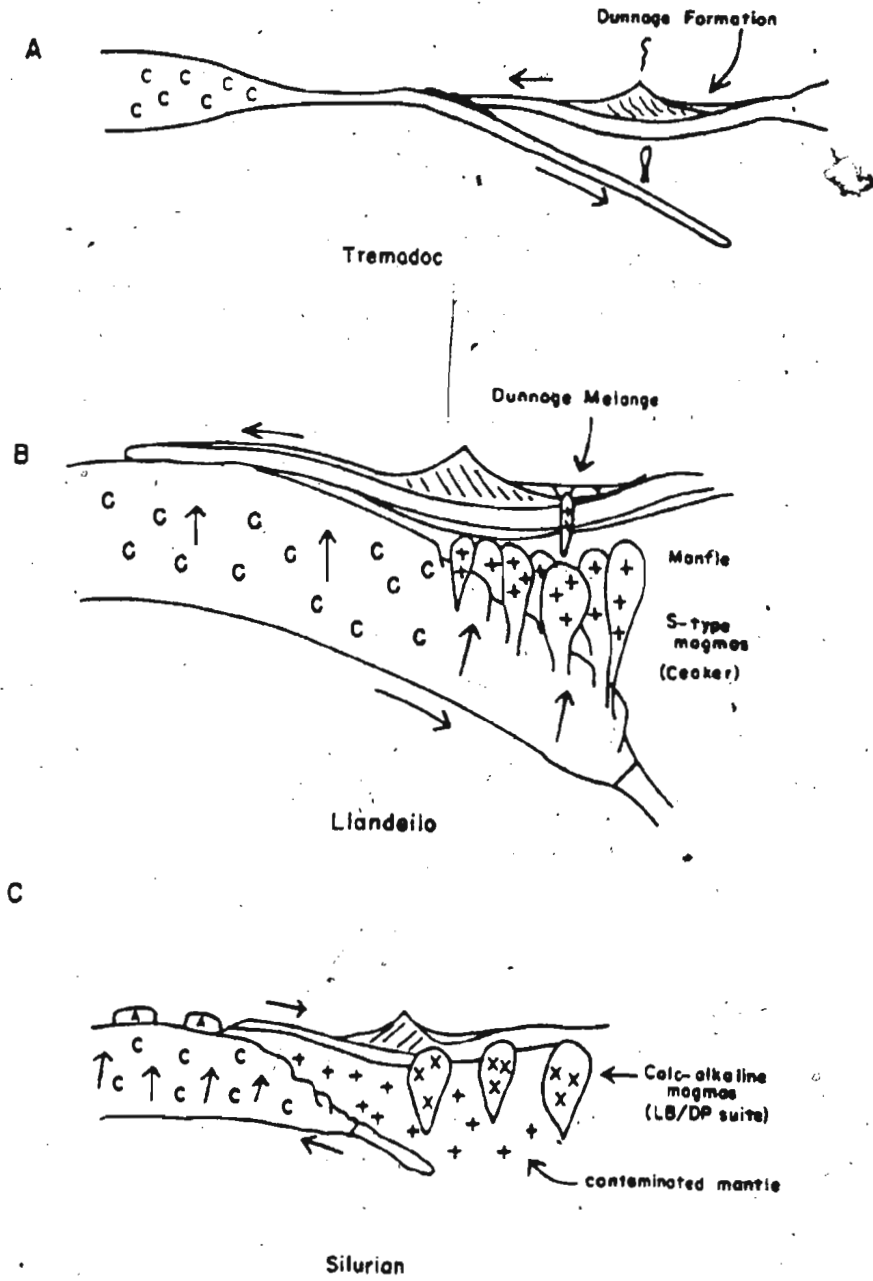
Bibliography

Burnham, C. W., and Ohmoto, H. 1980. Late stage processes of felsic magmatism. In Granitic Magmatism and Related Mineralization. Edited by S. Ishihara and S. Takenouchi. Mining Geology Special Issue ho. 8, Society of Mining Geologists of Japan, pp. 1-12.

Busch, W., Schnieder, G. and Mehnert, K. R. 1974. Initial melting at grain boundaries II: melting in rocks of granodioritic, quartzdioritic, and tonalitic composition. Neues Jahrbuch Mineralogie Mehnart, 345-370.

Cawthorne, R. G., and Brown, P. A. 1976. A model for the formation and crystallization of corundum-normative calc-alkaline magmas through amphibole fractionation. Journal of Geology, 84, pp. 467-476.

Cawthorne, R. G., Strong, D. F., and Brown, P. A. 1976. Origin of corundum-normative intrusive and extrusive magmas. Nature, 259, pp. 102-104.

Chappell, B. W. and White, A. J. R. 1974. two contrasting granite types. Pacific Geology, 8, pp. 173-174.

Clemens, J. D., and Wall, V. J. 1981. Origin and crystallization of some peraluminous (S-type) granitic magmas. The Canadian Mineralogist, 19, pp. 111-131.

Coleman-Sadd, S. P. 1980. Geology of south-central Newfoundland and evolution of the eastern margin of Iapetus. American Journal of Science, 280, pp. 991-1017.

Coleman-Sadd, S. P. 1982. Two stage continental collision and plate driving forces. Tectonophysics, 90, pp. 263-282.

Dean, P.L. 1978. The volcanic stratigraphy and metallogeny of Notre Dame Bay, Newfoundland. Memorial University of Newfoundland, Geology Report 7, 205 pp.

Deer, W. A., Howie, R. A., and J. Zussman. 1962. Rock-Forming Minerals, volume 2: Sheet Silicates. Longmans, Green and Co., Ltd., London.

Dewey, J. F. 1969. Evolution of the Appalachian/ Caledonian orogen. Nature, 222, pp. 124-129.

Didier, J., Duthou, J. L., and Lameyre, J. 1982. Mantle and crustal granites: Genetic classification of orogenic granites and the nature of their enclaves. Journal of Volcanology and Geothermal Research, 14, pp. 125-132.

Dunning, G. 1980. The Annieopsquotch Complex, Newfoundland's newest ophiolite. Geological Society of America Abstracts with Programs.

Floran, R. L. 1971. A petrologic investigation of the Loon Bay Batholith in north-central Newfoundland. Unpublished M. A. thesis, Columbia University, New York, 62 pp.

Flood, R. H., Vernon, R. H., Shaw, S. E., and Chappell, B. W. 1977. Origin of pyroxene-plagioclase aggregates in a rhyodacite. Contributions to Mineralogy and Petrology, 60, pp. 299-309.

Geological Society of Canada. 1964a. Point Leamington. Aeromagnetic Series Geophysics Paper 4461, Sheet 2 E/6, Map 4461G.

Geological Society of Canada. 1964b. Comfort Cove. Aeromagnetic Series Geophysics Paper 4462, Sheet 2 E/7, Map 4462G.

Green, T. H. 1977. Garnet in silicic liquids and its possible use as a P-T indicator. Contributions to Mineralogy and Petrology, 65, pp. 59-67.

Green, T. H. 1980. Island-arc and continent-building magmatism - a review of petrogenic models based on experimental petrology and geochemistry. Tectonophysics, 63, pp. 367-385.

Green, T. H. and Ringwood, A. E. 1972. Crystallization of garnet-bearing rhyodacite under high-pressure hydrous conditions. Journal of the Geological Society of Australia, 19, pp. 203-212.

Hanson, G. N. 1978. The application of trace elements to the petrogenesis of igneous rocks of granitic composition. Earth and Planetary Science Letters, 38, pp. 26-43.

Hanson, R. E., and Schweikert, R. A. 1982. Chilling and brecciation of a Devonian rhyolite sill intruded into wet sediments, northern Sierra Nevada, California. Journal of Geology, 90, pp. 717-7.24.

Harris, N.B. W., Duyverman, H. J., and Almond, D. C. 1983. The trace element and isotope geochemistry of the Subaloka Igneous Complex, Sudan. Journal of the Geological Society of London, 140, pp. 245-256.

Haworth, R. T., Lefort, J.-P., and Miller, H. G. 1978. Geophysical evidence for an east-dipping Appalachian subduction zone beneath Newfoundland. Geology, 6, pp. 522-526.

Helwig, J. A. 1967. Stratigraphy and structural history of the New Bay area, north-central Newfoundland. Unpublished Ph.D. dissertation, Columbia University, New York.

Helwig, J. A. 1969. Redefinition of the Exploits Group, Lower Paleozoic, northeast Newfoundland. American Association of Petroloeum Geologists Memoir 12, pp. 408-413.

Helwig, J. A. 1970. Slump folds and early structures, northeastern Newfoundland Appalachians. Journal of Geology, 78, pp. 172-187.

Heyl, G. R. 1936. Geology and mineral deposits of the Bay of Exploits area, Newfoundland. Newfoundland Department of Natural Resources, Geology section, Bulletin no. 3.

Hibbard, J. P. 1976. The southwest portion of the Dunnage Melange and its relationships to nearby groups. Unpublished M.Sc. thesis, Memorial University of Newfoundland, 131 pp.

Hibbard, J. P., Stouge, S., and Skevington, D. 1977. Fossils from the Dunnage Melange, north-central Newfoundland. Canadian Journal of Earth Sciences, 14, pp. 1176-1178.

Hibbard, J. P., and Williams, H. 1979. Regional setting of the Dunnage Melange in the Newfoundland Appalachians. American Journal of Science, 279, pp. 993-1021.

Hibbard, M. J. 1979. Myrmekite as a marker between preaqueous and postaqueous phase saturation in granitic systems. Geological Society of America Bulletin, 90, pp. 1047-1062.

Hine, R., Williams, I. S., Chappell, B. W. and White, A. J. R. 1978. Contrasts between I- and S-type granitoids of the Kosciusko batholith. Journal of the Geological Society of Australia, 25, pp. 219-234.

Horne, G. S. 1968. Stratigraphy and structural geology of southwestern New World Island area, Newfoundland. Unpublished Ph.D. dissertation, Columbia University.

Horne, G. S. 1969. Early Ordovician chaotic deposits in the central volcanic belt of northeastern Newfoundland. Geological Society of America Bulletin, 80, pp. 2451-2464.

Horne, G. S. 1970. Complex volcanic-sedimentary patterns in the Magog Belt of northeastern Newfoundland. Geological Society of America Bulletin, 81, pp. 1767-1788.

Horne, G. S., and Helwig, J. A. 1969. Ordovician stratigraphy of Notre Dame Bay, Newfoundland. American Association of Petroleum Geologists Memoir 12, pp. 388-407.

Hoyt, C. L. 1961. The Hammond Sill - An intrusion in the Yakima Basalt near Wenatchee, Washington. Northwest Science, 35, 2, pp. 58-64.

Huang, W. L., and Wyllie, P. J., 1973. Melting relations of muscovite-granite to 35 kbar as a model for fusion of metamorphosed subducted oceanic sediments. Contributions to Mineralogy and Petrology, 42, pp. 1-14.

Huang, W. L., and Wyllie, P. J. 1981. Phase relationships of S-type granite with H2O to 35 kilobars: Muscovite granite from Harney Peak, South Dakota. Journal of Geophysical Research, 86, pp. 10515-10529.

Hughes, C. J. 1982. Igneous Petrology. Elsevier Scientific Publishing Company, New York, 551 pp.

Irvine, T. N., and Baragar, W. R. A. 1971. A guide to the chemical classification of the common volcanic rocks. Canadian Journal of Earth Sciences, 8, pp. 523-548.

Jacobi, R. D., and Schweickert, R. A. 1976. Implications of new data on stratigraphic and structural relations of Ordovician rocks on New World Island, north central Newfoundland, Geological Society of America Abstracts with Programs, 8, p. 206.

Jayasinghe, N. R. 1978. Devonian alkalic basalt dikes of northeastern Newfoundland: Evidence of a tensional environment. Canadian Journal of Earth Sciences, 15, pp. 848-853.

Karlstrom, K. E., Van der Pluijm, B. A. and Williams, P. F. 1982. Structural interpretation of the eastern Notre Dame Bay area, Newfoundland: Regional post-Middle Silurian thrusting and assymetrical folding. Canadian Journal of Earth Science, 19, pp. 2325-2341.

Kay, M.   1970. Flysch and bouldery mudstone in northeast
        Newfoundland. Geological Association of Canada, Special
        Paper 7, pp. 155-164.

Kay, M.   1972. Dunnage Melange and Lower Paleozoic deformation in
        northeast Newfoundland. International Geological Congress,
        24th, section 3, pp. 122-133.

Kay, M.   1973. Tectonic evolution of Newfoundland. In Gravity and
        Tectonics.   Edited by K.   A. DeJong, and R. Scholten.
        Wiley and Sons, New York, pp. 313-326.

Kay, M.   1975. Campbellton sequence, manganiferous beds adjoining
        the Dunnage Melange, northeastern Newfoundland. Geological
        Society of America Bulletin, 86, 105-108.

Kay, M.   1976. Dunnage Melange and subduction of the Protacadic
        Ocean, northeast Newfoundland. Geological Society of
        America, Special Paper 175, 49 pp.

Kay, M. and Eldredge, N.   1968.   Cambrian trilobites in central
        Newfoundland volcanic belt. Geological Magazine, 105, pp.
        372-377.

Kokelaar, B. P. 1982. Fluidization of wet sediments during the
        emplacement and cooling of various igneous bodies. Journal
        of the Geological Society of London, 139, pp. 21-33.

Leake, B. E.   1978.   Nomenclature   of   amphiboles. American
        Mineralogist, 63, pp. 1023-1052.

Lorenz, B. E., and Fountain, J. C. 1982. The South Lake Igneous
        Complex, Newfoundland: A marginal basin - island arc
        association. Canadian Journal of Earth Sciences, 19, pp.
        490-503.

McKerrow, W. S., and Cocks, L. R. M. 1977. The location of the Iapetus Ocean suture in Newfoundland. Canadian Journal of Earth Science, 14, pp. 488-495.

McKerrow, W. S., and Cocks, L. R. M. 1978. A Lower Paleozoic trench-fill sequence, New World Island, Newfoundland. Geological Society of America Bulletin, 89, pp. 1121-1132.

Miyashiro, A. 1975. Classification, characteristics, and origin of ophiolites. Journal of Geology, 83, pp. 249-281.

Miyashiro, A., Shido, F. and Ewing, M. 1970. Crystallization and differentiation in abyssal tholeiites and gabbros from mid-ocean ridges. Earth and Planetary Science Letters, 7, pp. 361-365.

Naney, M. T., and Swanson, S. E. 1980. The effect of Fe and Mg on crystallization in granitic systems. The American Mineralogist, 65, pp. 639-653.

Pajari, G. E., Pickerill, R. K., and Currie, K. L. 1979. The nature, origin, and significance of the Carmanville ophiolitic melange, northeastern Newfoundland. Canadian Journal of Earth Sciences, 16, pp. 1439-1451.

Patrick, T. O. N. 1956. Comfort Cove, Newfoundland, map with notes. Geological Survey of Canada Paper 55-31.

Pearce, J. A., and Cann, J. R. 1973. Tectonic setting of basic volcanic rocks determined using trace element analyses. Earth and Planetary Science Letters, 19, pp. 290-300.

Pearce, J. A. and Norry, M. J. 1979. Petrogenetic implications of Ti, Zr, Y, and Nb variations in volcanic rocks. Contributions to Mineralogy and Petrology, 69, pp. 33-47.

Phillips, E. R. 1974. Myrmekite - one hundred years later. Lithos, 7, pp. 181-194.

Reynolds, P. H., and Murthy, G. S. in press. Devonian dikes from north central Newfoundland: A radiometric-paleomagnetic study. Geophysical Research Letters.

Schleicher, H., and Lippolt, H. J. 1981. Magmatic muscovite in felsitic parts of rhyolites from southwest Germany. Contributions to Mineralogy and Petrology, 78, pp. 220-224.

Sekine, T., and Wyllie, P. J. 1982a. Phase relationships in the system KAlSiO4 - Mg2SiO4 - SiO2 - H2O as a model for hybridization between hydrous siliceous melts and peridotite. Contributions to Mineralogy and Petrology, 79, pp. 368-374.

Sekine, T., and Wyllie, P. J. 1982b. Synthetic systems for modeling hybridization between hydrous siliceous magmas and peridotite in subduction zones. Journal of Geology, 90, pp. 734-741.

Sekine, T., and Wyllie, P. J. 1982. The system granite - peridotite - H2O at 30 kbar, with applications to hybridization in subduction zone magmatism. Contributions to Mineralogy and Petrology, 81, pp. 190-202.

Smith, J. V. 1974. Intergrowths of feldspars with other minerals. In Feldspar Minerals, Chapter 20, volume 2. Springer Verlag, New York, pp. 553-608.

Stevens, R. K. 1970. Cambro-Ordovician flysch sedimentation and tectonics in west Newfoundland and their possible bearing on a Proto-Atlantic Ocean. In Flysch Sedimentology in North America. Edited by J. Lajoie. Geological Association of Canada, Special Paper 7, pp. 165-177.

Strong, D. F. 1977. Volcanic regimes of the Newfoundland Appalachians. In Volcanic Regimes in Canada. Edited by W. R. A. Baragar, L. L. Coleman, and J. M. Hall. Geological Association of Canada, Special Paper 16, pp. 61-90.

Strong, D. F. 1980. Granitoid rocks and associated mineral deposits of eastern Canada and western Europe. In The Continental Crust and its Mineral Deposits. Edited by D. W. Strangway. Geological Association of Canada, Special Paper 20, pp. 741-769.

Strong, D. F., and Dickson, W. L. 1978. Geochemistry of Paleozoic granitoid plutons from contrasting tectonic zones of northeast Newfoundland. Canadian Journal of Earth Sciences, 15, pp. 145-156.

Strong, D. F., and Harris, A. 1974. The petrology of Mesozoic alkaline intrusives of central Newfoundland. Canadian Journal of Earth Sciences, 11, pp. 1208-1219.

Wasowski, J. J. and Jacobi, R. D. 1983. Geochemistry and tectonic significance of mafic volcanic blocks in the Dunnage Melange, north-central Newfoundland. Geological Society of America Abstracts with Programs, Northeast section, p. 189.

Watson, E. B. 1979. Zircon saturation in felsic liquids: Experimental results and applications to trace element geochemistry. Contributions to Mineralogy and Petrology, 70, pp. 407-419.

White, A. J. R., and Chappell, B. W. 1977. Ultrametamorphism and granitoid gneiss. Tectonophysics, 43, pp. 7-22.

Williams, H. 1962. Botwood (west half) map area - Newfoundland. Geological Survey of Canada Paper 62-9, 16 pp.

Williams, H. 1963. Twillingate map area, Newfoundland. Geological Survey of Canada Paper 63-36, 30 pp.

Williams, H. 1972. Stratigraphy of Botwood map area, northeastern Newfoundland. Unpublished manuscript, Geological Survey of Canada open file 113, 103 pp.

Williams, H. 1975. Structural succession, nomenclature, and interpretation of transported rocks in western Newfoundland. Canadian Journal of Earth Sciences, 12, pp. 1874-1894.

Williams, H. 1979. Appalachian orogen in Canada. Canadian Journal of Earth Sciences, 16, pp. 792-807.

Williams, H., and Hibbard, J. P. 1976. The Dunnage Melange, Newfoundland. Geological Survey of Canada, Paper 76-1A, pp. 183-185.

Williams, H. and Hatcher, R. D. 1983. Appalachian suspect terranes. Geological Society of America Memoir 158, pp. 33-53.

Winkler, H. F. 1976. Petrogenesis of Metamorphic Rocks, 4th edition. Springer Verlag, New York, 334 pp.

Wood, D. A., Tarney, J., Varet, J., Saunders, A. D., Bougault, H., Joron, J. L., Treuil, M., and Cann, J. R. 1979. Geochemistry of basalts drilled in the North Atlantic by IPOD Leg 49: Implications for mantle heterogeneity. Earth and Planetary Science Letters, 42, pp. 77-97.

Wyborn, D., Chapell, B. W., and Johnston, R. M. 1981. Three S-type volcanic suites from the Lachlan Fold Belt, Australia.

Wyllie, P. J., and Sekine, T. 1982. The formation of mantle phlogopite in subduction zone hybridization. Contributions to Mineralogy and Petrology, 79, pp. 375-380.

Appendix
Map Notes for Figure 2.3

1. (Coaker Island) Richly garnetiferous Coaker Porphyry.

2. Gabbro intrusion – possibly part of the Puncheon Diorite suite.

3. Small block of Coaker Porphyry in shale.

4. Carbonate block.

5. and 6. Dark Hole Shale surrounded by Dunnage Melange mudstones.

7. Enormous (up to 30 cm diameter) ultramafic xenoliths in Causeway-type Coaker Porphyry. Some xenoliths contain xenoliths themselves.

8. Silicified, brecciated Coaker Porphyry. Cataclastic texture in thin section.

9. Well-exposed contact between hornfelsed melange and Causeway-type Coaker Porphyry.

10. Abundant gabbroic xenoliths in Causeway-type Coaker Porphyry.

11. In mudstone: block of clast-supported conglomerate consisting of mafic glass pebbles in shale.

12. Causeway-type Coaker Porphyry peperite at contact with mudstone. Abundant silicic xenoliths (older Coaker Porphyry ?).

13. Melange matrix contains clasts of hornfels near contact with Coaker Porphyry. Nearby is a carbonate block.

14. Small, lobate body of banded Coaker Porphyry.

15. Large block of carbonate breccia.

16. Collected from Coaker Porphyry in this locality: a large (5x20 cm) rectangular xenolith or phenocryst of pure sericitized alkali feldspar. (Fox Island).

17. Peperite dikes in Coaker Porphyry.

18. Banded, vesicular Coaker Porphyry pillows in shale. (Fair Maid's Lookout).

19. Dikes of xenolith-rich Coaker Porphyry intruding purple hornfels. Darks are flow-differentiated with xenoliths concentrated in their centers. Hornfels preserves earlier folds.

20. Xenolith-rich Coaker Porphyry intruding an older body of Coaker

Porphyry that is paler in colour, has larger phenocrysts, and fewer xenoliths.

21. Very large diabase dike (or one with low angle of dip).

22. Carbonate block.

23. Dark Hole Shale – Dunnage Melange contact along shore.

24. Low-amplitude folds in Dark Hole Shale (approximately 1 m wavelength). The folds become tighter to the north and fracture along the hinge.

25. Intrusion of Dildo Porphyry, cutting across bedding in Dark Hole Shale. Intrusion contains abundant phenocrysts of milky-white quartz.

26. Bedding of Dark Hole Shale becomes gradually less distinct; Dunnage character takes over.

27. Large block of coarse conglomerate: pebbles and stringers of basaltic glass in calcite.

28. Raft of Dark Hole Shale in Dunnage Melange.

29. Cherty-looking, angular cobbles of Coaker Porphyry in black mudstone.

30. Puncheon Diorite, with schlieren near contact. Intruded by Coaker Porphyry. (Pomeroy's Island).

31. (White Islands). Pillowed, vesicular Coaker Porphyry in contact with purple hornfels.

32. Coaker Porphyry breccia in hornfels. Slickensides indicate tectonic brecciation rather than peperite.

33. Coaker Porphyry dike (85 cm across) sharply cuts a volcanic block.

34. Contorted, baked mudstone at contact with Puncheon Diorite.

35. Light grey, medium-grained Puncheon Diorite intruded by aplitic dikelets. Also contains cognate inclusions of both lighter and darker dioritic material. Puncheon Diorite here contains highly irregular banding or layering of leucocratic and mafic diorite.

36. Spectacular schlieren.

37. Dike of Coaker Porphyry intruding Puncheon Diorite.

38. Folded diabase dike in Coaker Porphyry, suggests folding contemporaneous with or later than intrusion of diabase dikes.

39. Block of autobrecciated spherulitic pillow basalt with carbonate selvedge.

40. Coaker Porphyry peperite in mudstone. Well-exposed along shore, parallel to contact between stock and mudstone.

41. Cooling cracks in contact surface of Coaker Porphyry stock.

42. Spectacular mixture of boudinaged Coaker Porphyry and mudstone.

43. Isoclinal folds in silty shale.

44. Well-bedded, undisturbed silty shale, or bedded tuff.

45. Breccia consisting of fragments of black shale, red shale, greywacke, scoriaceous basalt in a green shale matrix.

46. Coaker Porphyry with abundant large gabbroic xenoliths, both dark-coloured amphibolites and light grey prehnite-quartz assemblages.

47. Euhedral quartz megacrysts (up to 8 cm across) in Causeway xenolith phase.

48. Type locality of the Causeway xenolith phase of the Coaker Porphyry.

49. Birchy Islands - Intermingled and folded Coaker Porphyry and mudstone. Coaker Porphyry is locally vesicular with lobate contacts and cracked surfaces.

50. Coaker pillows, intermixtures with mudstone, and breccia. Some of this material is possibly extrusive. Mudstone and Coaker Porphyry are also intermixed with mafic volcanic pillowed flows and breccia.

51. Grapnel Gabbro stock containing small ultramafic xenoliths.

52. Small boulders of bedded carbonate.

53. Extremely fresh xenolith-rich Coaker Porphyry containing amphibole and garnet.

54. Folded Coaker Porphyry dike with lobate termination.

55. Coaker Porphyry - Grapnel Gabbro contact.

56. An island composed entirely of well-formed spherulitic pillow basalt.

57. Mudstone matrix containing sandy layers and lenses, and small carbonate blocks.

58. (Inspector Island) Cindery-looking, black Coaker Porphyry.

59. White Coaker Porphyry with extremely few phenocrysts, no xenoliths.

60. Intermixed and folded Coaker Porphyry and mudstone. Coaker Porphyry stock, from which dikelets emerge, is flow-banded and vesicular. Contains large (up to 8 mm across) muscovite phenocrysts.

61. Silty and sandy beds in black mudstone, some folded, some disrupted, some undisturbed.

62. A very large limestone block, locally known as "The Limestone", quarried approximately 50 years ago (E. C. Small, pers. com. 1981).

63. Complexly intermixed volcanics (tuff, pumice) and matrix, intruded by Causeway-type Coaker Porphyry.

64. Large lobate "pillows" of Coaker Porphyry (up to 3 m across) intruding black mudstone.

65. Spherulitic pillow basalt with spherules up to a cm across.

166. Old mine pit in a block of brecciated jasper fragments in a black Mn-oxide + magnetite matrix.

67. A series of mine pits in a mineralized dike. (Chalcopyrite + pyrrhotite + pentlandite).

68. Xenolith-rich Coaker Porphyry with small phenocrysts intruding xenolith-poor Coaker Porphyry with large phenocrysts.

69. Pillowed Coaker Porphyry in mudstone. Surrounding mudstone includes Coaker fragments, some of which are rounded.

70. Isoclinally folded beds of siltstone and shale. Siltstone layers show varying degrees of disruption, boudinage, rotation.

71. Isolated pillow of black, flow-banded Coaker Porphyry, approximately 2x1 m. Easily accessible in quarry.

72. Several small anastomosing diabase dikes, their orientation controlled by slickensided fractures (related to Reach Fault) and the presence of Coaker Porphyry.

73. One of several plutonic cobble conglomerates. Some of these cobbles are petrographically and geochemically similar to the Twillingate trondhjemite.

74. More plutonic cobble conglomerate.

75. Mudstone with disrupted bands of siltstone and sandstone, and a plutonic cobble conglomerate. Nearby Coaker Porphyry is cut by a peperite dike.

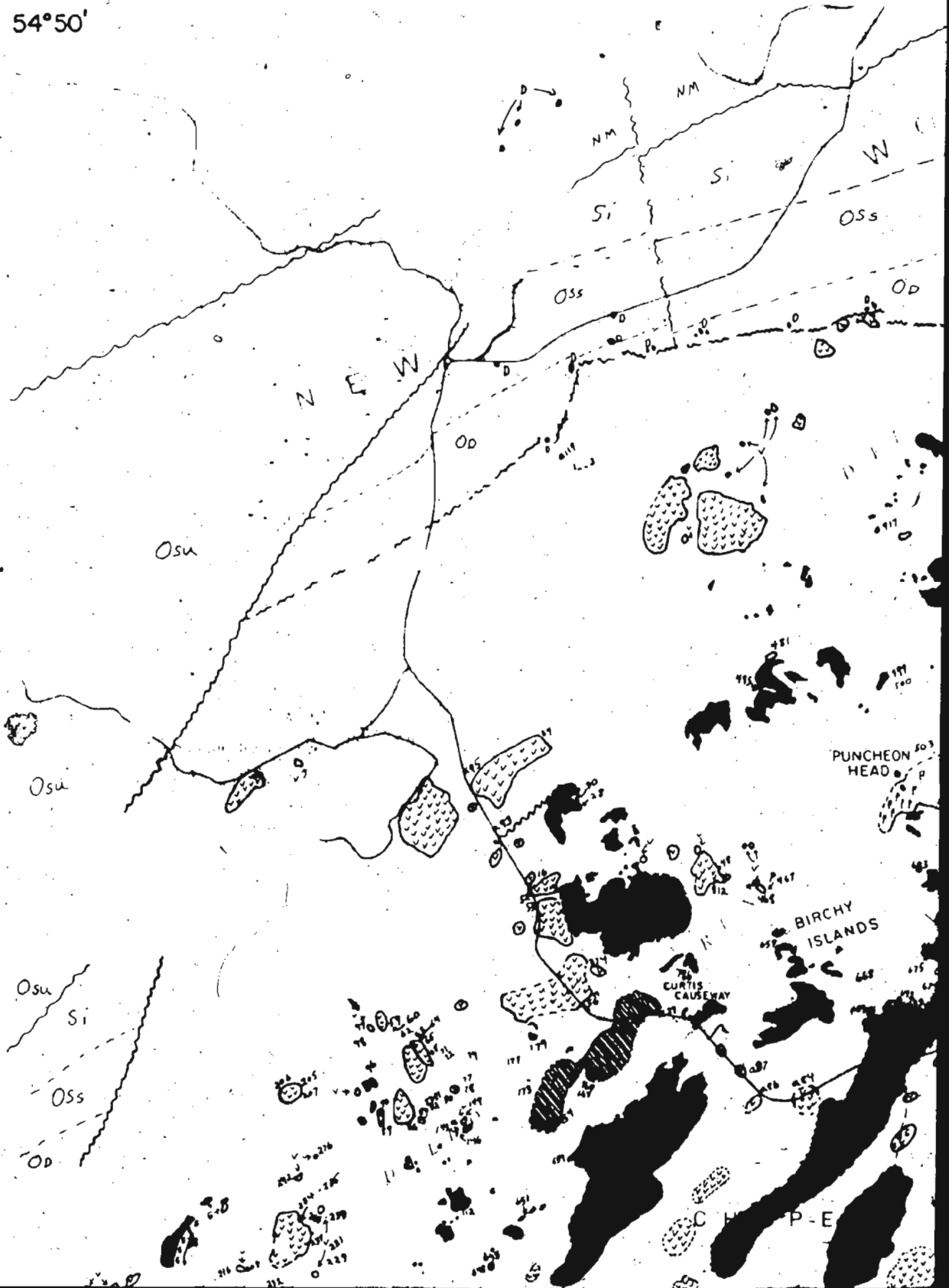Appendix B

Key to Figure 2.3 Maps of Northeast Dunnage Melange

Undifferentiated Silurian groups	Si
New World Island Complex	NM
Sansom Greywacke	OSs
Dark Hole Shale	OD
Chapel Formation	▨
Summerford Group	OSu
Volcanic blocks	▨
Dunnage Melange	☐

Intrusions

Late dikes	◺
Loon Bay Granite	⊞
Dildo Porphyry	[D]
Grapnel Gabbro	▨
Xenolith-rich Coaker Porphyry	▨
Coaker Porphyry	■
Puncheon Diorite	▨
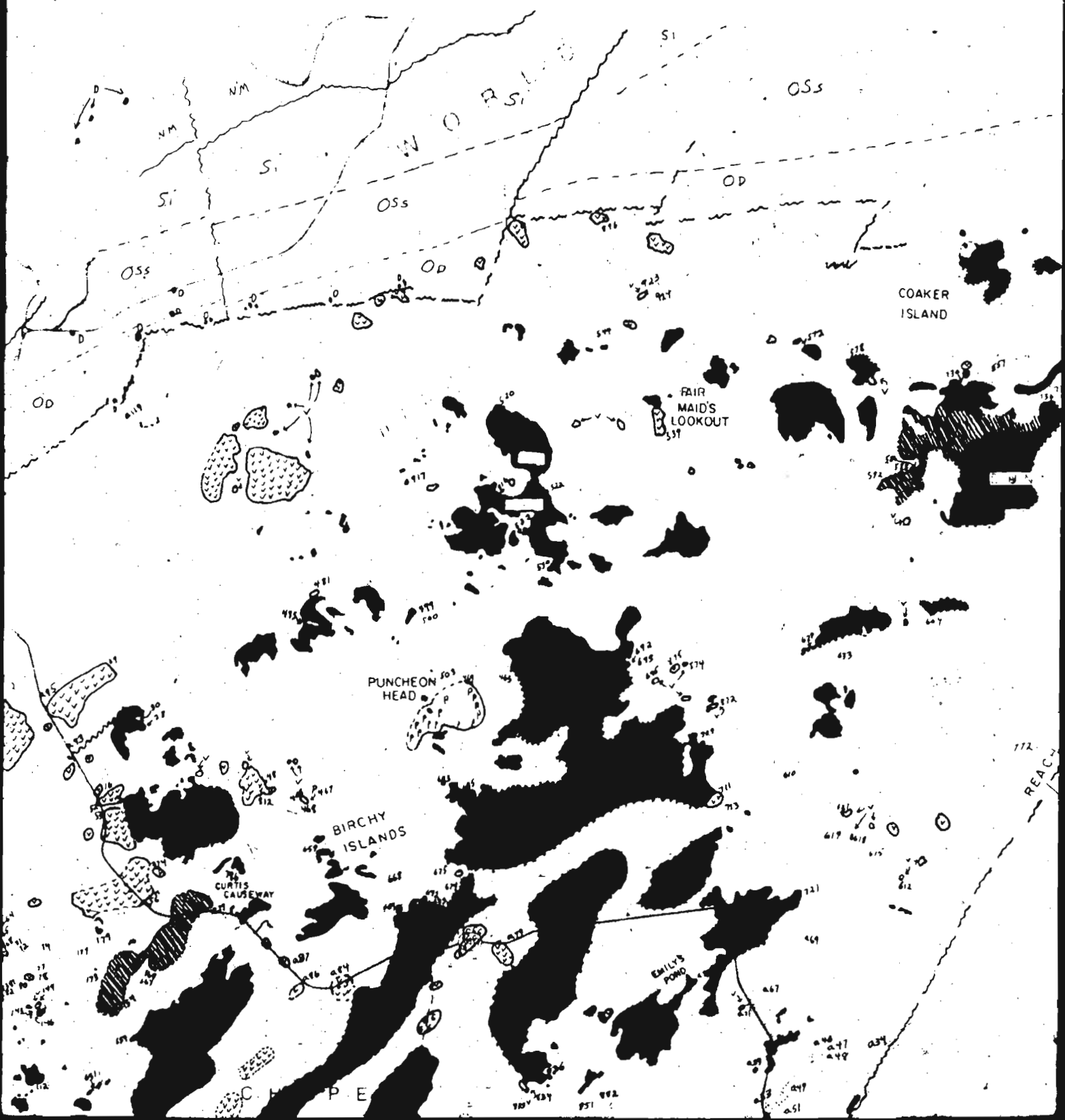
COAKER
ISLAND

FAIR
MAID'S
LOOKOUT

PUNCHEON
HEAD

BIRCHY
ISLANDS

CURTIS
CAUSEWAY

EMILY'S
POND

REACH

54° 35'

OSs

OD

Si

COAKER
ISLAND

FAIR
MAID'S
LOOKOUT

-49°30'

REACH FAULT

Si

EMILY'S
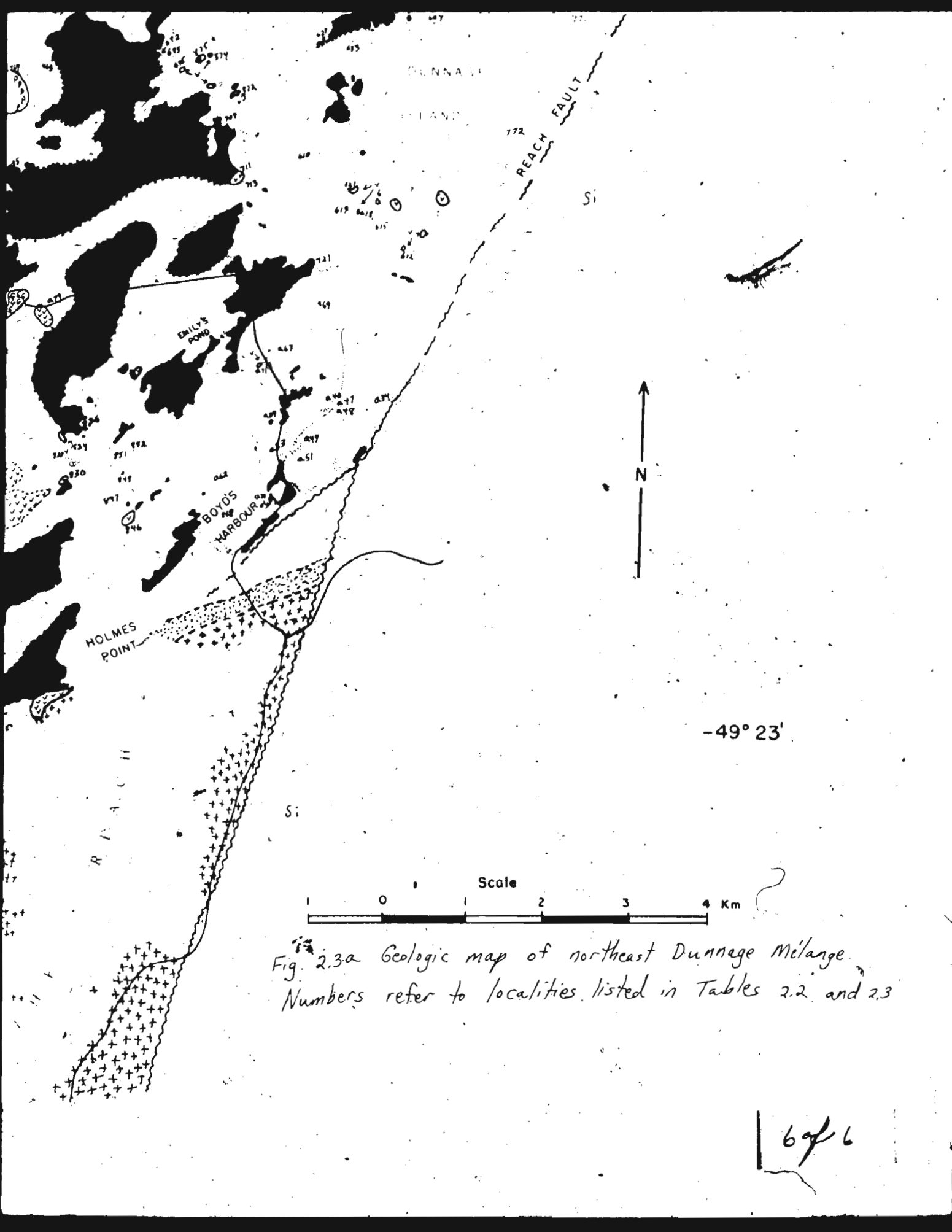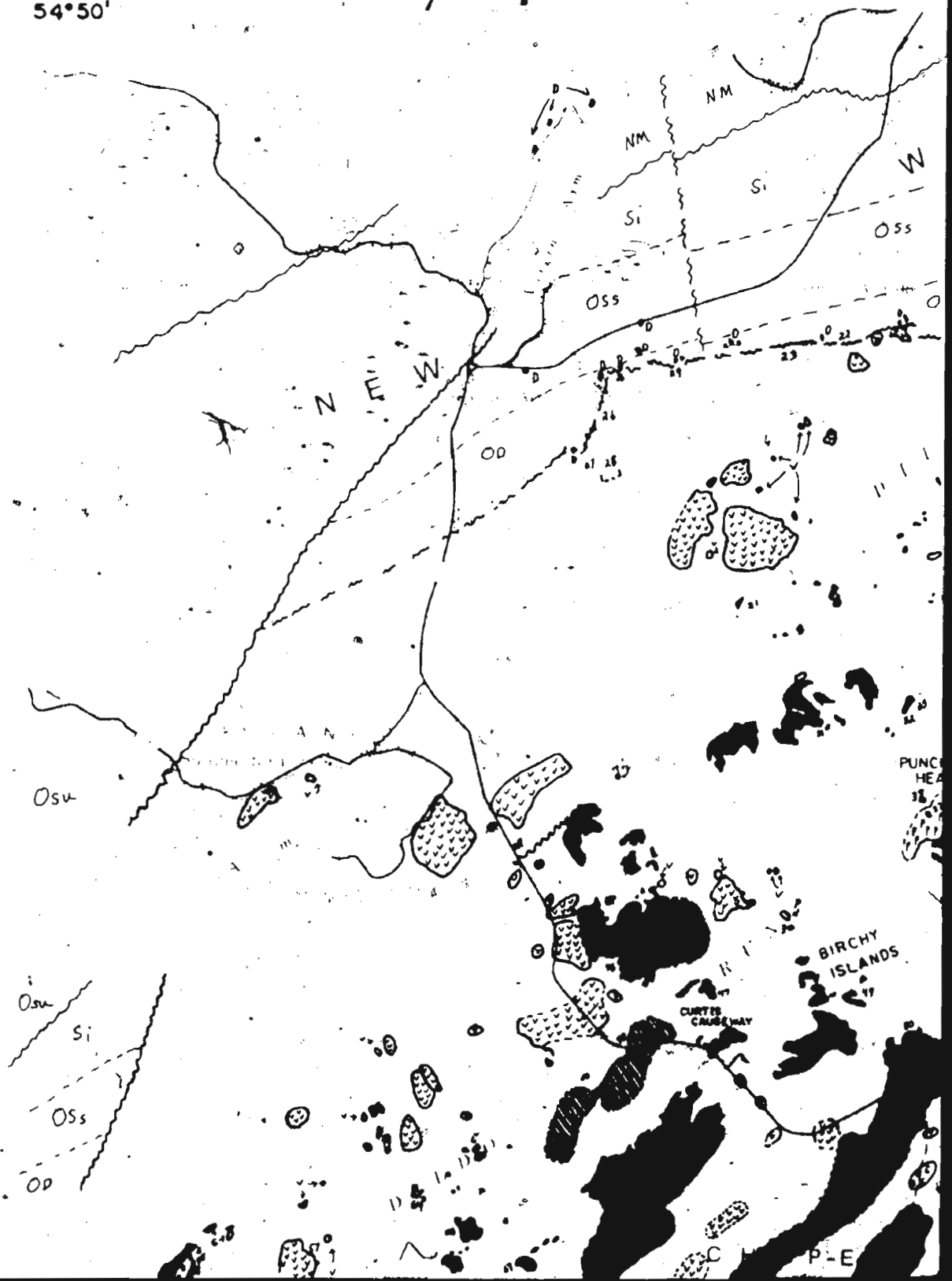POND

37

Fig. 2.3a Geologic map of no
Numbers refer to localities

5.9
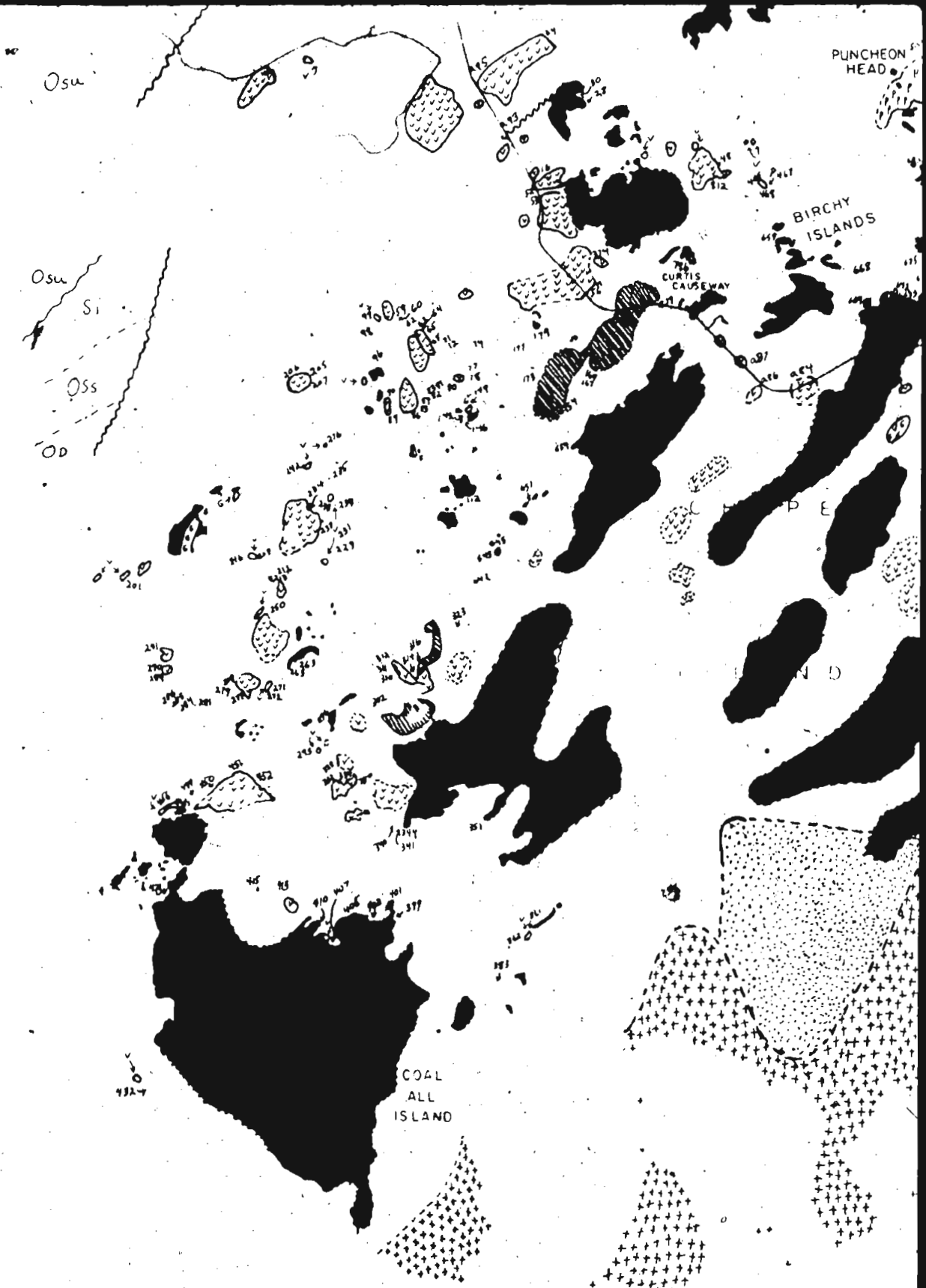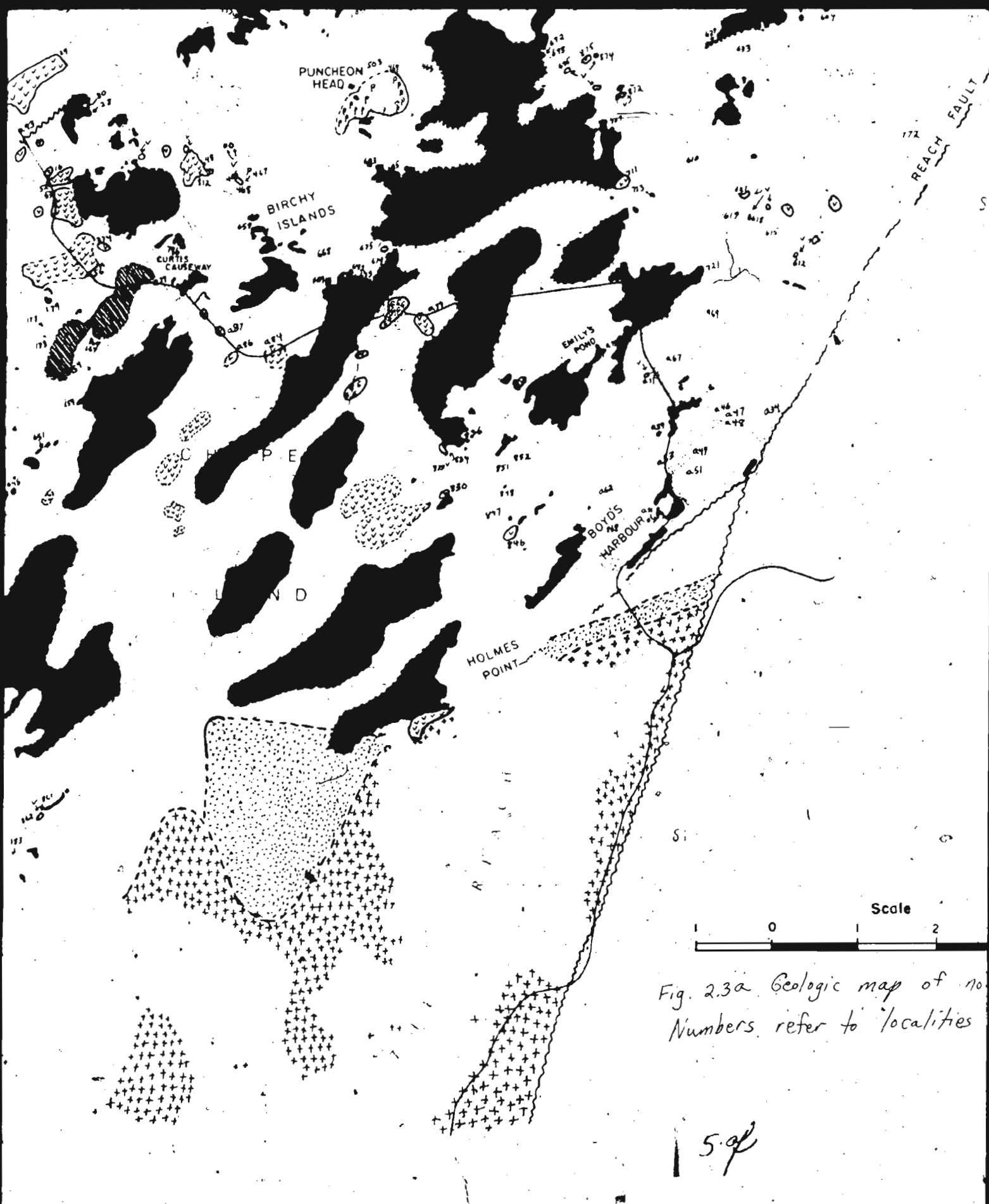
Fig. 2.3a Geologic map of northeast Dunnage Mélange.
Numbers refer to localities listed in Tables 2.2 and 2.3

54°50'

NM
NM
NM
Si
Si
W
Si
Oss
Oss
N E W
OD
Osu
Osu
Si
Oss
OD

PUNCH
HEAD
BIRCHY
ISLANDS
CURTIS
CAUSEWAY

C
P-E

W O R L D

NM

NM

NM

Si

Si

Si

Si

Oss

Oss

Oss

OD

OD

OD

OD

Oss

D

COAKER
ISLAND

FAIR
MAIDS
LOOKOUT

GUNNA

PUNCHEON
HEAD

REACH FAULT

Si

BIRCHY
ISLANDS

CURTIS
CAUSEWAY

EMILY'S
POND

C A P E

54°35'

RLD Si

OSS

OD

OD

COAKER
ISLAND

FAIR
MAIDS
LOOKOUT

-49°30'

REACH FAULT

Si

37

EMILY'S
POND

N

Osu

Osu

Si

CSs

OD

BIRCHY
ISLANDS

CURTIS
CAUSEWAY

CHAPEL
ISLAND

SLAND

P E

COAL
ALL
ISLAND

4 of

PUNCHEON
HEAD

BIRCHY
ISLANDS

CURTIS
CAUSEWAY

REACH FAULT

EMILY'S
POND

CHAPEL
ISLAND

BOYD'S
HARBOUR

HOLMES
POINT→

Si

Scale
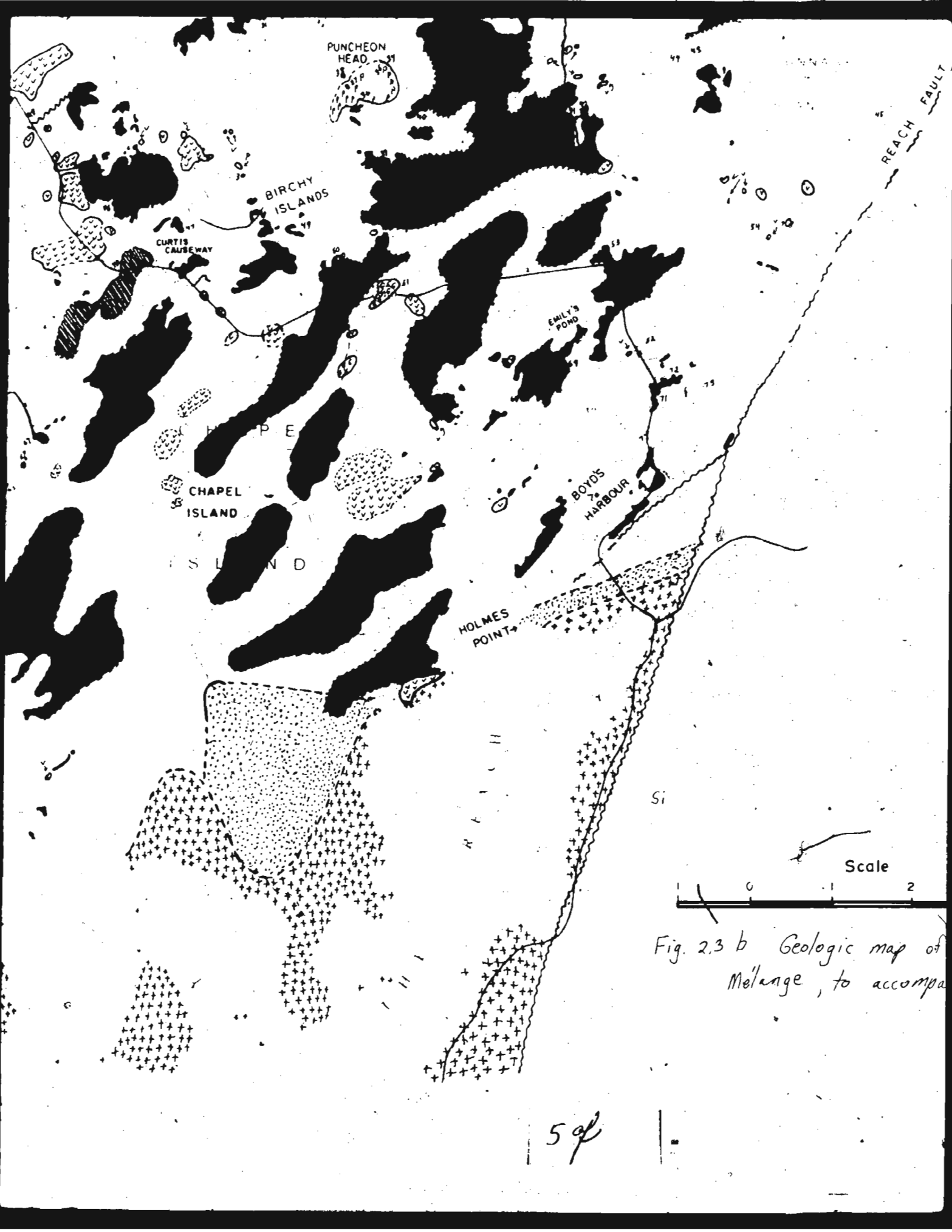
Fig. 2.3 b Geologic map of
Mélange, to accompa
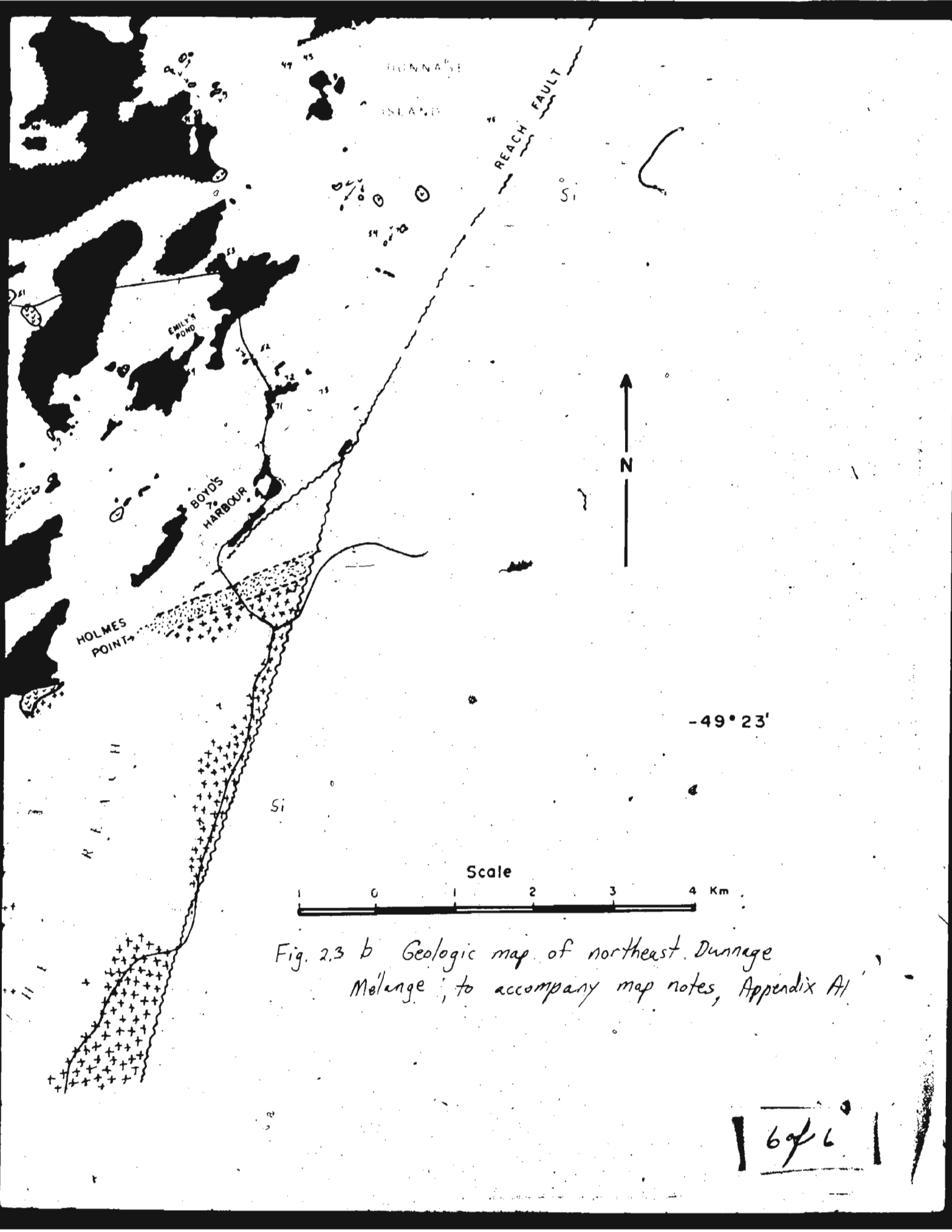
Fig. 2.3 b Geologic map of northeast Dunnage Melange; to accompany map notes, Appendix A1

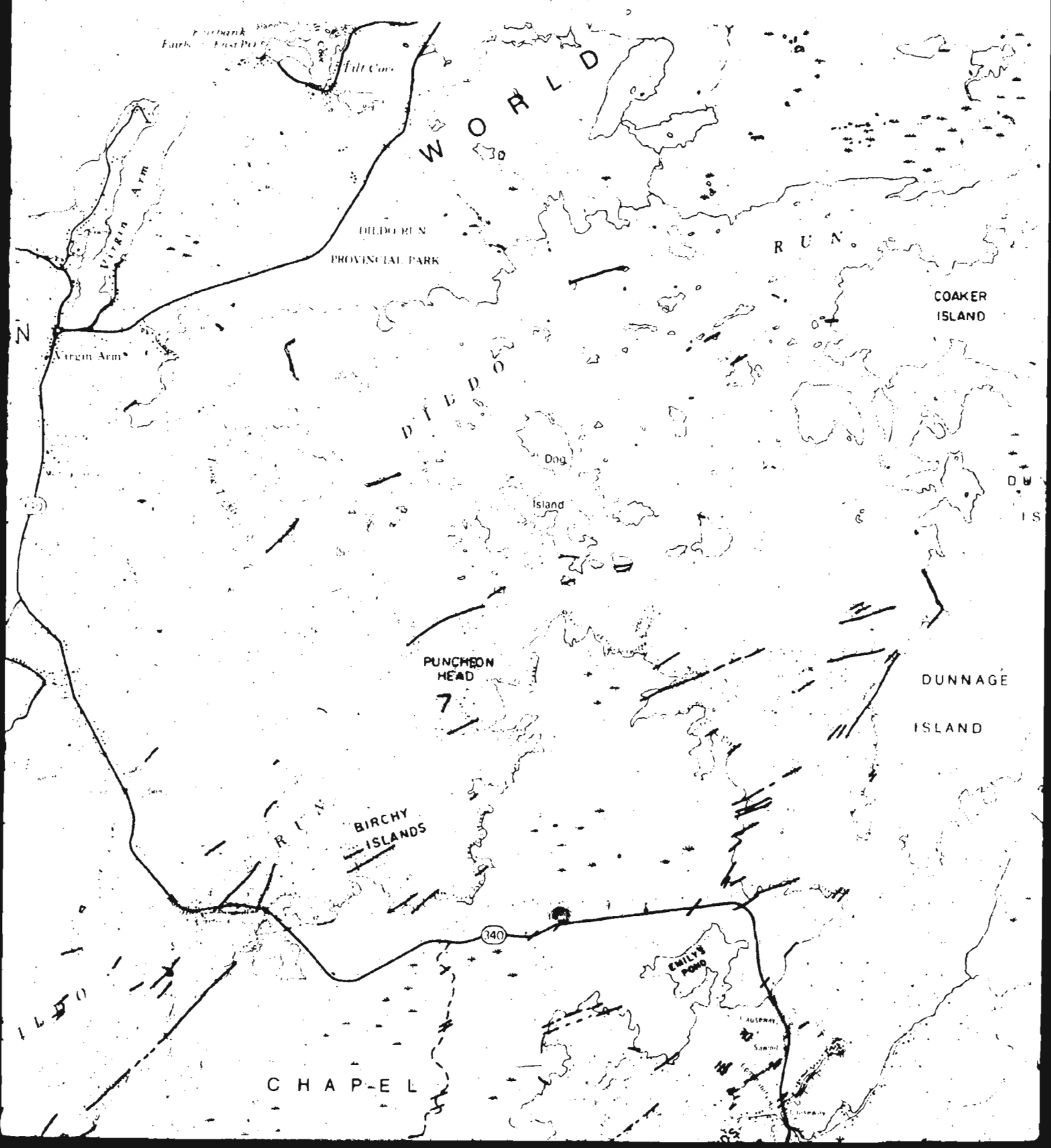DUNNAGE ISLAND

REACH FAULT

EMILY'S POND

BOYD'S HARBOUR

HOLMES POINT

REACH

N

-49°23'

Scale

1   0   1   2   3   4 Km

6 of 6

D
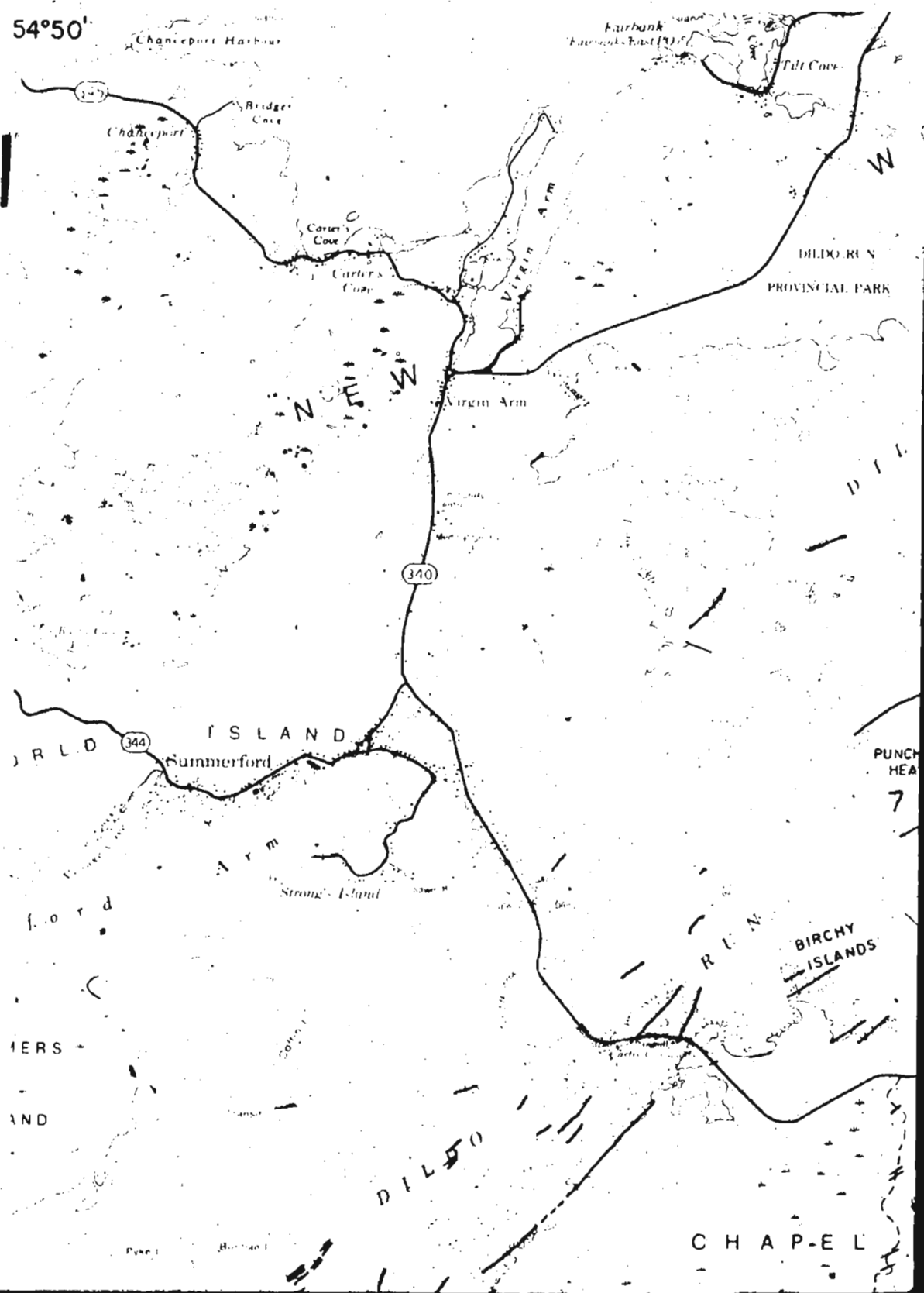
R U N

COAKER
ISLAND

DUNNAGE

ISLAND

54°35'

-49°30'

DUNNAGE

ISLAND

REACH FAULT

EMILY'S
POND

N

Summerford

ford   Arm

Strong's Island

BIRCHY
ISLANDS

RUN

IERS

AND

D I L D O

C H A P E L

I S L A N D

COAL   ALL
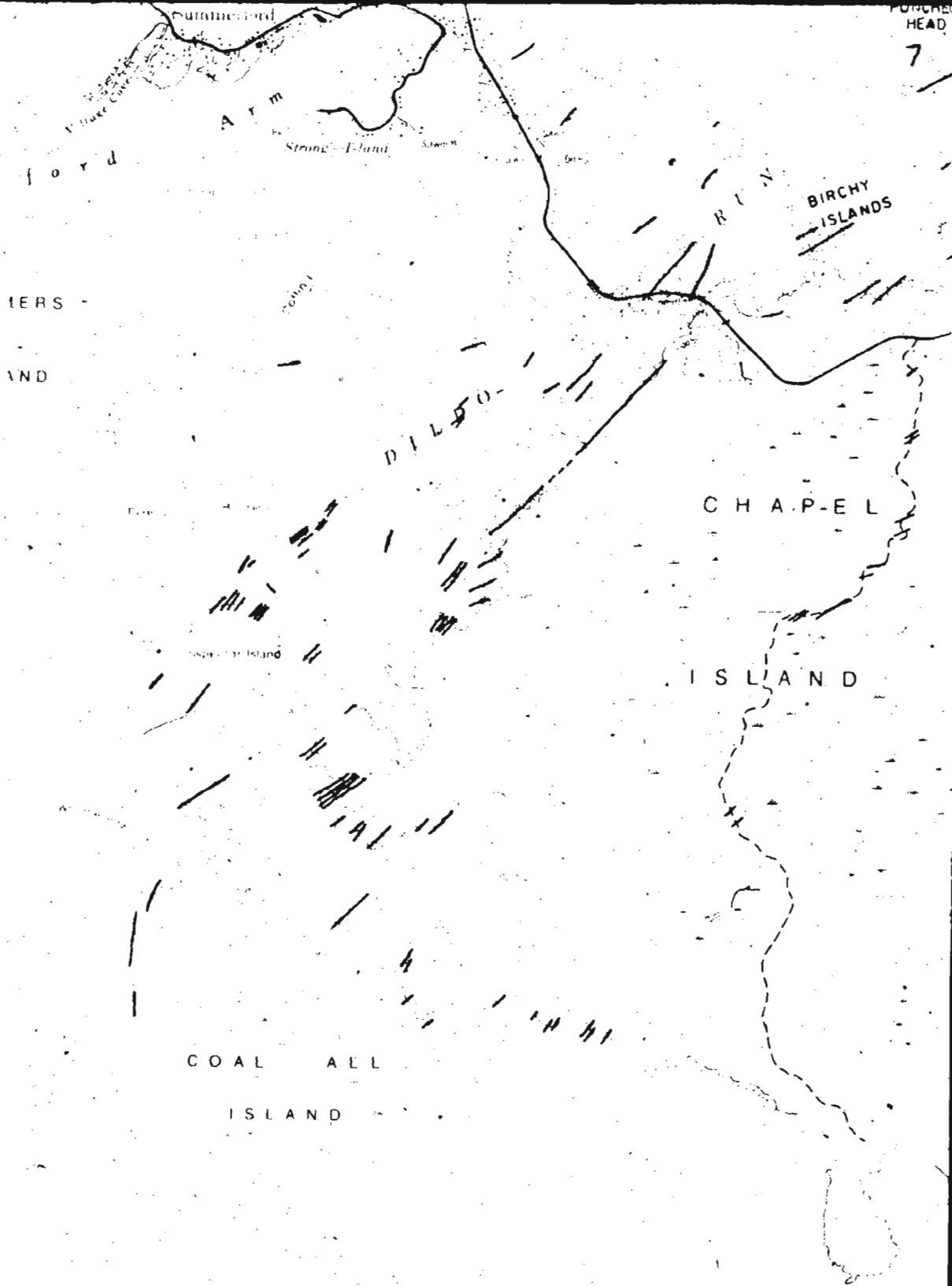
ISLAND

4 of
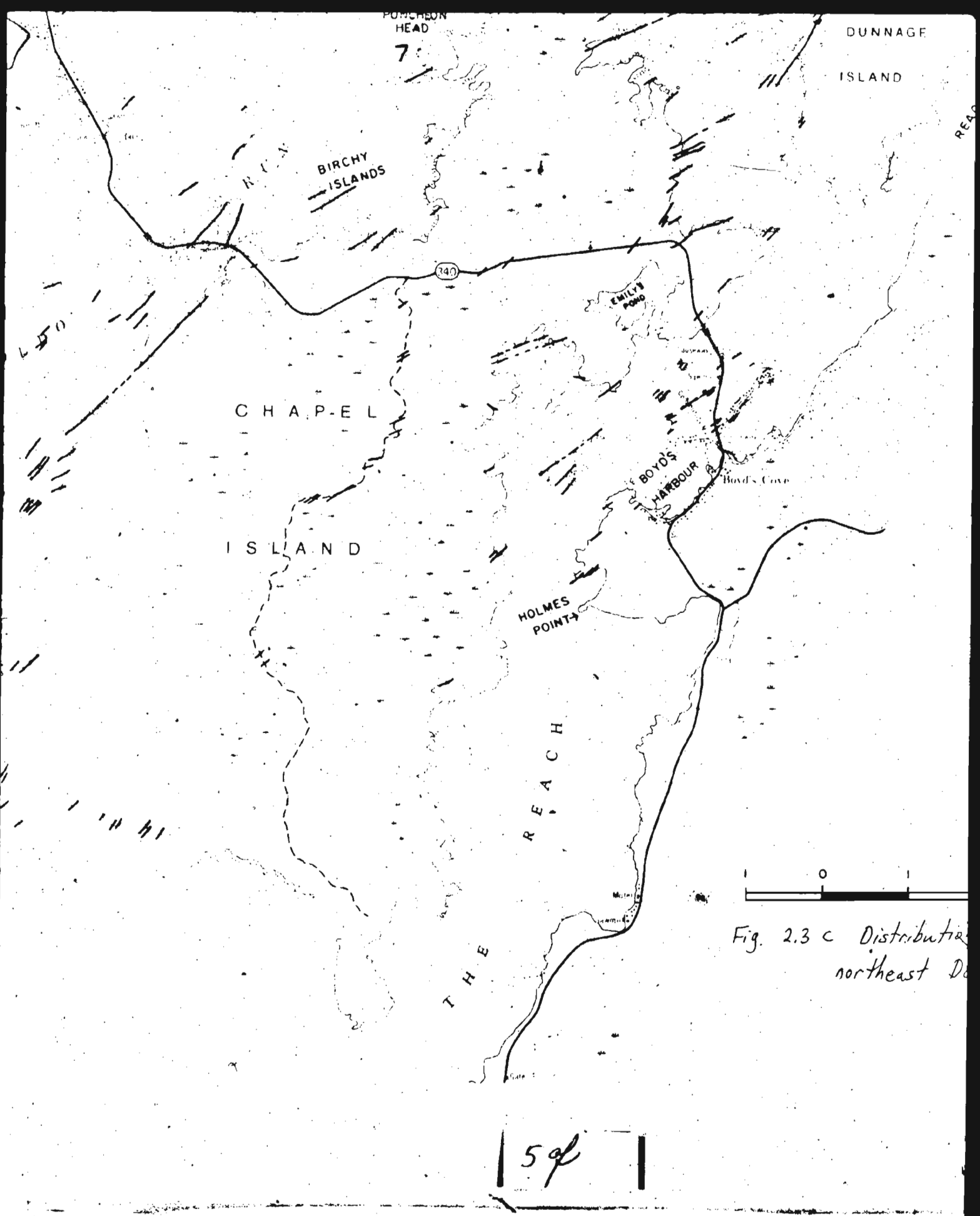
Fig. 2.3 c Distribution
northeast D...

5ℱ

DUNNAGE

ISLAND

REACH FAULT

EMILY'S POND

BOYD'S HARBOUR

Boyd's Cove

HOLMES POINT→

R E A C H
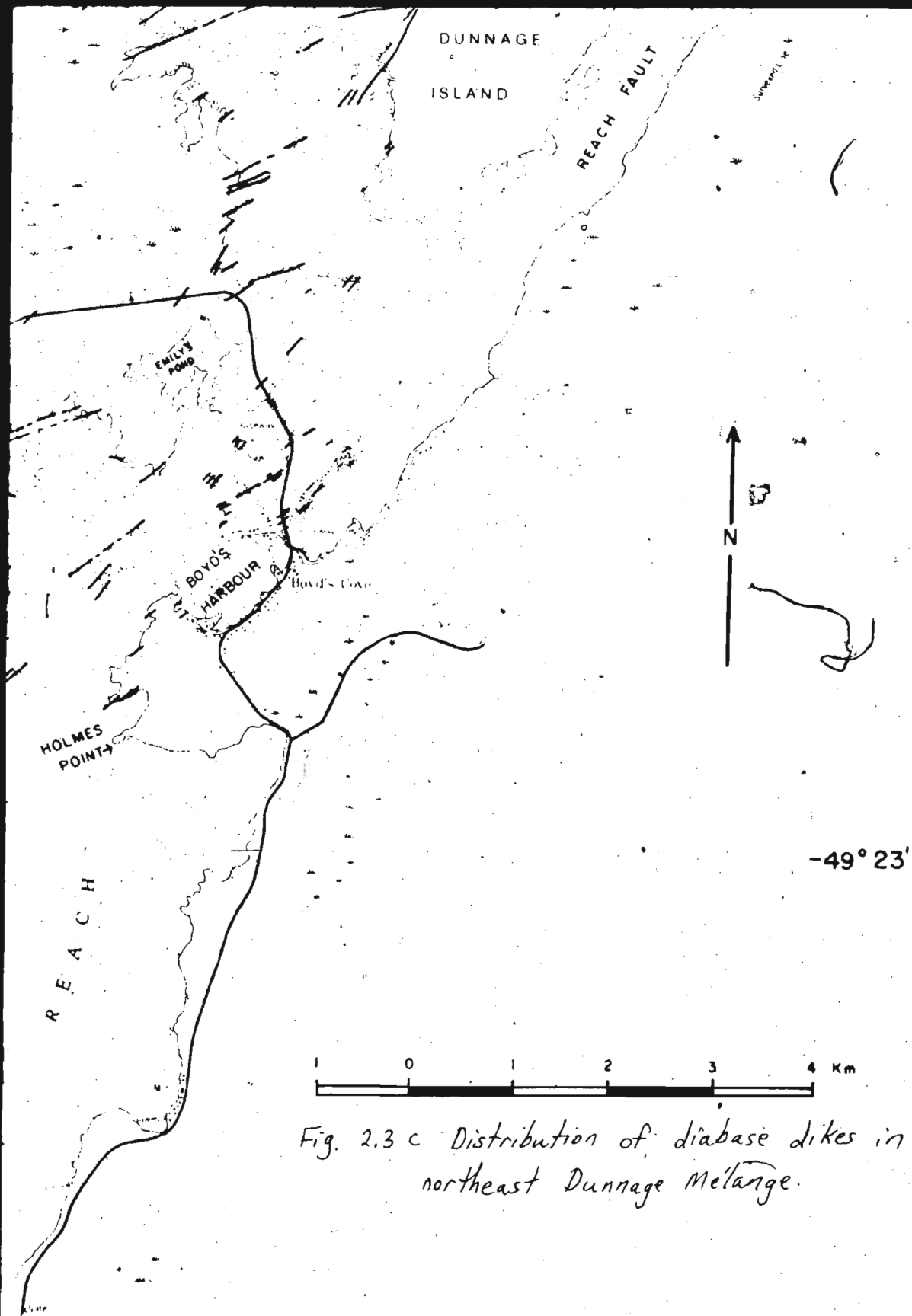
N

−49° 23'

| 1 | 0 | 1 | 2 | 3 | 4 Km |

Fig. 2.3 c Distribution of diabase dikes in
northeast Dunnage Melange.